THE UNIVERSITY OF OKLAHOMA

GRADUATE COLLEGE

OPTIMIZATION OF LIQUID CHROMATOGRAPHY WITH ELECTROCHEMICAL

DETECTION OF THREE MICRON REVERSED-PHASE COLUMNS

FOR NEUROCHEMICAL DETERMINATIONS

A DISSERTATION

SUBMITTED TO THE GRADUATE FACULTY

in partial fulfillment of the requirements for the

degree of

DOCTOR OF PHILOSOPHY

By

PETER YAU TAK LIN

Norman, Oklahoma

1984

OPTIMIZATION OF LIQUID CHROMATOGRAPHY WITH ELECTROCHEMICAL

DETECTION OF THREE MICRON REVERSED-PHASE COLUMN

FOR NEUROCHEMICAL DETERMINATIONS

A DISSERTATION

APPROVED FOR THE DEPARTMENT OF CHEMISTRY

By

ACKNOWLEDGEMENTS

The support of my family is especially noted. Thanks,
Uncle T. Y. for making it possible. To my parents, a very
special thank you is extended. This work would not have
been possible without your love, patience and encouragement.
To the rest of my family, I would just like to say, "Thanks
for having faith in me."

To a very special person, one who is so willing to give
so freely of himself — Dr. C. LeRoy Blank, I extend my most
sincere thank you. This is for everything. You have become
more than just my advisor, you have become a very special
friend.

To my wife, Lorrie, at times like this it is most
difficult to find the words that I would like to express. I
would like to thank you for being so understanding about the
long lonely nights. Without your loving support and gentle
encouragements this work would not have been possible.

To God, my Lord and Shepherd, thank you.

To my mom and dad,

and my wife, Lorrie.

TABLE OF CONTENTS

viii

LIST OF TABLES

LIST OF FIGURES

OPTIMIZATION OF LIQUID CHROMATOGRAPHY WITH ELECTROCHEMICAL

DETECTION OF THREE MICRON REVERSED-PHASE COLUMNS

FOR NEUROCHEMICAL DETERMINATIONS

CHAPTER 1

LIQUID CHROMATOGRAPHY WITH ELECTROCHEMICAL DETECTION

HISTORICAL PERSPECTIVE AND FUNDAMENTAL PRINCIPLES

I. Introduction

The first chromatographic separation experiment was re-
ported by Mikhail Tswett in 1906.[1] He separated pigments
from a green leaf of a plant on a chalk column, producing a
number of colored bands on the initially white column.   This
separation process was named chromatography, which is de-
rived from two Latin words meaning color and writing.

Since 1906, chromatography has developed into three
major categories − thin layer chromatography, gas chroma-
tography, and liquid chromatography.   Of these three, the
development of liquid chromatography (LC) has been the slow-
est.   Its development has been hampered by the lack of a
truly universal detector comparable to the thermal conducti-
vity and flame ionization detectors in gas chromatography.

A number of "universal" detectors have been reported

for LC. These include the refractive index, conductivity, and dielectric constant detectors. However, the relatively high detection limits of these detectors has restricted their application in modern LC. As a result, attention has turned to the development of LC detectors that are more selective and possess lower limits of detection. Among these, the most popular are the multi-wavelength ultraviolet-visible absorption, fluorescence, and electrochemical detectors. A number of connecting devices for coupling LC with mass spectroscopic detection have also been designed and demonstrated. Although these devices are commercially available, their complexity and the high cost of the combined instrument limits their practical utilization.

Electrochemical detection for liquid chromatography was first reported by Kemula in 1952.[2] He used polarography to detect liquid chromatographic eluents. However, it was not until 1973 that Kissinger *et al.* reported achieving detection limits for electrochemical detection in the picogram range.[3] Since that publication in 1973, this technique has received considerable attention. According to an August, 1982 report by BioAnalytical Systems, more than 700 papers have been published in this field.[4]

The basic instrument for liquid chromatography with electrochemical detection (LCEC) consists of two major parts. They are the liquid chromatograph and the electrochemical detector. The primary function of the liquid chro-

matograph is to separate a sample mixture into its consti-
tuent components.   The function of the electrochemical de-
tector is to detect the presence of the constituents as they
elute from the column.   Generally, the information obtained
from an electrochemical detector is more quantitative than
qualitative in nature.

II.   Liquid Chromatograph (LC)

The separation of an LC is afforded by the interactions
of the individual sample solutes with the mobile and sta-
tionary phases in the column.   The stationary phase may be
the packing material itself or a surface coating attached to
the packing material. The mobile phase is the liquid that
flows through the column. The sample is introduced into the
mobile phase at the inlet of the column.   As the sample
traverses through the column, the individual components
interact with both phases. Strong attraction between a
component and the stationary phase will increase its resi-
dence time in the column, while strong attraction between
the solute and the mobile phase will give it a shorter
retention time. Thus, based on the interactions between the
mobile and stationary phases with the sample components, the
individual species will elute from the column in different
time periods as bands or peaks.

A.   Pump

The primary function of the pump is to provide a flow

of mobile phase through the column.   Today,   there are many

pumps which are commercially available. These can be divided

into   two   basic categories: constant pressure   pumps   and

constant flow pumps.

1.   Constant pressure pumps.   Historically,   constant

pressure pumps have been popular because of their simplicity

and low cost.   Constant pressure is applied against   the

mobile phase at the column inlet,   thus forcing it   through

the column.   The constant pressure can be simply atmospheric

pressure,   but it is generally derived from a compressed gas

tank source.   However,   when a compressed gas is used,   the

gas is more likely to dissolve in the mobile phase and,

then,   degas out of the mobile phase and form bubbles   under

the   lower pressure conditions found at the column outlet or

the detector.   This is a serious problem for most LC detec-

tors.   But, the problem can be minimized by utilizing a pump

that   employs a diaphragm or baffles to separate the   mobile

phase from the applied compressed gas.

The   primary disadvantage of these pumps is   the   poor

reproducibility of retention times for the individual   elu-

ents.   Although a constant pressure is applied to the inlet

of the column, the flow rate through the column is primarily

dependent on the actual back pressure of the column   rather

than the externally applied pressure.   And, retention times

are directly related to flow rate. Accumulation of solid

portions of samples often occurs on the frit of the   column.

This introduces a pressure drop across the inlet frit and, thus, lowers the back pressure of the column. The resultant change in retention times makes identification and quantitation much more difficult.

2. Constant flow pumps. To eliminate the problems of irregular flow rate, constant flow pumps have been introduced. Today, constant flow pumps have replaced constant pressure pumps in almost all LC applications. Examples of constant flow pumps include the peristaltic pump, the single piston reciprocating pump, the dual piston reciprocating pump, and the syringe pump.

Constant flow is achieved by displacing a preselected volume of mobile phase from the pump in a fixed unit of time. This has been accomplished by two different methods. In the reciprocating pump, the volume within the pump head is successively discharged and replaced by an electric motor during each pump cycle. Although these pumps allow undisrupted analysis of many samples, they also produce a pulsating flow. This presents a problem for flow sensitive detectors.

The second class of constant flow pumps was designed to minimize this pulsation problem. These are the displacement, or syringe pumps. In this type, the electric motor drives the piston continuously and discharges a relatively small portion of the mobile phase in a constant and pulse-free manner. The volume of flow per minute is generally

very small compared to the total displacement capacity of the piston chamber. The primary disadvantage of this type of pump is that one must stop the analysis and refill the pump when the piston chamber has been completely discharged.

Due to the relatively higher cost and inconvenience associated with refilling the syringe pumps, reciprocating pumps have become more popular than displacement pumps. The exception to this generality is encountered when pulse-free flow is an overriding criteria in system requirements. Many modifications have been attempted to minimize the pulsation of reciprocating pumps, and some have been quite success-ful. One example is the dual piston reciprocating pump. While one piston is discharging, the other is filling. Thus, one piston is always delivering liquid to the system. Although this design eliminates the majority of the pulsa-tion problems, there is still a problem when the directional reversal of the two pistons occurs. Another improvement is represented by the single piston, rapid fill reciprocating pump. In this pump, the discharge portion of the pump cycle is set to be much longer than the refill portion. Since the pump spends a greater portion of time discharging than refilling, the pulsation is minimized. Once again, however, pulsation is minimized, but not completely eliminated. The latest attempt to minimize the effects of pulsation is represented by a high speed single piston reciprocating pump. The pumping frequency for this unit is greatly in-

creased from the normal units.   The usual one-half Hertz is
raised to twenty-seven Hertz and the volume displaced per
cycle is reduced by the same relative amount.   The small
discharges occur at such a high rate that the pulsation is
greatly diminished.   The much higher frequency of the pulsa-
tion also allows advantageous application of electronic
damping to the final signal.   The flow profile of this pump
is rather impressive.   However, there is a price to be paid
for the gain.   Since the displacement of the pump is so
small (on the order of microliters), it is extremely sus-
ceptibile to dissolved gases in the mobile phase.   Formation
of small gas bubbles in the piston chamber lead to drastic
reductions in flow rate.

<center>B.   Injector</center>

     The sole purpose of the injector is to deliver the
sample onto the top of the column.   This can be accomplished
in two distinct ways: stop-flow and continuous-flow injec-
tion.

     1.   Stop-flow injection.   In the stop-flow method, a
mechanical injector is not required.   Injection is accom-
plished by stopping the pump, disconnecting the pump from
the column, loading the sample onto the top of the column
with a syringe, reconnecting the pump to the column, and
starting the pump again.   Although this method is very
simple and economical, it is tedious and often irreproduci-

ble.   Thus,   for   most   applications,   this method has   been
replaced by continuous-flow injection.

2.   Continuous-flow injection.   In the continuous-flow
injection,   two different approaches are   available.   These
are represented by the septum and the loop injectors.

Septum injector.   With the septum injector,   a syringe
is   used   to pierce the septum and deposit the   sample   into
the flow stream   at the top of the column.   This system   is
relatively inexpensive and works quite well.   The main pro-
blem   with   this system is that   small pieces of the   septum
are   dislodged into the flowstream as the septum is   repeat-
edly   pierced.   These pieces accumulate at the column   inlet
and block the flow through the column.   Another   limitation
of this injector is that,   due to potential leaks, it cannot
be   used   with systems operating at pressures   much   greater
than one thousand pounds per square inch (psi).

Loop injector.   By far, the state of the art for injec-
tors is represented by the loop injector.   The loop injector
has   two basic positions: load and inject.   In the   load
position, the pump is connected directly to the inlet of the
column and the loop is accessible for sample loading.   Once
the sample is loaded by drawing it into the loop, the injec-
tor   is   turned to the inject position,   where the   loop   is
inserted   between   the pump and the inlet   of   column.   The
mobile   phase   flushes the sample out of the loop and   onto
the top of the column.   The loop injector can be operated in

two different modes.   It can be used in the partial filled

mode or the completely filled mode.   The partial filled mode

offers sample size flexibility while sacrificing injection

volume accuracy and reproducibility.   The completely filled

mode, on the other hand, offers excellent accuracy and

reproducibility, but requires physical removal and replace-

ment if a different sample size is desired.

C. LC Column

The heart of the liquid chromatograph is the column.

This is the portion in which the actual separation processes

occur.   In liquid chromatography, four major types of co-

lumns form the basis for liquid-solid chromatography (LSC),

liquid-liquid chromatography (LLC), ion exchange chroma-

tography (IC), and size exclusion chromatography (SEC).

1.   LSC.   In LSC, the stationary phase is the surface

of the packing material and the basic interaction mechanism

involves adsorption onto this surface.   Both solute and

mobile phase molecules compete for the available adsorption

sites on the surface.   The degree of adsorption is highly

dependent on the functional group(s) of the molecules in-

volved.   Solutes with functional groups that do not readily

adsorb on the stationary phase are weakly retained, while

solutes with functional groups that adsorb readily will be

strongly retained.   The most common stationary phases in LSC

are silica and alumina.   Since adsorption is heavily de-

pendent upon functional groups, LSC is extremely useful for the separation of a mixture into groups based on their functional groups. Tswett's separation of leaf pigments on a chalk column is an excellent example of LSC.

2. <u>LLC</u>. In LLC, the column is packed with a solid material usually referred to as the solid support, and the stationary phase is coated on the solid support. The basic interaction mechanism involves partition between the immiscible mobile and stationary phases. The solute molecules distribute themselves between the two phases according to their partition coefficients. Once again, the solute with the greater attraction for the stationary phase will be retained longer, while a solute with less attraction will be retained for a shorter period of time.

Columns with stationary phases that are merely coated on the solid support are subject to stationary phase stripping. This occurs when the stationary phase slowly dissolves in the mobile phase or, when extremely high flow rates are used, the stationary phase may be mechanically stripped. This problem was circumvented with the development of bonded phase LLC. In bonded phase LLC, the stationary phase is chemically bonded onto the surface of the solid support. The bonded columns are so much superior to the unbonded that the vast majority of commercially available LLC columns today are chemically bonded.

Since most LLC columns use silica as the solid support,

a secondary mechanism of adsorption occurs when the surface of the silica is not completely covered by the bonded stationary phase. Ideally, the stationary phase coverage should be one hundred percent, but this is seldom the case. Highly polar compounds are the most likely candidates for adsorption on the exposed silica. This leads to peaks for these compounds which exhibit serious tailing problems. The active sites can be substantially decreased, however, by silylation, and this process is commonly referred to as "endcapping".

Unbonded silica was one of the first packing materials used in the older LSC. The surface of this material contains many hydroxyl groups, which are highly polar in nature. To provide a polarity difference between the mobile and stationary phases, the mobile phase was chosen to be a nonpolar liquid. But, the advent of bonded columns allowed the silica stationary phase to become either polar or nonpolar. Thus, the term "normal phase" was coined for the historical case of a polar stationary phase and nonpolar mobile phase, while the term "reversed-phase" was used to refer to the case of a nonpolar stationary phase with polar mobile phase.

3. IC. In ion exchange chromatography, the stationary phase contains surface functional groups that are ionic in nature. These functional groups are usually attached to a resin based backbone which is cross-linked to give it structural rigidity. Different functional groups can be attached

12

to make the column suitable for strong anion, weak anion, strong cation, or weak cation separations. The primary interaction mechanism involves the adsorption of the ionic solute onto the attached functional group. But, the solute ion must compete with other ionic solute and solvent components for the limited number of ion-exchange sites. Solute molecules with a higher charge density will, thus, be retained relatively more than those with a lower charge density.

4. SEC. In size exclusion chromatography, also commonly known as gel permeation chromatography or GPC, the stationary phase is composed of a highly porous material, the surface of which is ideally chemically inert. The basic separation mechanism involves the diffusion of solute molecules into the pores of the stationary phase. Solute molecules that are bigger than the pores will elute initially, while smaller molecules that can diffuse into the pores will be retained longer. Thus, size exclusion chromatography separates solutes on the basis of their size or molecular weight.

A large number of stationary phases have been developed for GPC. The pore size of these stationary phases can now accommodate molecular weights in the range of 10^2 to 10^8. This type of chromatography is particularly applicable to the separation of high molecular weight polymeric and biological materials. Early packing materials were soft

gels made from styrene, styrene divinylbenzene, dextran, or agarose. These soft gels would operate properly only under very modest pressures. High flow rates causing high pressure would collapse the pores. This resulted in long separation times. The recent development of semi-rigid and rigid stationary phases has led to high speed size exclusion separations. These new materials, including Styragel[R], porous silica, and porous glass beads, can be operated at relatively high flow rates, thus allowing much faster analyses. They are especially useful for the separation of proteins and peptides.

For a more in depth treatment of the science of separation and liquid chromatography, a number of excellent books are recommended.[1,5,6]

III. Electrochemical Detector

The main function of the electrochemical detector is to detect the solutes in an LC effluent. This is usually accomplished by flowing the effluent through a small volume electrochemical cell. If the solute is electrochemically active at the applied potential of the working electrode, an electrochemical reaction occurs as it is swept across the electrode surface. As the reaction occurs, a current is generated. At a given flow rate, the current is directly proportional to the quantity of solute in the effluent. Limited qualitative information is also afforded by this detector. Only chemicals that are electrochemically oxidi-

zable or reducible at the applied potential will produce an observable signal. By judiciously selecting the applied potential, two co-eluting compounds having half-wave potential differences greater than one to two hundred millivolts may be distinguished. The degree of qualitative information is quite similar to that which can be obtained from a UV detector.

This method is based on one of the simplest and most sensitive methods of electrochemistry — amperometry. Thus, at the beginning of LCEC, most of the instrumentation was adopted directly from classical electrochemical procedures. As the technique matured, hardware which was more dedicated in nature was developed. Modern instrumentation is so specific to LCEC that it is virtually useless for general electrochemical experiments. The following sections will cover the evolution of LCEC potentiostats, cell designs, and electrode materials.

A. Potentiostats

The primary function of the potentiostat is to maintain a constant potential at the working electrode relative to the reference electrode and monitor the passage of current through the working electrode. Depending on the particular requirements of the experiment, the potentiostat may be no more complex than a battery with a variable resistor and an ammeter.[8] Although such two electrode systems are adequate

for measurements in the nano and picoampere range, three electrode systems are generally used to insure proper maintenance of the applied potential. The three electrodes are the auxiliary, reference and working electrodes. The additional auxiliary electrode provides a current source/sink for the working electrode.

1. <u>Single</u> <u>potentiostats</u>. The design of the three electrode potentiostat was substantially simplified by the advent of low cost operational amplifiers (op amps). Two fundamental op amp based designs have been developed: the DeFord and the Diefenderfer potentiostats, as seen in Figure 1-1.

The major component difference between the two designs is represented by the additional op amp in the feedback loop for the control amplifier of the Deford potentiostat. Since the cost of most op amps is currently less than ten dollars and exceptionally high performance op amps cost less than twenty dollars, the difference in the cost of these two potentiostats is not significant. Circuit analysis also reveals that the potential of the working electrode *versus* the reference has exactly the same sign and magnitude as the applied potential for the Deford potentiostat. In the Diefenderfer, on the other hand, the magnitudes are the same, but the signs are opposite. Although this sign reversal may occasionally be a slight inconvenience, it does not affect the operational quality of the potentiostat. Both designs
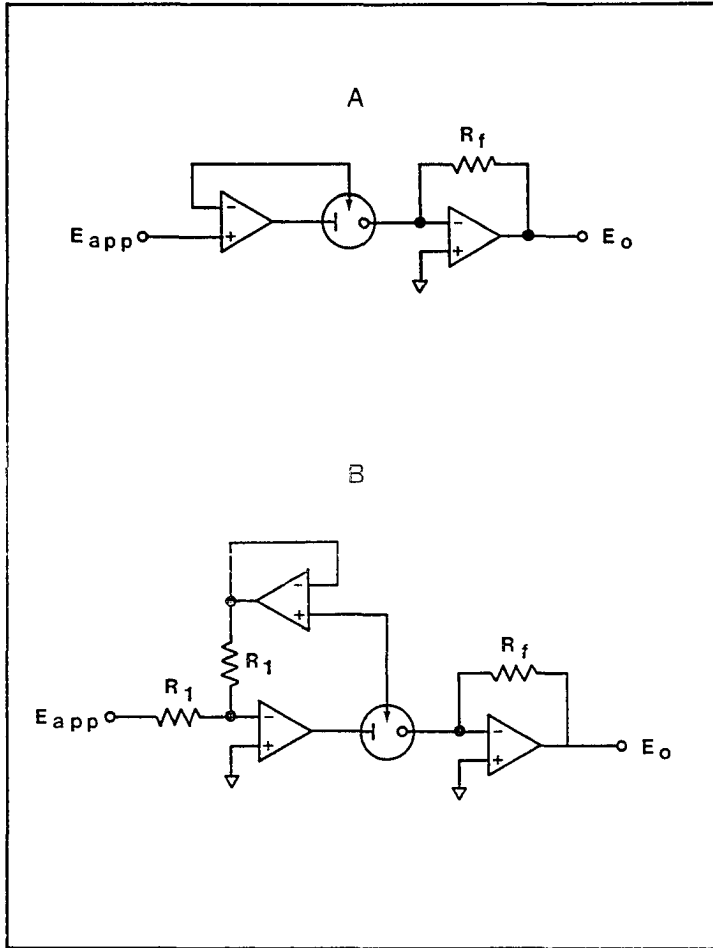
Figure 1-1. Fundamental Circuit Components for the Die-
fenderfer (A) and DeFord (B) Potentiostats.

perform equally well.

The primary advantage of using op amps in potentiostats
is afforded by their inherently high input resistance, which
is usually on the order of 10^8 to 10^9 ohms or higher. This
high resistance leads to only very small input or bias
currents at the inputs of each op amp. This keeps the
current flowing through the reference electrode at a mini-
mum, thus allowing the reference electrode to maintain its
desired potential. It also allows accurate measurement of
working electrode currents by minimizing dissipation of such
currents in the op amps themselves.

To quantitate the LC eluents, the current flowing
through the working electrode is continuously monitored.
Depending for the most part on the quantity of the eluent
and the surface area of the working electrode, this current
is typically in the picoamp to microamp range. Such cur-
rents can be directly monitored by a high sensitivity amme-
ter or galvanometer, but are normally converted into a more
easily handled voltage and amplified to the millivolt or
volt level. The voltage signal can be directed to a compu-
ter *via* an analog-to-digital convertor or, simply, to a
strip-chart recorder. Currently, there are approximately
ten versions of potentiostats available in the commercial
market based on the two fundamental designs.

2. Dual potentiostats. The first dual potentiostat
for LC was reported by Blank in 1976.[7] The concept of one

instrument simultaneously controlling the potentials of two different working electrodes is not new. Bipotentiostats have been used with rotating ring-disk electrodes for years.[8] Extending this concept into LCEC, however, has been an important step. This pioneering work paved the way for development of some very unique applications of dual LCEC. Some of these developments will be presented later. Currently, there are at least three commercially available dual potentiostats for LCEC.

Recently, a microprocessor-controlled dual potentiostat for voltammetry has also been reported.[9] A number of optional potential waveforms and current sampling methods can be programmed employing this unit. Although designed specifically for use with classical electrochemical investigations, it may also be found suitable for applications in LCEC.

3. Non-DC potentiostats. Since the initial publication of LCEC in 1973, various non-DC modes of LCEC have been evaluated. These include modifications of some of the classical electrochemical waveforms --- linear sweep, pulse, and differential pulse. More recently, very complex waveforms have been employed for some very specific applications.

B. Cell Design

The design of the detector cell is critical to its proper operation. It affects the dead volume, the hydrodynamic characteristics, and the IR drop of the cell. These three factors each play a very important role in the perfor-

mance of the cell.   The dead volume affects the band broa-
dening of the chromatographic peaks.   The hydrodynamic para-
meters and the impedance of the cell can affect the electro-
chemical reaction.

Several different designs of LCEC cells have been de-
veloped.   They include the thin layer, wall jet, tubular,
porous and polarographic units.   Many different detector
cells within each category have also been developed.

1.   Thin-layer cells.   The thin-layer cell consists of
two blocks of plexiglas or Kel-F separated by a thin fluoro-
carbon spacer.   The cell volume is defined by the size of
the slit cut in the spacer.   The top block contains two
drilled holes positioned over the two ends of the flow
cavity which serve as the inlet and outlet of the cell.   The
working electrode is usually located on the bottom block of
the cell.   The electrode may assume the shape of a small
circle in the middle of the flow stream or it may encompass
the entire flow stream, forming one wall of the channel.
The reference and auxiliary electrodes are usually placed
downstream from the cell.

The main advantage of this type of cell is afforded by
the small cell volume.   When used with most electrode mater-
ials, the cell volume is usually in the order of a few
microliters.   The one exception to this is provided by the
dropping mercury electrode.   Due to the bulkiness of this
electrode, a cell containing a dropping mercury electrode

has a significantly larger cell volume.

The major disadvantage of this cell design is the inherently high IR drop which is due to the downstream placement of the auxiliary and reference electrodes. When the spacer is extremely thin, the resistance between the working and the remaining electrodes can be very high. In the single electrode cell, the IR drop is usually not disastrous. But, in the case of a dual or multiple electrode cell, the IR drop can cause the working electrode to cross-talk and, thus, affect the performance of the cell. To alleviate this problem, the auxiliary electrode is incorporated into the cell near the working electrode. At the current time, the auxiliary electrode is typically located directly across from the working electrode when dual or multiple electrodes are used.

A good example of the thin-layer type of cell is the first high sensitivity LCEC detector reported by Kissinger et al. in 1973.[3] The working electrode of this cell was formed from carbon paste which was packed into a circular well drilled into the cell bottom. The diameter of the well was larger than the width of the channel. The inlet and outlet to the flow channel were angled at approximately 45° relative to the direction of flow in the channel to minimize turbulent flow.

In 1976, Shoup and Kissinger reported a versatile thin layer cell that is suitable for both thin-layer chronocoulo-

metry and LCEC.[10] The main difference between this cell and the previously mentioned cell is that the inlet and outlet are perpendicular to the flow stream rather than angled. Most LCEC cells used today are derived from this cell design. In that same year, Lankelma and Poppe designed a thin-layer coulometric cell using two plates of glassy carbon separated by a spacer as a working electrode/auxiliary electrode pair. This was the first utilization of a working electrode that spanned the total available area on one side of the channel. It was also the first time that an auxiliary electrode was placed directly across from the working electrode.[11] Also in that year, Swartzfager designed a thin-layer cell that had a removable working electrode.[12] This allowed a fairly rapid exchange of the working electrode material.

The first dual electrode thin-layer cell was also reported in 1976 by Blank.[7] This dual cell was very similar to the first single LCEC cell with the exception that an additional electrode was inserted downstream in the flow channel from the first electrode. Using this cell, he demonstrated the enhanced selectivity available with dual detection by resolving three chromatographically overlapping peaks.

In 1978, Weber and Purdy investigated the behavior of a variety of thin-layer cells.[13] They also derived a theoretical expression for the limiting current as a function of

both cell and chromatographic parameters.

In 1980, Hirata *et al.* developed a thin-layer cell for use with capillary LC columns.[14] The internal volume of this cell was approximately 0.1 µl. Also in that year, Pinkerton *et al.* designed an optically transparent thin-layer cell.[15] This allowed simultaneous spectrophotometric as well as electrochemical determinations.

Finally, Beauchamp *et al.* developed a thin-layer cell that not only allowed interchangeable working electrodes, but also an alternate mode of operation.[16] The normally thin-layer amperometric cell can be modified to become a wall jet cell by merely selecting a different inlet on the top of the cell.

This somewhat limited review of thin-layer LCEC cells is not by any means complete. Indeed, many more reports on thin-layer cells have been published. The intent of this discussion was simply to point out the major options which have been developed for these cells.

2. <u>Wall jet cells</u>. In this type of cell, the LC effluent is directed perpendicularly to a planar disk electrode *via* an inlet nozzle. After impinging on the electrode, the eluent forms a boundary layer on the surface of the electrode and disperses radially outward from the center of the electrode. It diffuses out of the cell using at least two opposing outlets which are equidistant from the electrode. The limiting current of the cell is a very complex

function of the flow rate, the nozzle inner diameter, the area of the electrode and the distance between the nozzle and the electrode.[17] The distance separating the nozzle outlet and the working electrode is particularly critical. Unimpeded development of the boundary layer is essential to obtaining an optimal limiting current. If the nozzle is too close to the electrode surface, the tip of the nozzle will disrupt formation of the boundary layer. If the distance is too large, the stream from the nozzle will dissipate prior to impacting on the electrode. A recent report indicated that the distance must be less than 1 cm at flow rates of 1-10 ml/min to avoid dissipation. Disruption of the boundary layer can also arise from another source. If a thin spacer is used, the presence of a restricted region on the cell top surrounding the nozzle may also impede proper formation of this boundary layer. In fact, a more recent report indicated that a wall jet electrode with a very thin spacer responded exactly like a radial thin-layer cell.[17]

The wall jet design has two important advantages. Due to the highly convective nature of the mass transfer process at the point of contact between the stream and the electrode surface, this design has a higher sensitivity and slightly less problems with electrode fouling than the thin-layer cell. However, the question of which provides better detection limits is uncertain at this time due to conflicting reports.[16,18-21]

The wall jet design has one rather unique feature. Its effective cell volume is only determined by the volume of the boundary layer and not the entire geometric cell volume.[22] This feature, confirmed by a second report,[17] allows the actual volume of the wall jet cell to be quite large without eliciting significant increases in band broadening.

The theory of the wall jet cell was first reported by Matsuda and Yamada in 1967.[65-67] Since that time, further studies on the theory of this cell's operation have been conducted by the groups of Fleet and Weber.[17,22] The first wall jet cell designed for use with an LCEC was reported by Fleet and Little in 1974.[23] Beauchamp *et al.*, as previously mentioned, reported an LCEC cell that can be used in both the thin-layer mode and the wall jet mode in 1981.[16] In the same year, Stulik *et al.* compared the sensitivity and the detection limit of the thin-layer cell to that of the wall jet cell.[19,20] In the following year, Slais and Krejei reported a wall jet cell with an effective cell volume of less than one nanoliter.[24]

3. <u>Tubular cells</u>. In a tubular cell, the working electrode is shaped like a hollow cylinder. It is placed in the cell so that only the inside of the tube is exposed to the flow stream. The auxiliary and reference electrodes are usually located down stream. The main advantage of this design is that the flow pattern and resultant currents are theoretically well defined. The main problem with this design is that the electrode is very difficult to resurface.

This design is not popular, and only a limited number of papers covering its application have appeared in the literature.[19,23,25-29]

4. <u>Porous cells.</u> The design of these cells is very similar to that for the tubular cells. However, instead of being a hollow tube, the working electrode is a porous plug. This plug can be shaped like either a rectangular block or a cylinder. The effluent is simply forced through the working electrode, resulting in very extensive mixing and electrolysis of solutes. The obvious advantage of this design is the coulometric, or complete, electrochemical conversion of the solutes. The disadvantages are the relatively large dead volume of the cell and the fact that resurfacing the electrode is either difficult or impossible.

A limited number of porous cells for LCEC have been reported with the first reports appearing in 1973.[25,30-33] Takata and Muto and Johnson and Larochelle both examined porous flow cells for use with LCEC.[30,31] In 1980, Schieffer developed a dual flow cell which had a porous coulometric electrode upstream to remove undesirable electroactive components from the effluent. The downstream carbon paste amperometric electrode was then used to detect the remaining compounds of interest.[34] Very recently, a commercial company has developed a dual porous cell which has a reported total cell volume of less than S μl.[35]

5. <u>Polarographic cells.</u> A very large number of mer-

cury electrode based cells for LCEC have been developed. This is partly due to the popularity of the mercury electrode in classical electrochemistry. The most common mercury electrode for general electrochemical applications is the dropping mercury electrode (DME). This popularity is due to the continuously and reproducibly refreshed electrode surface that is obtained with each new drop.

The DME has been incorporated into a thin-layer type of cell in two ways. The DME can be mounted in a vertical position so that the flow stream of the effluent impinges on the DME horizontally.[23] In the other case, the DME is placed horizontal and the flow stream is vertical.[36] The required cell volume can be somewhat minimized by using very short drop times.[37] The DME can be further used in a very different mode; for example, the Princeton Applied Research Co. has developed a wall jet DME cell.[38]

The hanging mercury drop electrode (HMDE) offers no obvious advantage over the DME in LCEC, thus, it has not been extensively examined. On the other hand, mercury film electrodes exhibit none of the mechanical bulkiness of the DME or the HMDE. But, switching to mercury film electrodes incurs a loss of the continuously renewed surface as well as a loss in the usable cathodic range due to amalgam formation. In spite of these disadvantages, the film electrode has experienced successful commercial exploition by BAS. They have incorporated such electrodes into thin-layer cells

for a variety of applications.[4,39]

C. Electrode Materials

The single most important component in an LCEC is frequently the electrode material. Often, the type of electrode material chosen will dictate the cell design. A wide variety of electrode materials have been used in LCEC. Among the most successful are carbon paste, carbon composites, glassy carbon, mercury and platinum. A number of characteristics must be considered when selecting the electrode material. One of the most important parameters is the potential range of the material. Other parameters include residual current, compatibility with the mobile phase, useful lifetime and ease of resurfacing the electrode.

1. <u>Carbon paste electrodes</u>. Carbon paste is made from Ultrapure[R] carbon and a high molecular weight organic binder. Several organic binders have been evaluated. They are Nujol[R] (a paraffin mixture), ceresin wax, silicone grease and α-bromonaphthalene. The most popular binder is Nujol[R].

Carbon paste has a wide aqueous potential range spanning approximately −1.6 to +1.1 volts *versus* the saturated calomel electrode (SCE).[3,19] It has an extremely low anodic residual current, but the cathodic residual current is rather high. It is also extremely inexpensive and quite easy to resurface. A new carbon paste surface can be installed in less than five minutes by an experienced opera-

tor.   A well surfaced electrode can last from one day to several months depending on the environment and the nature of the samples to which it is exposed.   Due to its inherently low background noise in the anodic range, it exhibits a very low limit of detection.

Carbon paste suffers from several problems.   Since organic binders are employed in its production, it is incompatible with very nonpolar mobile phases.   However, it may be used with aqueous mobile phases containing small amounts of nonpolar liquids (typically less than 5-10%) without any substantially deleterious effects.   It is also susceptible to adsorption of solutes and fouling of the electrode surface.   Because it is soft, it is not applicable to wall jet designs.   It is difficult, if not impossible, to produce a carbon paste surface that is perfectly smooth and planar. The electrode material frequently bulges out slightly after surfacing.   This precludes the use of carbon paste as an opposing auxiliary electrode with a very thin spacer.   And, it is not very suitable for cathodic work due to the high residual current in this potential range.

2.   <u>Carbon</u> <u>composite</u> <u>electrodes</u>.   These electrodes were designed to alleviate the short-comings of the carbon paste electrode, namely the pliant nature of the paste.   A number of matrices have been tested.   The most successful include polyvinyl chloride, polyethylene, polypropylene, Kel-F and high molecular weight waxes.[20,26,13,40,41]

These electrodes can generally be polished to obtain quite smooth and highly planar surfaces. They are compatible with aqueous mobile phases and even with many organic solvents. They also possess a wide anodic potential range. In general, however, they are less sensitive than carbon paste with comparable or even higher residual currents. Thus, they exhibit higher detection limits. They are slightly more expensive than carbon paste and are harder to resurface. Currently, there are several commercial instrument manufacturers offering these kinds of electrodes for LCEC detectors.

3. <u>Glassy carbon electrodes</u>. Glassy carbon is a solid carbon material that exhibits high purity, great mechanical strength, and extremely low permeability to gases or liquids. It is made from organic materials which are carbonized followed by a carefully programmed thermal treatment. Current theory concerning the nature of this material implicates the presence of both trigonal and tetrahedral bonded carbons. The conditions employed in the heat treatment determine the ratio of the types of carbon contained in the final material.

The useful aqueous potential range of glassy carbon is approximately −0.8 to +1.2 volts *versus* SCE.[4,16,19] Due to its relatively low residual current in this entire potential range, it can be advantageously employed for both anodic and cathodic reactions. Its hard surface can also be polished

to a mirror-like finish. Thus, it can be used in both the thin-layer and wall jet designs. In an LCEC cell, however, glassy carbon is susceptible to surface adsorption and film formation. Electrode resurfacing is more difficult and tedious than for carbon paste. It has a slightly lower sensitivity and a slightly higher residual current when compared to carbon paste. Thus, it exhibits a slightly higher detection limit. The performance of this electrode is highly dependent on the surface smoothness obtained by electrode polishing.

The first group to use this material in an LCEC cell was that of Poppe *et al.* in 1976.[11,42] Due to its physical and electrochemical attributes, it is currently very popular, and its use is widespread. In fact, glassy carbon is probably the most frequently used electrode material in LCEC today.

4. <u>Mercury electrodes</u>. The DME has seen extensive use in the field of electrochemistry. The advantages afforded by a fresh and reproducible electrode surface with each new drop are unmatched by any other material. It has an aqueous potential range of approximately -1.9 to +0.4 volts *versus* the SCE.[16,19] While it is extremely well suited for cathodic work, some anodic work is also possible using compounds requiring only relatively low potentials for oxidation.

To alleviate the mechanical awkwardness of the DME, the mercury film electrode was developed. In the most common

commercial cell (BAS TL-9A), the substrate is gold and mercury is applied to the gold surface to form an amalgam film. This electrode material has lost the advantage of periodical surface renewal of the DME, and the aqueous potential range has been decreased to -1.0 to +0.4 volts *versus* SCE. In spite of these compromises, the mercury film electrode, together with the glassy carbon electrode, is one of the major materials used for cathodic investigations in modern LCEC.

5. Platinum electrodes. Platinum (Pt) is a very malleable substance and is easily polished to obtain a smooth surface. It has an aqueous potential range of about -0.5 to +1.2 volts *versus* SCE.[61,64] The potential range of Pt is much wider in organic solvents. The use of Pt in LCEC is very limited due to the formation of oxides in the anodic region and adsorption or filming in the cathodic region. A relatively small number of LCEC papers have been published using this material.[30-32,43]

Pt electrodes are very useful, however, in certain very specific cases. By irreversibly adsorbing iodide onto the Pt surface, Johnson and Larochelle prevented oxide formation.[44] This allowed the detection of certain inorganic ions. Recently, this same group has used an ingenious pulse sequence on Pt electrodes to detect amino acids without any prior derivitization. The electrode surface is kept clean by briefly pulsing into the anodic region during each se-

quential cycle.

6. Other graphite electrodes. Other graphite materials have been used to alleviate the short-comings of carbon paste. One such material is pyrolytic graphite. The electrode surface is extremely flat on the basal plane. The surface is easily renewed by simple pealing with an adhesive tape. The aqueous potential range is approximately -1.5 to +1.2 volts *versus* an SCE.[45] Wightman *et al.* have demonstrated that this material has anodic detection limits that are similar to that of carbon paste, yet it is usable in both the anodic and cathodic regions.[14,46]

Another material used in LCEC cells is the carbon fiber electrodes of Wightman *et al.* These workers have fabricated a working electrode consisting of one hundred strands of 5 μm dia. carbon fibers.[47] This array is formed so that neighboring fibers are approximately 0.25 to 0.50 mm apart. They have found that this cell is relatively insensitive to flow pulsation. The carbon fiber array electrode was also used for the rapid voltammetric scanning of LCEC effluents to facilitate the identification of the components.[48] A disadvantage of the scanning mode is that the detection limit increases by three orders of magnitude when compared to the normal amperometric mode.

Curran and Fougas used reticulated vitreous carbon (RVC) as the working electrode material for an LCEC coulometric cell.[49] Due to the large dead volume of the electrode,

the entire cell possessed an effective overall dead volume
of approximately 8.5 µl. The authors claimed that the
detection limits of the cell were comparable to most ampero-
metric cells; they reported detection limits of 0.132 ng and
0.366 ng for dopamine and epinephrine, respectively.

D. Modes of Operation

Since the first demonstration of high sensitivity LCEC
by Kissinger *et al.* in 1973, several other modes of LCEC
have been developed. The first experimental LCEC actually
used a small electrode held at a constant potential. This
approach only produces electrolysis of a small fraction of
the total available effluent, and, thus, is commonly known
simply as "amperometry". In contrast to amperometry, com-
plete electrolysis of the effluent components is referred to
as "coulometry". The constant potential mode is called the
"DC" mode. On the other hand, when the applied potential is
varied as a function of time, this case will be referred to
as the "non-DC" mode. In addition to these two options, one
other choice is available: the number of the working elec-
trodes. Theoretically, any number of electrodes may be used.
Practically, only single and dual electrode cells are em-
ployed. From these three options, eight different LCEC
modes of operation are possible, but not all have yet been
attempted.

In addition to these modes, one other highly successful
use of LCEC, which is not discussed here, has been de-

veloped.[61-64] One of the fundamental requirements for a compound to be determined by LCEC is that the compound be electrochemically active. Post-column and pre-column derivatization as well as enzymatic transformations have allowed electrochemically inactive compounds to be detected by LCEC. This approach has greatly expanded the applicability of LCEC to include many previously inaccessible compounds.

    1. *Amperometry* vs. coulometry. The first reports of both amperometric and coulometric detection in LCEC appeared in 1973.[3,30] The report of the amperometric mode preceded that of the coulometric mode by about three months. In the formative years of LCEC, it was fairly clear that amperometry had the edge over coulometry due mainly to its lower detection limit and smaller dead volume. Currently, this issue has become somewhat clouded because of recent advances in coulometry.

    Amperometric cells typically have smaller cell volumes because only very small electrode areas are needed. Due to the smaller surface area, they usually have lower detection limits. Most amperometric cells utilize either the thin-layer design or the wall jet design. The innately flat electrode cells are easily disassembled and resurfaced.

    Coulometry. In order for a coulometric detector to achieve complete electrolysis, it must expose all the solute molecules to the electrode surface. This can be accomplished in two ways. One way is to increase the residence

time of the effluent in the cell so that there is sufficient time for all the solute molecules to diffuse to the electrode surface. But, a good detector should not place any flow rate limitations on the system. To avoid this possible restriction, the surface area and, thus, the cell volume must be increased. Another alternative is to increase the degree of mixing so that convection, rather than diffusion, will become a more prevalent mode of transport to the electrode surface. This is usually accomplished by using porous electrodes which also, simultaneously, provide an increased surface area.

The first reported coulometric LCEC cell is an example of the latter case. In 1973, Takata and Muto used a cell with internal dimensions of 48 mm by 15 mm by 2 mm, and they packed carbon cloth, platinum gauze or silver wire netting into this cavity. This approach yielded an electrolytic efficiency of more than 99.5% with flow rates up to 6 ml/min.[30] On the other hand, an example of the first kind of coulometric detector was reported in 1976 by Poppe and Lankelma.[11] They used a glassy carbon electrode with a surface area of 80 mm by 7 mm. The extra long flow channel subtantially increased the residence time of the eluting solutes. However, they found the coulometric efficiency of this cell to be highly dependent on both the flow rate and the spacer thickness. With a 0.05 mm spacer and a flow rate of 0.33 ml/min, a coulometric yield of 96% was achieved.

This flow rate dependence represents a severe limitation on the use of this device in modern LC separations. From these investigations, it is clear that the best coulometric cells incorporate the flow through electrode design. The thin-layer and wall jet designs are inappropriate for coulometric determinations. Since 1976 only three further reports on coulometric cells have appeared.[35,49,50] All three reports have used flow through electrodes. The first of these reported the use of a coulometric cell as a precolumn device for removal of electroactive impurities in the mobile phase. This decreases the pump pulsation noise and some faradaic derived noise sources associated with the electrode. The second cell is a commercially available cell which has two porous flow through electrodes which can operate with flow rates of up to 4 ml/min. The third cell uses an RVC material as its porous working electrode.

Several advantages of coulometry over amperometry have been cited. These include an increase in the faradaic current, less sensitivity to pump pulsation, direct correlation of peak area to the amount of compound present, and less susceptibility both to electrode surface imperfections and to deactivation caused by solute adsorption.[11] Assuming a conversion efficiency of roughly ten percent for an amperometric cell, the increase in current provided by a coulometric cell can, at most, be factor of ten. But, the noise is directly proportional to the electrode surface area, and the

surface area of a coulometric cell is greater than that of an amperometric cell by more than a factor of ten.[11] Thus, the gain in signal for a coulometric cell is negated by its increase in noise, and the signal to noise ratio is actually decreased. Further, in order to convert the peak area directly into the amount of solute, the number of electrons involved in the electrochemical reaction must be accurately known and eluting peaks must be completely resolved.[51] Baseline resolution of all peaks is difficult to achieve and, practically, requires an inordinate amount of time. The number of electrons transferred is frequently unknown for many compounds and is rather difficult to determine experimentally. This number is highly dependent on the solvent and may well change if the mobile phase is altered. Besides, quantitation by amperometry with an internal standard is at least as effective as coulometry and places less demand on the LC, since baseline resolution is not required. Often, the extra surface area required for coulometry is accompanied by an increase in cell volume. Excessively large cell volumes can have seriously detrimental effects on the band spreading of individual peaks. But, notably, recent advances in coulometric cells have decreased the cell volume to the region of 5 to 8 μl.[35,49] Other problems associated with this type of cell include complex cell design, bulkiness, and difficult or impossible electrode resurfacing.

In spite of these problems, the dual coulometric cell merits special attention. The two electrodes are arranged serially in the cell, leading to three possible modes of operation. These are the screen mode, the redox mode, and the differential mode. In the screen mode, the first electrode is used to screen out mobile phase impurities, potentially interferring compounds, and even pump noise, while the second electrode is used to monitor the peaks of interest. This is only possible in an anodic application if the half-wave potentials of the compounds of interest are at least moderately greater than those of the interferring components. In the redox mode, the first electrode is used to oxidize or reduce the electrochemically reversible compound of interest and the second electrode is used to perform the opposite reaction. This is comparable to a similar rotating ring-disk experiment, with the exception that the dual coulometric unit exhibits a much greater collection efficiency. Both of these modes are used to increase the selectivity of the compound of interest. To lower the detection limit, the differential mode may be used. In this mode, the first electrode is used to react with all the electroactive components in the effluent, while the second electrode is used to monitor the background noise. By subtracting the output of the second electrode from that of the first, the signal to noise ratio of the resulting chromatogram is enhanced.

Summary. Amperometry utilizes small flat electrodes in

small flow cells. With carbon paste electrodes, subpicogram detection limits are possible. On the other hand, coulometry uses flow through electrodes with larger cell volumes. Their detection limits are higher, usually in the range of a few picograms to nanograms. Amperometric cells should be used when the volume of the cell or the detection limit is critical, while dual coulometric cells are appropriate when enhanced selectivity is needed.

2. **DC** *versus* non-DC. The issue concerned with the choice of the proper applied waveform is similar to the issue of amperometry *versus* coulometry. The fundamental concern is once again detection limit *versus* selectivity. As usual, there are advantages and disadvantages to both choices.

DC mode. In this mode, the applied potential is held constant, and the residual current is at a minimum because of the absence of charging currents. The current output of the cell is due primarily to faradaic processes. Selectivity is inherent in the DC mode because only those compounds whose half-wave potentials are near or below the applied potential will be detected in anodic applications.

Non-DC mode. A variety of waveforms have been used for the applied potential. This discussion will be limited to pulse waveforms because triangular waveforms and their constant, large charging currents have been shown to be of little use in LCEC. Three different types of pulse wave-

forms have been used in LCEC.   The first type is the normal pulse waveform.   The second type is the differential pulse waveform.   The third type is labelled special application or specific waveforms.

Normal pulse.   In this waveform, an initial potential, E_0, is selected at which the desired electrochemical reaction will not occur,   whereas the pulse potential, E_1, is one at which the reaction will occur.   The current is sampled for a short time near the very end of the pulse period, shown as interval A in sample waveform A of Figure 1-2. Sampling the current at the end of the pulse step allows the charging current to decay to a minimum value, and, thus, maximizes the faradaic fraction of the total measured value.

Swartzfager found that the normal pulse mode offers little or no advantage over the DC mode, while increasing the detection limit by ten- to twenty-fold.[12]   Poppe's group likewise reported an increase in detection limits of a factor of ten for the normal pulse operation, but they also stated that this technique is very useful for the detection of strongly adsorbing compounds.[52] The reverse step, back to the initial potential, helps to remove adsorbed compounds.

Differential pulse.   The voltage waveform used in this mode is identical to that used in the normal pulse mode. The difference arises from the fact that the currents are recorded for two periods in each pulse cycle.   Both inter-
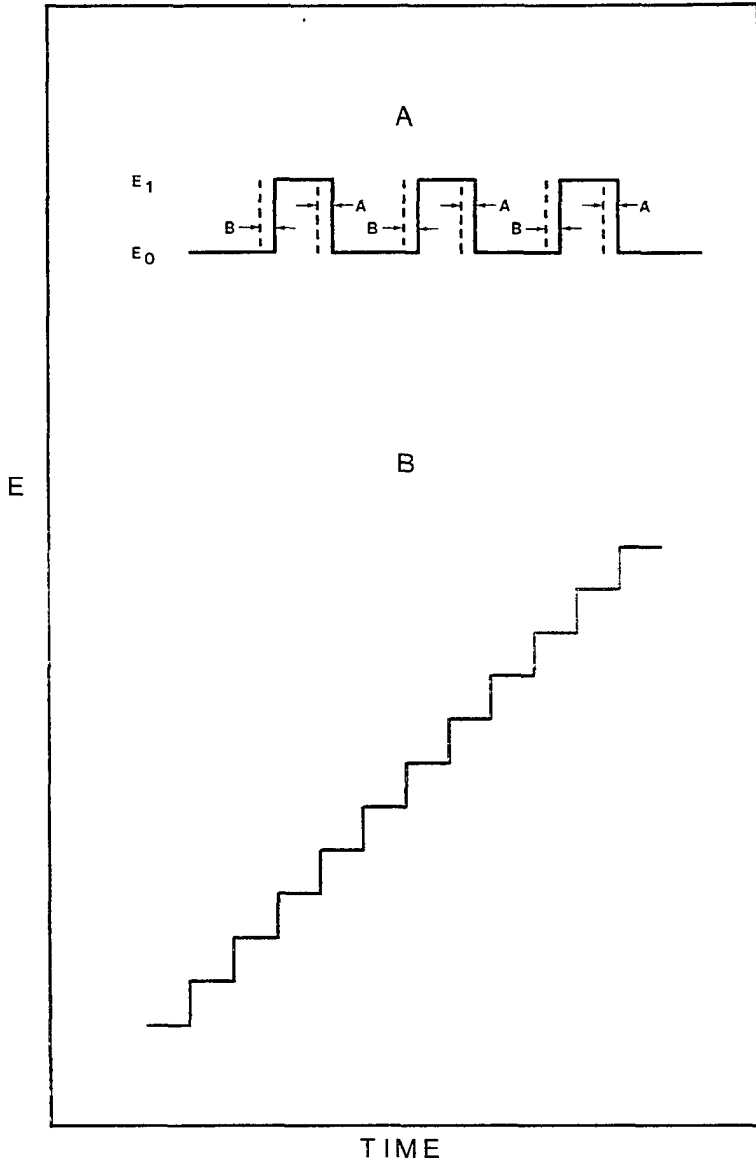
Figure 1-2. Non-DC Waveforms. A. Pulse and Differential
            Pulse. B. Staircase Voltammetry.

vals A and B are sampled, as shown for waveform A in Figure 1-2. The current difference obtained between intervals A and B roughly corresponds only to compounds whose half-wave potentials lie near the range defined by E_0 and E_1. This method can remove signals due to mobile phase impurities, pump pulsation, or any compounds with half-wave potentials significantly less than E_0 or significantly greater than E_1.

Several papers on this technique have been published. Swartzfager demonstrated the utility of the differential pulse mode in a determination of 3,4-dihydroxyphenol, which was detected in spite of the presence of the co-eluting p-aminophenol by judiciously selecting E_0 and E_1.[12] Enhanced selectivity from the differential pulse mode was also reported by the groups of Poppe and Stulik.[52,19] Once again, however, all three papers reported a significant increase in the detection limit of the differential pulse when compared to the DC mode.

Scanning pulse. In an effort to obtain more information from each chromatogram, scanning LCEC techniques were developed. Several reports have used mercury electrodes and solid electrodes for this purpose.[53-55] This technique is comparable to rapid scanning UV absorption, but the "spectra" obtained are simply voltammograms. Staircase voltammetry, shown as waveform B in Figure 1-2, for example, has been used. Once again, the current sampling period is selected to be near the end of each pulse.

One report by Wightman *et al.* merits attention because of its relatively low detection limit.[47] Using the carbon fiber array cell and a staircase waveform, they were able to record voltammograms of compounds as they eluted from the LC column. Detection limits were reportedly in the sub-nanomolar range. When lower detection limits are required, this cell can be rapidly switched to DC operation. This switch can even be accomplished in the middle of a chromatographic run.

Summary. The DC mode of LCEC exhibits the lowest detection limits. Normal pulse LCEC can be useful with strongly adsorbing compounds. Differential pulse offers considerably greater selectivity with appropriate compounds. Rapid scanning LCEC offers the greatest amount of qualitative information.

3. Single *versus* dual electrodes. A preview of the capabilities of dual electrode cells was presented in the previous coulometry section with the example of the dual coulometric cell. This section will be limited to dual amperometric thin-layer cells. Dual wall jet cells have, for obvious reasons, not been reported.

In a thin-layer cell, the two electrodes can be arranged serially, adjacent (parallel), or on opposite sides of the flow channel. Each configuration has its own inherent advantages and associated applications.

Series dual electrodes. In this configuration, the dual amperometric cell is very similar to the dual coulome-

tric cell discussed earlier. The three previously mentioned modes for the dual coulometric cell are also applicable to this cell. Due to the nature of amperometric cells, however, the collection efficiency between the electrodes is significantly less than one hundred percent. Reported collection efficiencies of dual thin-layer cells are between three and forty-two percent.[56] This wide difference in collection efficiencies exerts its greatest effect in the screen mode. In this mode, the first electrode is used to remove various interferring compounds and impurities from the effluent. An appropriate potential for this electrode would be the E_o we discussed for Figure 1-2A. The second electrode is used to detect only the compounds of interest. Because the first electrode is amperometric in nature, removal will not be complete and the second electrode will, thus, be exposed to a considerable amount of undesirable material. Although selectivity is enhanced, this cell is not as effective for this purpose as the coulometric cell. Recently, Schieffer addressed this problem by developing a dual coulometric/amperometric cell, where complete removal is made possible by the upstream coulometric electrode.[57]

The series dual cell can also be used in the redox mode. In this case, the first electrode is used to electro-generate a reactant which is then electrochemically active at the second electrode. Selectivity is enhanced in this mode. However, only compounds which are reversible under

these two applied potentials will be detected at the second electrode. Examples of this approach have been reported for the detection of thiols, disulfides, and o-sulfate derivatives of dopamine, norepinephrine, and serotonin.[58,59]

   Parallel dual electrodes. In this configuration, two electrodes are placed side by side in the flow channel. One application of this cell is conceptually similar to the differential pulse technique. E_0 and E_1 (Figure 1-2A) are the applied potentials. The difference between the resultant currents from the two electrodes emphasizes compounds whose half-wave potentials are in the neighborhood of E_0 and E_1. This general approach was used to selectively detect homovanillic acid.[56]

   Another application of the parallel dual electrode involves operation of the two electrodes at considerably different potentials. The high potential chromatogram will exhibit a larger number of compounds. This chromatogram can be used to quantitate the harder to oxidize (or reduce) compounds. The lower potential chromatogram which exhibits fewer peaks can be used to quantitate compounds with lower oxidation (or reduction) potentials under conditions which experience less noise and less interference. An example of this enhanced selectivity was demonstrated in the first report of a dual LCEC cell by Blank.[7] Although Blank used the series configuration to demonstrate this enhancement, all three configurations are appropriate to this applica-

tion.

An extension of this approach was conducted by Meyer and Shoup.[60] Using a parallel dual cell at two different potentials, they were able to provide reproducible peak height ratios for both samples and standards, while discriminating between two nearly coeluting compounds and obtaining qualitative information about unknown peaks.

Opposing dual electrodes. In this cell, the two working electrodes are located directly across the channel from one another. The potentials of the electrodes are typically selected so that oxidation of the compounds of interest will occur at one electrode and reduction will occur at the other electrode. The sum of the two signals should enhance the detectability of the compound. In order for this to occur, however, the compound must be reversible and must diffuse from one electrode to the other many times. Due to the high linear velocities of modern LC, such diffusion is highly unlikely. A possibly advantageous application of this method might be in capillary LC, where the flow rate is on the order of a few microliters per minute.

In all dual configurations, the auxiliary electrode must be located as near the two working electrodes as is physically possible. In the dual series and parallel cells, the auxiliary electrode should be located across the channel. In the case of the opposing dual electrodes, the auxiliary electrode should be located downstream in the

channel near one of the working electrodes.

Comparison. Since dual thin-layer cells use the DC thin-layer mode, all inherent advantages of this mode are retained --- namely, the low cell volume and the low detection limit. This is a rare case in LCEC in which enhancements can be obtained with no substantial loss in applications or abilities. For a thorough review of dual thin-layer electrode LCEC, the reader is referred to a recent paper by Roston.[56]

4. Conclusion. Optimum detection limits and cell volumes are currently obtained by using DC amperometric cells. In most cases, coulometric cells have larger cell volumes and higher detection limits. The dual coulometric cells have some very important selectivity advantages with a slight cell volume and detection limit penalty. Non-DC operation offers selectivity enhancements, but the penalty in detection limits is considerable. The informational gain of the rapid scanning multiple fiber cell may occasionally justify the detection limit penalty, but this is highly dependent on the application. Dual and multiple electrode cells offer a significant gain in selectivity with only minor concessions in cell volume. If selectivity enhancement is needed, dual electrodes would currently appear to be preferable to the use of the non-DC mode for most circumstancies.

CHAPTER 2

OPTIMIZATION OF THE LIQUID CHROMATOGRAPH

FOR 3 μm COLUMNS

I. Introduction

Over the past ten years, our laboratory has directed its attention to the determination of catecholamines, indoleamines and related enzymes in various mammalian tissues and fluids.[68-75] Procedures for these determinations have included a variety of cleanup steps such as extraction, centrifugation, and/or filtration. But, the primary and final process has always included separation by liquid chromatography. The detection and quantitation has been accomplished mainly by electrochemical detection. Various catecholamines, indoleamines, and related compounds along with their acronyms have been collected in Table A-1 of the Appendix as an aid for the reader.

The early procedures for these compounds incorporated anion and cation exchange columns. Due to the low efficiencies of these columns, however, separations for only two or three compounds required ten to twenty minutes per sample.[69-71] During the late 1970's, 10 μm and 5 μm reversed-phase columns began to appear as viable alternatives

to their ion exchange predecessors. Using these columns, up
to 10,000 theoretical plates could be obtained with only a
15-25 cm length, and eleven to thirteen compounds could be
separated in about eighteen to twenty minutes.[74,75]

Due to the demand for greater efficiency and shorter
analysis times, 3 μm columns were developed in the very late
1970's.[89,92,93] By 1980, Cooke and Olsen reported the use
of the 3 μm column in the reversed-phase mode.[76] In 1981, 3
μm reversed-phase columns became commercially available, and
DiCesare *et al.* became the first group to report on the use
of these columns.[77-79] Because of the small size of the 3
μm packing material, the new columns have much higher back
pressures than columns with larger packing materials.   To
avoid excessive system pressures, the new columns were pre-
pared in shorter lengths.   A 3 μm column 7.5-10 cm long is
approximately comparable in efficiency to a 15-25 cm long 5
μm column.   Although substantial increases in efficiency
cannot practically be obtained with the 3 μm column due to
pressure limitation, a decrease in analysis times is readily
achievable.   For a given separation with similar efficiency
and resolution values for all pertinent peaks, the total
analysis time required for a 3 μm column is approximately
three times less than that required for a 5 μm column.[77,80]
Thus, 3 μm LC has been called "high speed" LC by the commer-
cial manufacturers.

Due to the size of the packing material, the eluting

peaks on a 3 µm column are extremely narrow. The 4σ value, which encompasses approximately 90% of the total band area, for peaks with a capacity factor (k′, see page 62) equal to 1 and 2, respectively is only 45 µl and 67 µl.[80] Thus, Cooke *et al.* have calculated that the variance of the peak due to the entire LC system must be held below 36 µl^2 in order to keep the loss in efficiency of a rapidly eluting peak below 20%.

To realize the full potential of the 3 µm column, the LC and the detection system must both be optimized. The dead volumes associated with the LC and the detector must be minimized so that the eluting peaks do not experience excessive band broadening. The electronics of the detector must also be sufficiently fast to follow the eluting peaks without degrading the peak shapes.

Instrumental band broadening has been thoroughly investigated by practitioners of capillary LC.[81-88] Extra column dispersion is even more detrimental in capillary LC than in 3 µm LC, because of the extremely small dead volumes in capillary columns. Yet, although band broadening has been thoroughly studied and is well understood for capillary LC, these studies are not directly applicable to 3 µm LC because of the considerable size discrepancy of the hardware involved.

The investigation of extra-column effects in conventional LC has been less extensive. This is partly due to

the slower evolution of conventional size, high efficiency LC columns. In 1977, Kirkland *et al.* examined the extra-column effects of the sample injection, the inlet and outlet configurations of the column, the detector cell, the connecting tubing, and the guard column.[89] Lauer and Rozing determined the dynamic dead volume of an entire, optimized LC system and of a 4 µl UV flow cell.[90] DiCesare *et al.* demonstrated the high speed capabilities of the 3 µm column using an optimized LC with a 2.4 µl UV flow cell.[77-79] They were able to separate a five or six compound mixture in less than two minutes. Cooke *et al.* used an optimized LC system to compare 3 µm and 5 µm reversed-phase columns.[80] Scott and Simpson used a 0.44 µl conductivity detector to evaluate the extra-column dispersion of connecting tubing and injection valves. They also examined the effects of coiling the capillary connecting tubing, sintered frits, connecting unions, and flow cells.[88] Finally, Scott and Katz used a 4 x 0.4 cm i.d., 3 µm silica gel column with a 1.4 µl flow cell to resolve an eight component mixture in less than sixteen seconds.[91] Using a very rapid gradient, they were able to separate thirteen compounds in approximately twenty-two seconds, but re-equilibration of the column required five to six minutes.

In light of the expected throughput advantage of the 3 µm column, we decided to proceed to investigate the feasibility of utilizing this column for the analysis of biogenic

amines.   In this chapter, we will discuss the optimization
of the   entire liquid chromatographic   instrument for the
separation of these compounds.

II. Experimental

A. Liquid Chromatograph

The liquid chromatograph is a home-assembled apparatus
consisting of parts from various manufacturers.   The pump is
a   single piston,   reciprocating Milton Roy minipump   (model
number 13906-1) rated to deliver a maximum pressure of 5000
psi.   The sample injector is a Rheodyne loop injector (model
7010),   equipped with a 5 µl sample loop (model   70-205L).
The injector is attached to a Rheodyne model 7001 pneumatic
actuator. The pneumatic actuator is powered by one pole of a
double-pole,   triple-throw (ON-OFF-ON) switch.   The   other
pole of the switch serves as the injection signal for the
computer. A 0-5000 psi pressure gauge (Weksler Instruments)
is used to monitor the system pressure and pulsation.   To
minimize the pump pulsation, a Mark III Pulse Damper (La-
boratory Data Control model number 920251) is included be-
tween the pump and the injection port. Pulsation is further
reduced by the addition of a one meter length of thin wall,
1/4 in. o.d., stainless steel tubing.   Connection of the
column to the injector is made with a 6 cm long, 1/16 in.
o.d., 0.006 in. i.d., stainless steel tubing with both ends

deburred and polished (Stainless Steel Micropolish). A Perkin Elmer, model HS-3, 4.6 mm x 10 cm reversed-phase column (part no. 258-1501) was used exclusively for the investigations presented in this chapter. See Figure 2-1 for a diagram of the complete LCEC system.

B. Electrochemical Detector

The potentiostat was especially designed to contain a low-pass, three pole Butterworth filter with a frequency cutoff that is user selectable. This potentiostat was designed and constructed in-house. Figure 2-2 is a schematic of the unit.

Various electrochemical cells and electrode materials were evaluated. Several Plexiglas^R cells with a 1/8 in. dia. carbon paste electrode (model TL-3), three KEL-F^R cells with a 1/8 in. dia. glassy carbon electrode (model TL-5), and a special low dead volume stainless steel cell top for 3 μm columns were all obtained from BioAnalytical Systems (BAS). Three KEL-F^R cells with, respectively, 1/32 in. dia., 1/16 in. dia. and 1/8 in. dia. carbon paste electrodes were fabricated by a local machine shop. Both the 0.002 in. and 0.005 in. spacers were obtained from BAS. Ag/AgCl reference electrodes were used (BAS model RE-1) with standard reference electrode holders (BAS model RC-2A). The carbon paste employed was model CP-O, also from BAS.

A dual pen (OmniScribe^R model 5212-1) strip chart recorder was used to record all the chromatograms. The output
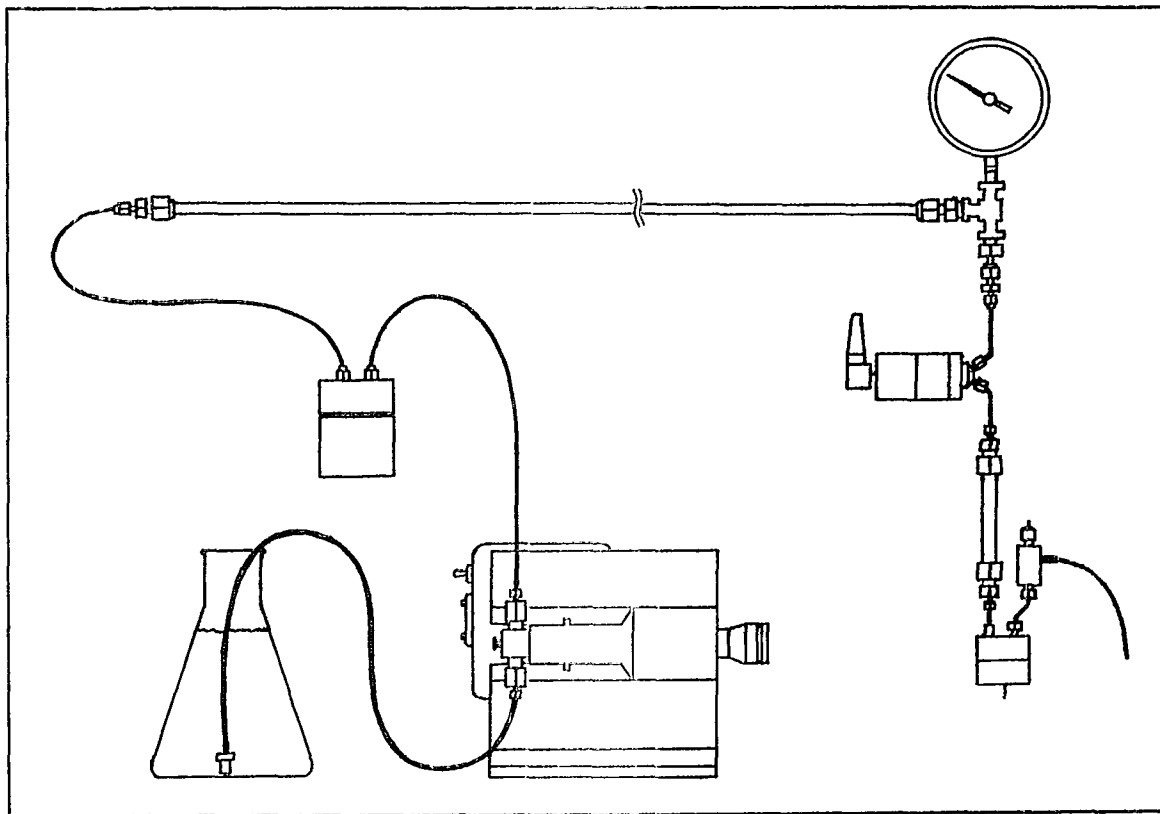
Figure 2-1. Setup for Liquid Chromatography with Electro-
chemical Detection.

Figure 2-2. Schematic Diagram of LCEC Potentiostat.

of the potentiostat was also connected to an analog-to-digital converter board, which uses a 12 bit Analog Devices (part no. ADC-12QM) analog-to-digital converter. The digital output was connected to either a Compupro or a Cromemco microcomputer for data manipulation. The data collection and analysis programs were all developed in-house by Dr. C. L. Blank.

C. Reagents and Preparations

Chemicals. The chemicals used for the preparation of the mobile phase were obtained from the following sources:

Citric acid monohydrate (Baker Analyzed Reagent) - J. T. Baker Chemical Co. (Phillipsburg, NJ)

Ethylenediaminetetraacetic acid, disodium salt (EDTA) - Aldrich Chemical Co. (Milwaukee, WI)

Octyl Sodium Sulfate (SOS) - Eastman Kodak Co. (Rochester, NY)

Sodium hydroxide pellets (NaOH) - J. T. Baker Chemical Co.

Acetonitrile (ACN) - Sigma Chemical Co. (St. Louis, MO)

Diethylamine (DEA) - Aldrich Chemical Co.

1. Mobile phase. The mobile phase used contained 0.100 M citric acid, 0.050 mM EDTA, 0.255 mM SOS, 0.060% (wt/vol) DEA, and 7.5% (vol/vol) ACN. It was titrated to a final pH of 2.55 with solid NaOH. The citric acid/NaOH combination provide adequately buffered pH control of the mobile phase. The EDTA has been noted by others to provide lower detector noise. The SOS acts as an ion pairing reagent (vida infra).

The DEA is necessary to eliminate the tailing of peaks commonly observed for amines. Finally, the ACN, used as an organic modifier, is added to provide a decrease in retention times for the individual solutes.

Filtration apparatus (all parts from Millipore Corp.). The mobile phase preparations were always filtered prior to use. The apparatus employed included [1] a 47 mm dia. (0.2 μm pore size) membrane (GVWP-0477-00), [2] a 300 ml glass funnel top (10-047-04), [3] a glass funnel base with stainless steel screen, gasket and neoprene stopper (10-047-04), and [4] an anodized aluminum spring clamp (10-047-03). The filtered solvent was collected in a 2 liter suction flask. An aspirator was connected to the apparatus to increase the rate of filtration. The volume of the 300 ml glass funnel was also increased to 1300 ml by attaching a one liter round bottom flask to the top funnel. This eliminated the frequent need to refill the 300 ml funnel.

TYPE 1 water. All water used for mobile phase preparations was obtained directly from a Milli-Q Reagent Water System (Continental Water Systems, El Paso, TX).

Preparation. The mobile phase was usually prepared in 4 liter batches. It was prepared by first dissolving approximately 1 g of NaOH in 3.70 liters of Type 1 H_2O. 74.45 mg of EDTA was added to this basic solution, in which it dissolves quite rapidly. After dissolution, 84.06 g of citric acid monohydrate and 236.92 mg of SOS were added with stir-

ring.   This mixture was filtered with the Millipore appara-
tus.   3.40 ml of DEA and 300 ml of prefiltered ACN were then
added to the filtered mixture,   and the solution was titra-
ted, with stirring, to a pH of 2.55 using solid NaOH.

2. Standards.   All   standards were obtained from   the
suppliers   at the highest purity level and used as received.
The   full   names and chemical structures for each   of   these
compounds is given in the Appendix.   From Aldrich   Chemical
Co. (Milwaukee, WS), we obtained:

DA	DHBA
DOPA	DOPAC
DOPEG	HVA
MEL	NE
MHPG	N-MET
N-Ac-5HT	5HT
3MT	

From Sigma Chemical Co. (St. Louis, MO), we obtained:

EPI	EPIN
MET	NM
TP	TYR
VMA	4MT
5HIAA	5HTOL
5HTP	

Stock   solutions.   1.0 mM solutions of each   standard
compound were prepared.   For example, a 1.0 mM solution of
DA   was   prepared by dissolving 18.96 mg of dopamine   hydro-
chloride (DA.HCl,   F.W.=189.64) in 100 ml of 1.0 mM HCl. The
1.0 mM HCl solution was prepared by adding 50 µl of   conc.
HCl   to 1.0 liter of Type 1 H_2O.   The stock solutions   were
divided   into   15 ml portions and stored   at $-90^{\circ}C$.   When
prepared   and   stored in this   manner,   the   solutions   were

usable for at least one year.   When stored at 5°C, they are only usable for about three months.

Working solutions.   The working solutions were made by diluting the stock solutions on the day of the experiment. Two different working solutions are used in this chapter. The first solution contained approximately 2.5x10^{-6} $\underline{M}$ NE dissolved in the mobile phase.   Dilution of NE with the mobile phase was especially important for these studies (*vide infra*) because this minimized the possible interference from the undesirable solvent front peak.   This solution was used solely in the columnless experiments (short circuited mode) for the determination of the experimental variance of the chromatograph.

The second solution was a mixture of four compounds with widely varying capacity factors and functional groups. They are VMA (an acid, k' = 1.7), EPI (an amine, k' = 3.4), 5HTOL (an alcohol, k' = 7.5), and 5HTP (an amino acid, k' = 11).   This solution was made on the day of the experiment by diluting the appropriate stock solutions by a factor of a thousand with 1.0 m$\underline{M}$ HCl. The final concentration of each of the four compounds was approximately 1x10^{-6} $\underline{M}$.   This solution was used to determine the efficiency of the column at various capacity factors in the normal mode experiments (*vide infra*).

D. Procedures

The main purpose of the experiments reported in this

chapter was to determine the band broadening effect of each portion of the LC. Once these effects were determined, the optimum condition for each parameter could be selected.

The determination of the band broadening is conducted by two methods. The first method utilizes a columnless LC system. For this, we will borrow the name coined by Lauer and Rozing, *i.e.*, the "short circuited mode".[90] The second method involves the system with a column, and this will be called the "normal mode".

1. <u>Short circuited mode</u>. In this mode, the detector was connected directly to the injector. To determine the experimental standard deviation, 5 µl of 2.5×10^{-6} M NE was injected. Typical LCEC operating conditions included a flow rate of 1.5 ml/min, a 0.05 s time constant, a modified cell top and a 0.002 in. spacer. Exceptions to these conditions are noted as appropriate. The resultant chromatogram was recorded by the computer, and the experimental variance and standard deviation of the peak was calculated. The experimental standard deviation determined corresponds to the band broadening due to the whole system with the exception of the column and the piece of connecting tubing used to join the column and injection port.

The system standard deviation was calculated indirectly from experimental standard deviation data. In this experiment, the experimental standard deviation was determined for various injection volumes, namely 5 µl, 20 µl, 50 µl, and

100 µl. This was accomplished by physically changing the loop of the injector to the appropriate volume. The system standard deviation was then obtained by extrapolating the results for the experimental standard deviation to an injection volume of zero. This value corresponds to the band broadening due to everything in the LC system except the injection, and the column, and the piece of tubing connecting these two items.

2. <u>Normal mode.</u> In this mode, the 3 µm column was included in the LC system. This mode was used to determine the effect of the parameter of interest on the efficiency of the column. This was accomplished by injecting 5 µl of the mixture containing 1×10^{-6} M VMA, EPI, 5HTOL and 5HTP. The LCEC conditions were typically the same as for the short circuited mode. The chromatogram was recorded by the computer. From the individual retention times and the width of the peak measured at one-half of its maximum height, the efficiency and the capacity factor for each component were calculated. Using the results for all peaks, a plot of efficiency *versus* capacity factor was constructed corresponding to the single value of the parameter investigated. This same process was repeated using different values of the parameter in question to obtain a family of plots on the same graph.

The families of plots for different parameters may be advantageously employed by practitioners of LCEC. The ear-

liest eluting peak is the most severely affected by changes in parameters (*vide infra*). Thus, knowing the capacity factor of the earliest eluting peak and *referring* to the graphs, the user can rapidly determine the expected effect on their separation by switching to either more or less optimal LCEC parameters.

E. Calculations

1. Capacity factor, k'. The capacity factor is an indication of the affinity of the solute for the stationary phase relative to the mobile phase. Solutes with smaller k' values will have less attraction to the stationary phase and, thus, will elute faster than compounds with larger k' values. By definition:

$$k' = (t_r - t_o)/t_o \qquad (2-1)$$

where t_r and t_o are, respectively, the retention times of the solute and the void volume or solvent front. See Figure 2-3. The capacity factor can also be calculated from the retention volumes. V_r and V_o are substituted for t_r and t_o in equation 2-1, where V_r is the retention volume of the solute and V_o is the void volume.

2. Efficiency, N. Efficiency, or the number of theoretical plates, is a measure of band broadening due to the LC column. If one has two columns that exhibit identical retention times for a given solute, the column that elutes
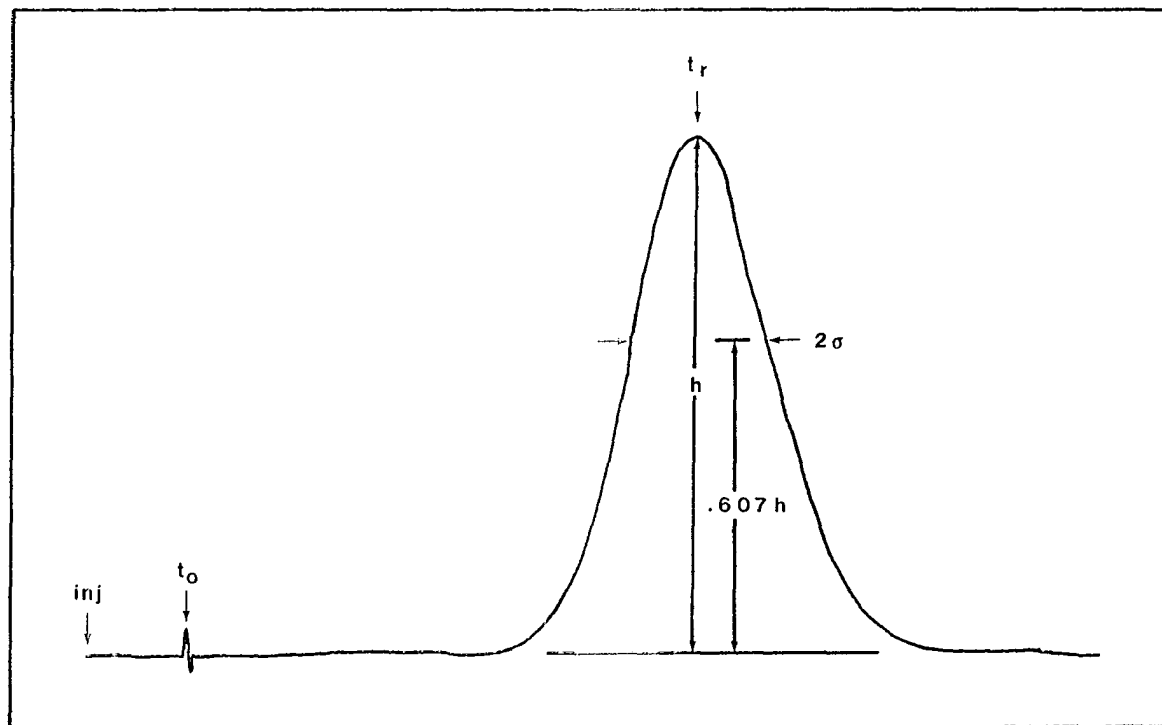
Figure 2-3. Chromatographic Peak Parameters.

the solute in a narrower band is the one with a higher efficiency. Efficiency is defined as:

$$N = (t_r/\sigma_t)^2 \qquad\qquad (2-2)$$

where t_r is the retention time and σ_t is one-half of the width of the peak measured at 60.7% of the maximum peak height, as shown in Figure 2-3.

There are actually several ways to determine σ_t. The most accurate way is *via* the statistical moment method.[89,94] In theory, the normalized n^{th} moment of the peak, m_n, is given by:

$$m_n = [\int t^n f(t)dt]/[\int f(t)dt] \qquad\qquad (2-3)$$

where t is the instantaneous time, f(t) is the instantaneous peak height at time t, and the integrations are performed for all values of t.

The zeroth moment of a peak is its area. The first moment defines the location or the center of gravity of the peak. If the peak is symmetrical, the first moment is equal to the retention time of the peak. The second moment is a measure, with respect to the first moment, of the broadness of the peak. The third moment, also calculated with respect to the first moment, is a measure of the symmetry of the peak. Normally, all the higher moments (n greater than one) are calculated with respect to the first moment.

In practice, the integrations are easily handled by a

computer. The calculation of the second moment, or the variance of the peak, can be performed with the following equation:

$$\sigma_t{}^2 = [(\Sigma_i h_i t_i{}^2)/\Sigma_i h_i] - [(\Sigma h_i t_i)/\Sigma h_i]^2 \qquad (2-4)$$

where t_i is the instantaneous time and h_i is the instantaneous peak height at t_i. All calculations based on the statistical moment method in the current investigation employed equation 2-4. The main advantage to this approach is that it yields values for σ_t which are not sensitive to the shape of the peak. In another words, it can be used to characterize a square peak, a skewed peak, or a Gaussian peak equally well. The major disadvantage of this method is that it is particularly sensitive to the assignment of the position of the baseline as well as the baseline noise.[80,94]

Another method for the estimation of σ_t is particularly useful if a computer is unavailable and the peak is Gaussian. In this approach, σ_t is calculated by physically measuring the width of the peak at half-height, $W_{1/2}$.

$$\sigma_t = W_{1/2}/[8(\ln 2)]^{1/2} \qquad (2-5)$$

Substituting the expression for σ_t from 2-5 into equation 2-2 yields:

$$N = 5.54(t_r/W_{1/2})^2 \qquad (2-6)$$

Equation 2-6 is strictly applicable only to Gaussian peaks.

Application of this equation to a moderately tailing peak, *e.g.*, one with a skew of 1.43, can lead to an overestimation of the efficiency by more than one hundred percent.[89] Since the solute peaks in the current study are all fairly symmetrical, equation 2-6 could be reasonably used as an alternative method to calculate the efficiency when operating in the normal mode.

3. Experimental and System Standard Deviations. A useful way to establish the effective dead volume of an LC is to measure the standard deviation of the system, σ_{sys}. The total variance of the observed output is generally given as the sum of variances of the individual components of the system.

$$\sigma_{exp}^2 = \sigma_{col}^2 + \sigma_{inj}^2 + \sigma_{sys}^2 \qquad (2-7)$$

where σ_{exp}^2 is the observed variance of the output signal and σ_{col}^2, σ_{inj}^2 and σ_{sys}^2 are the variances due to the column, the injection, and the rest of the system, respectively. In the short circuited mode, the column was eliminated and the detector cell was connected directly to the injector. Thus, σ_{col}^2 is zero, and equation 2-7 reduces to:

$$\sigma_{exp}^2 = \sigma_{inj}^2 + \sigma_{sys}^2 \qquad (2-8)$$

Sternberg has theoretically determined the effect of input peak shape on σ_{inj}^2.[95] He has shown that the volume vari-

ance, $\sigma_{v(inj)}{}^2$, of a rectangular input peak is $V_{inj}{}^2/12$ and for a Gaussian input peak is $V_{inj}{}^2/2\pi$, where V_{inj} is the injection volume. Simply, substituting a constant, C, for the denominator portion of these expressions for $\sigma_{inj}{}^2$ and rewriting the variances in equation 2-8 in units of volume yields:

$$\sigma_{v,exp}{}^2 = (V_{inj}{}^2/C^2) + \sigma_{v,sys}{}^2 \qquad (2-9)$$

More recently, Lauer and Rozing have reported that the variances of the individual components of an LC are not mutually independent as the above approach implies.[90] Indeed, their data suggest an interdependence of the system variance and the input variance. Thus, they proposed the following:

$$\sigma_{v,exp} = (V_{inj}/C) + \sigma_{v,sys} \qquad (2-10)$$

$$\sigma_{v,exp}{}^2 = (V_{inj}{}^2/C^2) + (2\sigma_{v,sys}V_{inj}/C) + \sigma_{v,sys}{}^2 \qquad (2-11)$$

From equation 2-10, it can be seen that a plot of $\sigma_{v,exp}$ versus V_{inj} should yield a slope of 1/C and a y-intercept of $\sigma_{v,sys}$. Finally, the volume experimental standard deviation can be readily calculated from the time experimental standard deviation derived from equation 2-4 in combination with the mobile phase flow rate U (ml/min):

$$\sigma_{v,exp} = \sigma_t \times U \qquad (2-12)$$

This equation was exclusively used in the current investiga-
tion to calculate the volume experimental standard deviation
for the short circuited mode.

III. Results and Discussion

A.   Optimization of the Liquid Chromatograph

LC systems in this laboratory have been optimized in
the past for 5 μm columns.[73,75] Due to the relatively large
particle size, an injection volume in the range of 20-200 μl
was quite easily tolerated for these systems.   Also, 1/16
in. o.d., 0.010 in. i.d. stainless steel tubing was used
throughout the system with no significant effect on perfor-
mance.   Substitution of a 3 μm column directly into one of
these LC systems, however, would almost completely obscure
the full potential of the 3 μm column.

1.   Injector.   DiCesare *et al.* have recently reported
that 3 μm columns can only withstand injection volumes less
than or equal to 7 μl before substantial band broadening
effects are encountered.[77] The Rheodyne 7010 loop injector
is sold with a standard 20 μl loop.   Thus, this had to be
remedied by replacing the 20 μl loop with the commercially
available Rheodyne 5 μl loop.

2.   System volume. System dead volume is another para-
meter that must be minimized in the 3 μm LC. In reality, the
volumes in only two places are important.   The first is the
volume between the outlet of the injector and the inlet of

the column.   The second is the volume between the outlet of
the column and the inlet of the detector.   The volumes of
components preceding the injection port or following the
detector in the flow path of the system are totally irrele-
vant.

The volume between the injector and the column is
minimized by using a connecting tube with a practical mini-
mum length and inner diameter.   The selected tubing was 6 cm
long and 0.006 in. i.d.   Both ends were deburred and micro-
polished to minimize turbulent flow.   The total volume of
this tubing is 1.09 µl.   When compared to an equivalent
length of a 0.010 in.   i.d. tubing, which has a total volume
of 3.04 µl, this substitution offers a dead volume reduction
of about threefold.

Short circuited mode.   To determine the system standard
deviation of the LC, the detector cell was connected di-
rectly to the injector.   Four different injection volumes
and two different flow rates were investigated.   Time exper-
imental standard deviations, $\sigma_{t,exp}$, were determined for 5
µl, 20 µl, 50 µl and 100 µl at flow rates of both 1.5 ml/min
and 2.0 ml/min.   The modified, low dead volume detector cell
(vide infra) was also employed for these experiments.   Vol-
ume standard deviations were calculated by multiplying the
time standard deviations by the appropriate flow rate.   The
experimental results are presented in Table 2-1.

A graphical representation of this data was then used

TABLE 2-1.   EXPERIMENTAL STANDARD DEVIATION AND VARIANCE
OF SHORT CIRCUITED LC SYSTEM

Injection Volume		Standard Deviation and Variance		
		$\sigma_{t,exp}$(min)	$\sigma_{v,exp}$(µl)	$\sigma_{v,exp}^2$(µl^2)
1.5 ml/min				
5 µl	($\bar{x}$)	0.003638	5.457	29.78
	(s.d.)	0.000137	0.206	
	(n)	7	7	
20 µl	($\bar{x}$)	0.01133	17.00	289.0
	(s.d.)	0.00098	1.47	
	(n)	7	7	
50 µl	($\bar{x}$)	0.02234	33.51	1123.
	(s.d.)	0.00029	0.43	
	(n)	7	7	
100 µl	($\bar{x}$)	0.03864	57.95	3359.
	(s.d.)	0.00032	4.80	
	(n)	8	8	
2.0 ml/min				
5 µl	($\bar{x}$)	0.003438	6.876	47.29
	(s.d.)	0.00529	1.058	
	(n)	8	8	
20 µl	($\bar{x}$)	0.008659	17.32	299.9
	(s.d.)	0.000827	1.65	
	(n)	8	8	
50 µl	($\bar{x}$)	0.01715	34.29	1176.
	(s.d.)	0.00108	2.15	
	(n)	9	8	
100 µl	($\bar{x}$)	0.02938	58.75	3452.
	(s.d.)	0.00075	1.49	
	(n)	8	8	

to determine the value for $\sigma_{v,sys}$, as shown in Figure 2-4. According to equation 2-10, a plot of $\sigma_{v,exp}$ *versus* V_{inj} should yield the $\sigma_{v,sys}$ as the y-intercept. Using this approach, values of 2.41 µl and 3.73 µl are obtained for the system standard deviation at 1.5 ml/min and 2.0 ml/min, respectively.

Since the approach of Lauer and Rozing indicates a linear relationship between the experimental standard deviation and the injection volume, a second obvious approach is to apply a least squares fit to the experimental results. The linear least squares method is readily obtained from a statistics textbook.[96] The results of this approach are presented in Table 2-2. The calculated lines produced y-intercept values of 4.781 µl and 5.717 µl for the 1.5 ml/min and 2.0 ml/min cases, respectively.

The correlation coefficient, r, obtained from a regression analysis is a statistical parameter which measures the goodness of fit between the data points and the calculated function. A correlation coefficient of +1 or -1 denotes a perfect fit while a correlation coefficient of 0 denotes an absence of a fit. The correlation coefficients obtained from the linear least squares fit are 0.996860 and 0.997911. Although these values may appear to indicate a good fit, in fact they denote only a moderate fit.

Since the linear least squares fitted values are only moderately good, and since they do not agree too well with
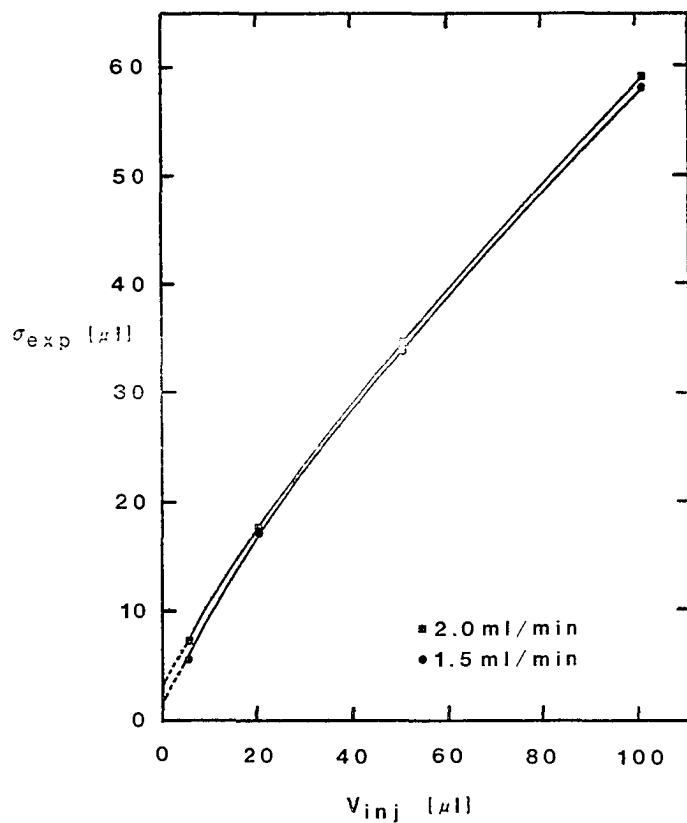
Figure 2-4. Effect of Injection Volume on the
Experimental Standard Deviation.

TABLE 2-2.   LINEAR AND NONLINEAR LEAST SQUARES REGRESSION
             TO DETERMINE THE SYSTEM STANDARD DEVIATION

Linear Regression

1.5 ml/min			2.0 ml/min		
X	Y_{exp}	Y_{cal}	X	Y_{exp}	Y_{cal}
5	5.457	7.490	5	6.876	8.413
20	17.00	15.61	20	17.32	16.50
50	33.51	31.86	50	34.29	32.68
100	57.95	58.95	100	58.75	59.64

Slope=0.5417   Slope=0.5393
Y-intercept=4.781   Y-intercept=5.717
Corr. Coef.=0.996860   Corr. Coef.=0.997911

Second Order Regression

1.5 ml/min			2.0 ml/min		
X	Y_{exp}	Y_{cal}	X	Y_{exp}	Y_{cal}
5	5.457	6.015	5	6.876	7.133
20	17.00	16.04	20	17.32	16.86
50	33.51	34.02	50	34.29	34.53
100	57.95	57.86	100	58.75	58.71

Fitted Function: Fitted Function:
 $Y=-.001533X^2+.7067X+2.52$ $Y=-.001321X^2+.6816X+3.76$
Y-intercept=2.519   Y-intercept=3.759
Corr. Coef.=0.999523   Corr. Coef.=0.999890

the results of the graphical approach, a nonlinear regres-
sion was used in an attempt to improve the results. To cor-
rectly apply nonlinear regression, one should select a func-
tion that best describes the data. Since we have no idea
what such a nonlinear function would be for this data, we
employed the simplest nonlinear function, *i.e.*, a second
order polynomial.

$$Y = aX^2 + bX + c \qquad (2-13)$$

A complete description of the nonlinear method can be found
in reference 96.

The results of applying the second order regression to
the present data are also given in Table 2-2. The correla-
tion coefficient for the regressions are 0.999523 and
0.999890 for flow rates of 1.5 ml/min and 2.0 ml/min, re-
spectively. These correlation coefficients denote adequate
fits. The resultant calculated values for the system stan-
dard deviation are 2.519 µl and 3.759 µl for the 1.5 ml/min
and 2.0 ml/min cases, respectively.

A cursory examination of the experimental values (Y_{exp})
and the calculated values (Y_{cal}) strongly suggest that the
second order fit is better than the first order fit. This
suggestion is affirmed by a comparison of the correlation
coefficients.

The results for the determination of $\sigma_{v,sys}$ by the
three methods are summarized in Table 2-3. Taking into

TABLE 2-3.   SYSTEM STANDARD DEVIATION OBTAINED
            BY DIFFERENT METHODS

Technique Used	$\sigma_{v,sys}$	
	1.5 ml/min	2.0 ml/min
Graphical Method	2.41 µl	3.73 µl
Linear Least Squares Regression	4.781 µl	5.717 µl
Second Order Regression	2.519 µl	3.759 µl

account the poor fit of the linear least squares approach and the relatively good agreement between the graphical and second order regression approaches, one can conclude that the system standard deviation for 1.5 ml/min is approximately 2.5 µl, and, for 2.0 ml/min, it is approximately 3.8 µl.

As previously mentioned, Cooke *et al.* have calculated that the system variance for a 3 µm column must be less than 36 µl^2, or the system standard deviation must be less than 6 µl, in order to keep the loss in efficiency below 20% for a peak with k' = 1.[80] The current results indicate that this criteria is easily met regardless of the theoretical approach employed. Since all the peaks we want to determine (c.f. Chap. 3) have k' values greater than 1.0, the current system will clearly not cause excessive band broadening to any of these peaks.

In Figure 2-5, the experimental variances $(\sigma_{v,exp}^2)$ were plotted *versus* the injection volume. The result is very similar to the plots reported by both Kirkland *et al.* and Lauer and Rozing.[89,90] This further suggests that the current system is operating in a manner that is similar to other optimized LC systems.

The system standard deviations obtained from the current work can also be compared with the results of other publications. This comparison, presented in Table 2-4, clearly indicates that the current system has been accepta-
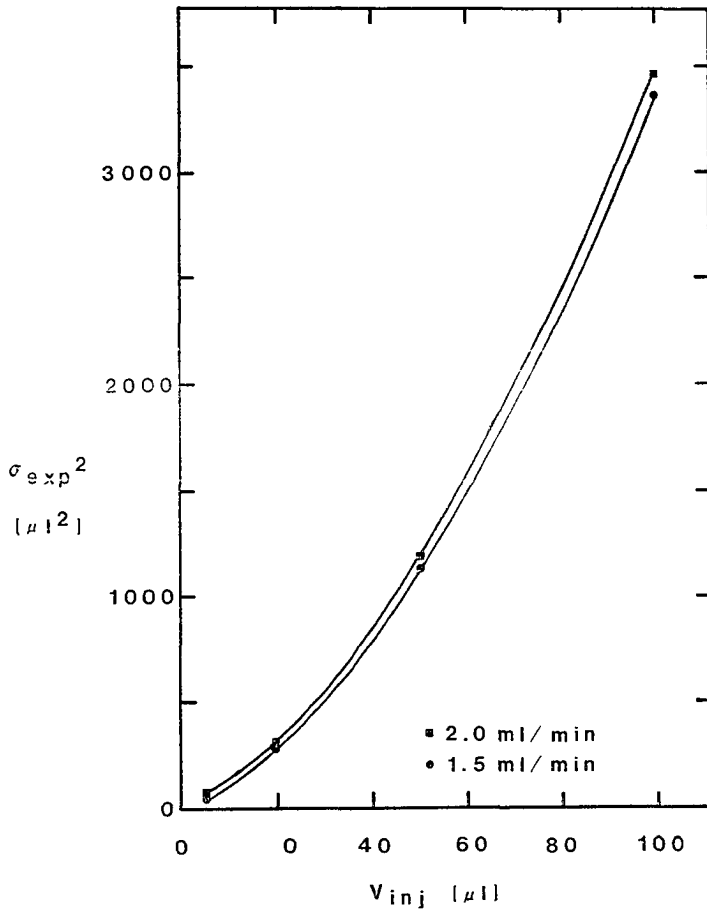
Figure 2-5. Effect of Injection Volume on the
Experimental Variance.

TABLE 2-4. COMPARISON OF REPORTED SYSTEM STANDARD
            DEVIATION VALUES

Reference	Calculated Volumes (μl)		V_{inj} (μl)	U (ml/min)	$\sigma_{V,sys}$ (μl)
	Cell	Tubing			
Kirkland	3.2	7	6.7	0.5	7.1
et al.(ref.89)	3.2	7	6.7	2.0	14.
Lauer and Rozing(ref.90)	4	---	6.5	0.54	6.5
DiCesare	2.4		6	0.5	8.0 *
et al.(ref.78)	8		6	0.5	18. *
Cooke	5	4	5	2.0	4.9
et al.(ref.80)	5	4	5	4.0	7.0
This Work	2.2	1.1	5	1.5	2.5
	2.2	1.1	5	2.0	3.9

* Values reported may be experimental standard
deviation instead of system standard deviation.
These were not clearly distinguished in the article.

bly optimized. The system standard deviation of the current system is the lowest of all the reported results. Since the other results were obtained using UV detection, however, a direct comparison may be inappropriate. Nonetheless, the work of Cooke *et al.* utilized conditions most similar to those of the current report.[80] The only major exception was in their use of a cell with a larger cell volume. And, the resultant, slightly higher system standard deviation they obtained, thus, correlates quite well with our work.

3. Pump pulsation. A major weakness of the current LC system is the pump. Single piston reciprocating pumps are well noted for their noisy flow profiles. The pulsation, fortunately, does not substantially affect the separation process within the LC column. But, it is bothersome when the detection system is flow sensitive. In such systems, the pulsation increases the noise level of the baseline and, thus, increases the limit of detection. Electrochemical detectors are definitely flow sensitive, and, therefore, they are affected by pulsation.

If the frequency of the desired output signal is signi- ficantly different from that of the noise, an electronic filter can be incorporated into the detector circuitry to remove the noise. This approach has been frequently used by our laboratory in the past. With a larger packing material, such as that in the 5 µm RPLC columns, the peak widths, measured at the base of the peak, can range from approxi—

mately fifteen seconds to several minutes.[73,75] The Milton Roy minipump cycle is approximately two seconds. Thus, the signal frequency is much lower than the pump frequency. In such cases, we have been successful in eliminating the flow pulsation from the output signal by adding a low pass filter to the potentiostat of the electrochemical detector. A low pass filter is simply an electronic circuit that allows signals with frequencies lower than the chosen cutoff frequency to pass unaltered, and it attenuates or completely eliminates signals with frequencies that are higher than the cutoff frequency. The cutoff frequency is selected by the circuit designer. By choosing the cutoff frequency of the low pass filter to be a value that is between the frequency of the desired signal(s) and the frequency of the pump, one makes the detector insensitive to pump pulsations. Although this does not actually eliminate the pulsation, the final output is free of pulsation effects.

While this signal conditioning method is very effective for 5 μm columns, it is not directly applicable to 3 μm columns. In this case, the signal frequencies, unfortunately, overlap the frequency of the noise. The band width ($4\sigma_v$) of a compound with k′=1 is about 45 μl at a flow rate of 2.0 ml/min. This translates to a band width in time units of about 1.35 seconds. Since the frequency of this peak is even higher than the noise frequency (0.74 Hz *versus* 0.5 Hz), any straightforward attempt to filter out the noise

will completely eliminate the signal. Thus, the only remaining alternative is to physically remove the pulsation. An obvious way to remove the pulsation is to install a pulse-free pump. Since this alternative is not practically available, we have to resort to the best possible form of mechanical pulse dampening. A number of devices were, thus, evaluated for their potential effectiveness in reducing pulsation.

Before these devices were evaluated, the noise level of a system without dampening had to be established. This was accomplished by connecting the pump with a piece a stainless steel tubing directly to the injector with no additional devices between these two units. The remainder of the LC was left intact. The pump was set at 1.5 ml/min, and the peak-to-peak noise level was recorded. The results are tabulated in Table 2-5, while samples of the noise are shown in Figure 2-6.

The first device investigated was one which is not commonly associated with pulse dampening: a pressure gauge. The active element of most LC pressure gauges is a Bourdon tube. This tube changes its physical shape as a function of the pressure within the tube. Dampening is provided since the Bourdon tube absorbs part of the energy during the discharge stroke of the pump and releases it during the intake stroke.[97] An electrochemical detector and a flow rate of 1.5 ml/min were used to determine the noise level.

TABLE 2-5. EFFECT OF VARIOUS DAMPING DEVICES
ON SYSTEM PULSATION AND NOISE

Dampening Device	System Pressure (psi)	Pressure Fluctuation (psi)	Peak-to-Peak Noise (pA)
A. None			120.9 ± 0.5
B. Pressure Gauge	2150-3240	1090	39.7 ± 0.7
C. Pressure Gauge and MARK III Pulse Damper	2500-3000	500	18.9 ± 0.7
D. Pressure Gauge, MARK III Pulse Damper, and 1 m of 1/4 in. o.d. Stainless Steel Tubing	2650-2680	30	11.6 ± 0.5
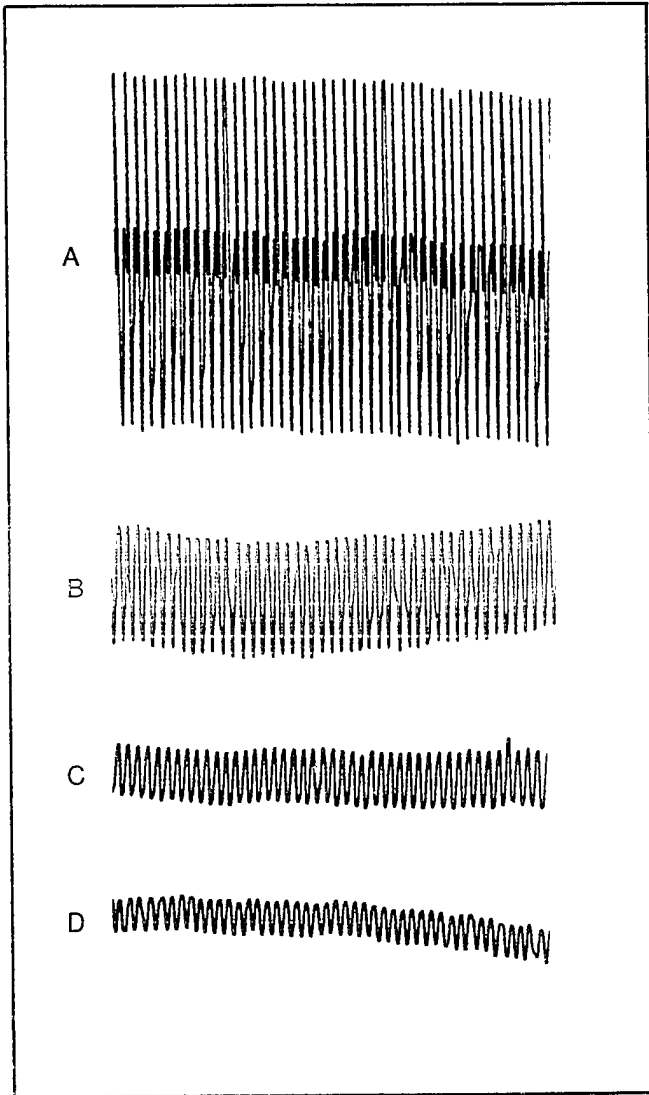
Figure 2-6.   Detector Noise Associated with Various Damping
                Devices.   [See Table 2-5 for conditions A-D].

The noise of the baseline was reduced from 120.9 pA without the pressure gauge to 39.7 pA with it. This represents a threefold reduction.

The next item tested was a commercial device, a Mark III Pulse Damper. Inserted between the pump and the pressure gauge, this device decreased the noise level and overall pressure fluctuation to 18.9 pA and 500 psi, respectively. This is equivalent to a twofold reduction from the previous noise level and a sixfold decrease from the original level.

The final stage of pulsation reduction was achieved by inserting a one meter long piece of 1/4 in. o.d., thin wall, stainless steel tubing between the pump and the Mark III Pulse Damper. This final system, which contained all three devices, yielded a noise level of 11.6 pA and a pressure fluctuation of only 30 psi. The final noise level represents more than a tenfold reduction from the original damperless system.

The amount of dampening that is practically needed is dependent on the detection limit required by the experiment. If the experiment requires only high detection limits such as those typically accessible with a 100 nA full scale output setting, then no damping is needed. The 120 pA of noise will only represent 0.12% of the total signal. On the other hand, if the experiment requires low detection limits such as these which would be obtained with the 1 nA setting,

then all three of the devices mentioned above are essential.

B. Optimization of the Potentiostat

Optimization of the detection system is just as criti-
cal as the optimization of the remainder of the system for 3
μm columns. Using a detector that was designed for 5 μm
columns with a 3 μm setup is comparable to playing a stereo
record with a monaural turntable. In the case of the re-
cord, the inherently dual nature of the information is never
revealed. In the case of the LC, on the other hand, the
full inherent separation potential of the 3 μm column is
never observed. To realize the full potential of the 3 μm
column, the electronics of the potentiostat must be fast
enough to follow the extremely narrow peaks without introdu-
cing significant attenuation. This also implies that the
detector dead volume must be small enough to avoid causing
any broadening of the peaks.

1. Time Constant. One of the most important parame-
ters of the potentiostat to optimize is the response time.
Most potentiostats contain low pass filters to prevent in-
terference from high frequency noise, such as the 60 Hz
noise derived from the line voltage, and to prevent the
operational amplifiers of the units from experiencing oscil-
lation. The cutoff frequency is the reciprocal of the time
constant for the filter. For example, a filter with a 0.5
Hz cutoff frequency is exactly the same as a filter with a
2.0 second time constant. A potentiostat designed for

columns containing 5 μm and larger packing materials will typically have a range of time constants between 0.2 and 5.0 seconds.

Normal mode. To determine the effects of various time constants on the peaks obtained from a 3 μm column, the potentiostat was modified so that the time constant could be changed to 0.05 s, 0.10 s, 0.25 s, or 0.50 s. Four determinations were made for each time constant. The results, presented in Table 2-6, reveal that, for any given compound, the width of the peaks at half-height increases as the time constant increases. Statistically, there is no difference for any of the peaks between the widths of the 0.05 s and 0.10 s time constants, while both the 0.25 s and 0.50 s results are different from the lower time constants and from each other.

To more easily determine the effects of the time constant on efficiency, a plot of efficiency *versus* capacity factor was constructed. As Figure 2-7 demonstrates, compounds with a smaller k′ are more susceptible to time constant changes than compounds with a larger k′. This trend is exactly as expected. When the width of the peaks becomes comparable to or smaller than the time constant of the filter, the peak shape becomes attenuated by the filter. If the peak width is sufficiently smaller than the time constant, it will be greatly attenuated or even eliminated by the filter. Since compounds with a smaller k′ are generally

TABLE 2-6. EFFECT OF DETECTOR TIME CONSTANT ON PEAK WIDTH
         AT HALF-HEIGHT AND EFFICIENCY

Compound*		$W_{1/2}$(min.)			
		0.05s	0.10s	0.25s	0.50s
VMA	$(\bar{x})$	0.02183	0.02217	0.02300	0.02675
	(s.d.)	0.00043	0.00043	0	0.00032
	(n)	4	4	3	4
EPI	$(\bar{x})$	0.03217	0.03259	0.03317	0.03650
	(s.d.)	0.00019	0.00042	0.00019	0.00058
	(n)	4	4	4	4
5HTOL	$(\bar{x})$	0.05742	0.05767	0.05850	0.06084
	(s.d.)	0.00032	0	0.00020	0.00019
	(n)	4	3	4	4
5HTP	$(\bar{x})$	0.08359	0.08367	0.08433	0.08658
	(s.d.)	0.00092	0.00027	0	0.00032
	(n)	4	4	4	4

		N			
		0.05s	0.10s	0.25s	0.50s
VMA	$(\bar{x})$	6528	6350	5891	4407
	(s.d.)	57	236	5	105
	(n)	4	4	3	4
EPI	$(\bar{x})$	8095	7911	7633	6371
	(s.d.)	92	212	88	192
	(n)	4	4	4	4
5HTOL	$(\bar{x})$	9420	9366	9104	8498
	(s.d.)	91	19	66	47
	(n)	4	4	4	4
5HTP	$(\bar{x})$	8842	8857	8746	8402
	(s.d.)	192	58	27	70
	(n)	4	4	4	4

* Capacity factors for compounds are: VMA-1.693,
  EPI-3.412, 5HTOL-7.479, and 5HTP-10.93.
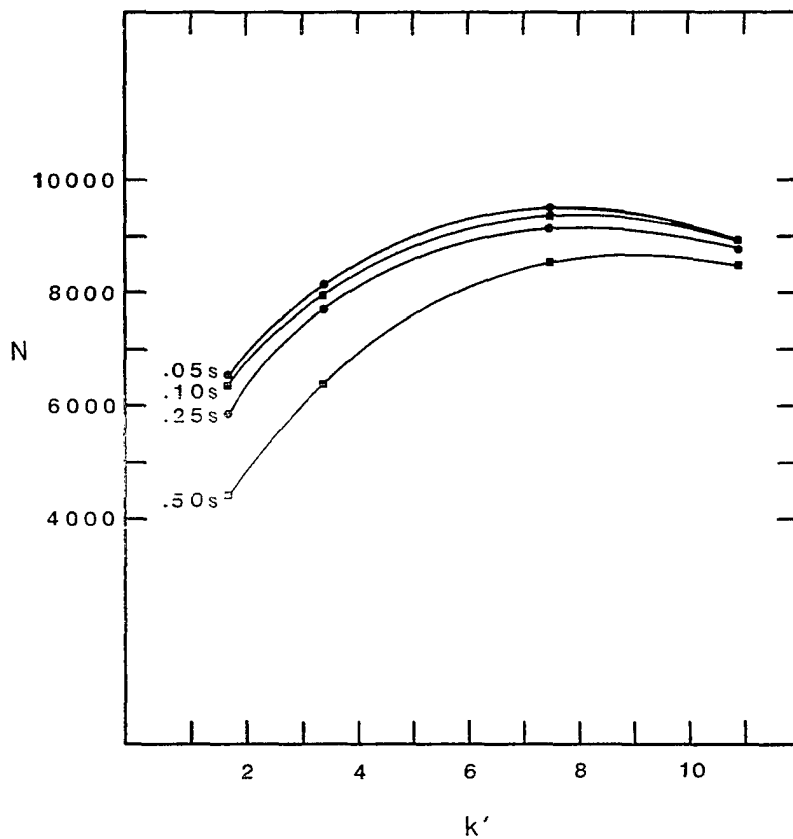
Figure 2-7. Effect of Detector Time Constant on the
Efficiency for Various Solutes.

eluted as narrower peaks than compounds with a larger k′, the smaller k′ compounds are always more likely to be attenuated. For example, VMA, a compound with a k′ of 1.7, loses about six hundred theoretical plates when it is detected with a 0.25 s time constant instead of a 0.05 s time constant, while 5HTOL, a compound with k′ equal to 7.5, can withstand a time constant of ca. 0.50 s before it experiences a comparable loss in efficiency. Note that for large k′ values, such as for 5HTP (k′=11), the peak width is so inherently large that essentially none of the tested filters cause substantial attenuation. This lack of effect on peaks with high k′ values explains why the curves for the four different time constants converge at high k′ values. This plot can be used to guide one in the selection of an appropriate time constant for a particular separation on a 3 μm column. Once the k′ of the earliest desired peak is determined, a quick look at the curves will reveal the largest time constant which will not reduce the efficiency of the peak at that k′ below the acceptable level. The largest possible time constant is chosen, since it will be most effective in rejecting noise. For example, if the earliest peak elutes with a k′ equal to 3, then a time constant of 0.25 s will probably be sufficient. On the other hand, if the earliest peak elutes with a k′ equal to 1.5, then a time constant of 0.10 s would be needed.

C. Optimization of the Detector Cell

The detector cell is considered by some to be the single most important part of the entire electrochemical detector. Thus, great care should be exercised in determining the optimum cell for utilization with 3 μm columns. The performance of the cell is highly dependent on its internal volume, the spacer thickness, the type of electrode material and the area of the working electrode. Each of the above parameters is individually evaluated to determine the optimum condition.

1. <u>Cell volume</u>. The internal volume of the cell is particularly important because it may contribute directly to band broadening. The actual flow pattern of the cell will determine which portion of the entire volume will contribute to band broadening. Sternberg has shown that, in general, if either total mixing or turbulent flow occur within a detector cell, the variance of the detector, $\sigma_{v,det}^2$, is equal to the square of the cell volume, V_c^2.[22] Since turbulent flow only occurs at very high flow rates, and such high flow rates are seldom used in LC, this result can be used as an upper limit for $\sigma_{v,det}^2$. This leads to:

$$\sigma_{v,det}^2 \leq V_c^2 \qquad (2\text{-}14)$$

Kirkland et al. have further suggested that, in practice, if the volume of the detector is less than one-tenth of the volume of the peak of interest, then detector band broa-

dening will be insignificant.[89] Using these reports as a guideline, we proceeded to determine the volume of a typical electrochemical cell (BAS TL-3). A drawing of this unit is presented in Figure 2-8. There are three regions which combine to form the total cell volume. These are the volumes of the tubing connecting the cell to the column, the detector inlet volume located within the top half of the cell, and the volume of the flow channel in the cell formed by the cutout portion of the teflon spacer. The typical connecting tubing used with the manufacturer supplied units is a six inch long piece of 1/16 in. o.d., 0.02 in. i.d. teflon tubing (BAS part no. CCT-1). A simple calculation reveals that the total volume of this tubing is 30.89 µl. Even if the length was decreased to a practical limit of 6 cm, this volume would still be 12.16 µl. The volume of the inlet in the top of the cell is 1/32 in. i.d. and 1/8 in. long. This translates into a volume of 1.57 µl. The shape of the flow channel is basically rectangular with half circles on each end. The channel is 0.625 in. long including the rounded ends and 0.185 in. wide. Since the electrode is in the middle, lengthwise, of this channel, only the regions preceding and directly above the electrode, as shown in Figure 2-8 are included in the calculation of the dead volume. Two different spacers are normally used. One has a thickness of 0.005 in. (BAS part no. TG-5M), and the other has a thickness of 0.002 in. (BAS part no. TG-2M).
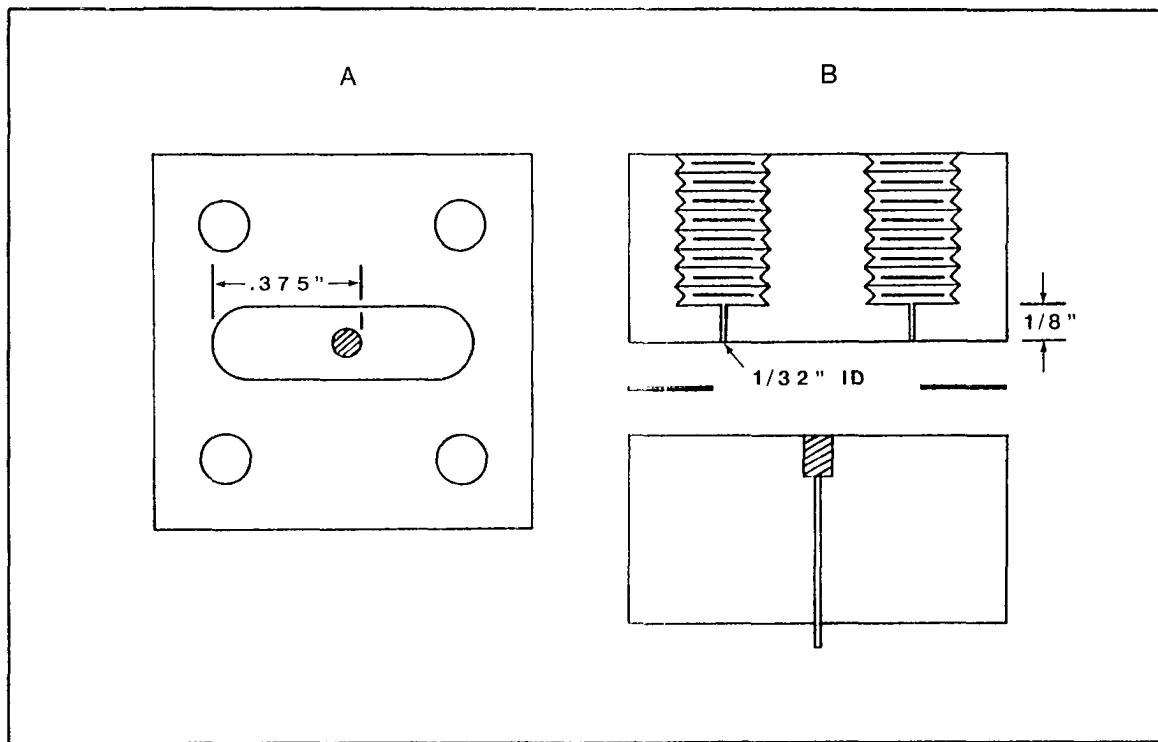
Figure 2-8.   BAS TL-3 Electrochemical Cell.   A. Top view of
              spacer and cell bottom.   B. Cross-sectional side
              view of the entire cell.

The volume of the flow channel is, thus, 5.38 µl and 2.15 µl for the 0.005 in. and 0.002 in. spacers, respectively. For the best case with this standard cell, in which a 6 cm long tubing and 0.002 in. spacer are used, the total volume of the cell is 15.88 µl. The worst case, when a 6 in. piece of tubing and a 0.005 in. spacer are used, results in a total cell volume of 37.85 µl. The calculations of these cell volumes, notably, assumes that the points of connection between the tubing and the column, as well as between the tubing and the cell, are perfect abutments. If this is not true, and it very seldom is in practice, the calculated volumes are even higher.

If the first peak of interest has a k' of 1, then the peak volume is approximately 45 µl. According to Kirkland's guideline, a suitable cell for the detection of this peak should have a total cell volume less than 4.5 µl. No confi-guration for this cell can meet this requirement. The best case has a cell volume that is about four times too large, and the worst case has a cell volume that is about eight times too large.

Since this cell was deemed to be unsatisfactory, and no other commercial cell could be found which did meet this requirement, we undertook a modification of the cell to reduce the volume. An examination of the previous cell reveals that two regions of the cell are particularly suita-ble for volume reduction. These regions are the connecting

tube and the inlet of the top.   The 0.020 in. i.d. teflon tubing can easily be replaced by a piece of 0.006 in. i.d., 1/16 in. o.d., stainless steel tubing.   The cell inlet volume, and the fitting between the tubing and the cell, can be completely eliminated by enlarging the inlet to 1/16 in. i.d. and inserting the connecting tube through the inlet so that its end is flush with the inner surface of the top. See Figure 2-9 for a detailed drawing of the final modified cell top.

The modification described is quite simple to produce, requiring approximately three hours. The inlet of the top is first enlarged by carefully drilling through it with a 1/16 in. drill bit. A small amount of epoxy is applied to the outside of one end of the stainless steel tubing.   Care is taken so that the capillary hole of the tubing is not sealed with the epoxy.   The epoxy coated end of the tube is inser- ted through the enlarged hole so that it extends approxi- mately 1/4 in. beyond the inner surface of the cell top. A very small amount of epoxy is applied to the exposed tubing, and it is retracted into the block until about 1/64 in. of tubing is still exposed.   A standard 1/4 in. - 28 threaded tube end fitting is inserted over the other end of the tubing and epoxied into the female fitting on the outside of the top half of the cell.   Additional epoxy is added to the outside of the tubing and the fitting such that it flows onto the flat region of the outside portion of the top half
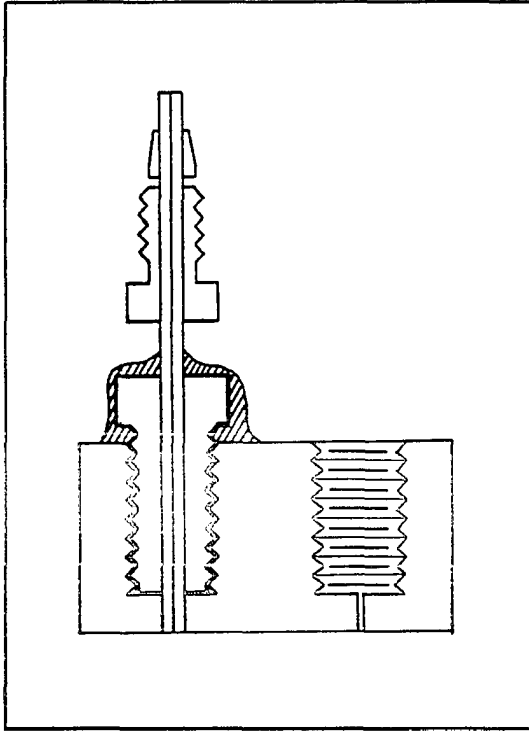
Figure 2-9. Modified Cell Top for 3 μm Columns.

of the cell. This adds mechanical strength to the final assembly. Adequate time is allowed for the epoxy to cure. Five minute epoxy is perfectly adequate for this application. Once the epoxy has hardened, the excess epoxy and tubing protruding from the inner portion of the top half of the cell is removed by sanding with a 600 grit piece of sandpaper. The resulting large scratches are quickly removed by polishing with 0.3 μm alumina polish (Buehler part no. 40-6352-006). A mirror like surface is achieved by polishing with 0.05 μm alumina polish (Buehler part no. 40-6353-006). The alumina is removed by washing with ultrasonication.

This modified top is combined with the unmodified bottom using a 0.002 in. spacer. The total volume of the tubing and top is now 1.09 μl, while the volume of the flow channel remains at 2.15 μl. Thus, the total volume of the modified cell is approximately 3.25 μl. This is a volume reduction of about five- to twelvefold when compared with the unmodified cell. The total volume of this cell is less than one-tenth of the volume of the desired peak, mentioned above, with a peak width of 45 μl. Even if maximum mixing occurs within the cell, band broadening due to the modified electrochemical cell should now be insignificant.

Short circuited mode. The modified cell was used to examine the system standard deviation of the LC. The experiment was conducted with the modified cell connected di-

rectly to the injector. The system standard deviation should include combinations from all system components except the injection and the column, as seen from equation 2-7. Thus, the system standard deviation includes the standard deviation of the connector from the injection to the column and the standard deviation of the detector. If the standard deviation due to the fitting is negligible, then the cell standard deviation should be equal to the measured system standard deviation. The results of Table 2-3 for $\sigma_{v,sys}$, in fact, agree quite favorably with the calculated volume for the modified cell. Since these values are approximately equal, very nearly total mixing must be occurring within the cell for a flow rate equal to 2.0 ml/min. Since the system standard deviation is actually greater than the calculated cell volume, the assumption of a negligible standard deviation of the fitting may be questionable.

These results further indicate that the modified cell is completely adequate for the determination of even low k' peaks with the 3 μm column. Also, the data indicate that this cell may have characteristics which are flow sensitive in nature.

2. Electrode resurfacing. Carbon paste electrodes require periodic resurfacing to maintain the optimum operating condition. Resurfacing, however, could have an effect on the experimental standard deviation of the cell. This possibility was, thus, investigated. In this experiment, a

modified top was used and the electrode was resurfaced with fresh carbon paste prior to each of four separate determinations.   A columnless system was used, eliminating both the column and the connecting tubing between the injector and the column.   The resulting experimental standard deviation was 5.30 ± 0.30 µl.   This is consistant with the results of the previous experimental standard deviation of the LC, determined in both cases with a 5 µl injection (Table 2-1).

3.   Cell reassembly.   The effect of cell reassembly on the experimental standard deviation of the cell was determined with a modified top, a 0.002 in. spacer, a 1/4 in. dia. carbon paste electrode,   and a 5 µl injection. Prior to each determination, the cell was removed from the injector and completely dissassembled and reassembled.   Five determinations were made with the same columnless system as described above.

The resultant experimental standard deviation of this experiment was 5.44 ± 0.44 µl.   This result is entirely consistent with that obtained from both the resurfacing experiment and the previous LC experimental standard deviation experiment.   In fact, the results from all three of these experiments are not significantly different.

Even though the effects of resurfacing and reassembling the cell were not significantly different from the original determination of $\sigma_{v,exp}$, it was, nontheless, decided to make all subsequent experimental determinations without electrode

resurfacing and cell assembly where possible to minimize additional possible uncertainties.

4. Spacer thickness. It is obvious from the previous discussion of the calculated cell volume that the spacer thickness plays an important role in the the detector dead volume. A decrease from 0.005 in. to 0.002 in. caused a reduction in the calculated cell volume from 6.48 μl to 3.25 μl. Although these two values are considerably different, their effects on the dynamic performance of the cell had not been established. Two experiments are performed to evaluate these possible effects.

But, before these experiments were conducted, the thickness of each of the spacers needed to be determined. This proved to be a fairly difficult task to perform with any degree of accuracy. For example, it is easily observed that the spacers are quite compressible and that spacers which have been used are slightly thinner than new spacers. Thus, it was decided that a number of spacers of both thicknesses would be separately installed in a cell for a fixed amount of time (2 hrs.) and the thickness would be determined by a micrometer immediately upon removal. The results are presented in Table 2-7. Although the standard deviations are quite large, the measured values of both the 0.002 in. spacer and the 0.005 in. spacer are quite close to the expected values.

Short circuit mode. The detector was connected di-

TABLE 2-7.   EMPIRICAL DETERMINATION OF SPACER THICKNESS

Manufacturer Specified Spacer Thickness		Measured Thickness(in.)			
		Trial Spacer#1	Trial Spacer#2	Trial Spacer#3	Average
0.002 in.	$(\bar{x})$	0.0018	0.0020	0.0019	0.00191
	(s.d.)	0.0004	0.0005	0.0003	0.00006
	(n)	5	5	5	15
0.005 in.	$(\bar{x})$	0.0046	0.0050	0.0047	0.00477
	(s.d.)	0.0005	0.0006	0.0005	0.00021
	(n)	5	5	5	15

rectly to the outlet of the injector, and the experimental standard deviation was determined for each thickness value. The results are presented in Table 2-8. The injection volume for these studies, it should be noted, was also fixed at 5.0 µl.

The results of Table 2-8 show that there is a significant difference in effect between a 0.002 in. spacer and a 0.005 in. spacer. Although the somewhat more lengthy determination of the system standard deviation, $\sigma_{v,sys}$, for each spacer would have given results which could have been directly compared to the calculate volume of the cell, this approach still gives a good indication of the relative effects of the two different spacers. This same method has been used by Kirkland *et al.* to determine the effects of replacing an 8 µl ultraviolet absorption cell with a 1 µl cell when using a 3 µm column.[89]

Normal mode. Although the previously presented data clearly show a difference between the spacers, the effects of the two spacers on actual chromatographic peaks also needs to be determined. This requires a second set of experiments using the normal mode. Additionally, it was decided to incorporate the effects of various electrode diameters into this same set of experiments. The results are presented in Table 2-9 and Figure 2-10. For all three electrode diameters, the 0.002 in. spacer produces higher efficiencies than the 0.005 in. spacer. The 1/32 in. dia.

TABLE 2-8. EFFECT OF DETECTOR SPACER THICKNESS ON
            THE EXPERIMENTAL STANDARD DEVIATION

Spacer Thickness		$\sigma_{t,exp}$ (min)	$\sigma_{v,exp}$ (µl)
0.002 in.	($\bar{x}$)	0.002661	5.32
	(s.d.)	0.000159	0.32
	(n)	18	18
0.005 in.	($\bar{x}$)	0.003315	6.63
	(s.d.)	0.000115	0.23
	(n)	7	7

TABLE 2-9. EFFECT OF ELECTRODE DIAMETER ON EFFICIENCY FOR TWO DIFFERENT SPACER THICKNESSES

| Compound | | N | | |
| | | Electrode Diameter (in.) | | |
		1/32	1/16	1/8
0.002 in. Spacer				
VMA	$(\bar{x})$	6373	5975	5669
	(s.d.)	96	90	99
	(n)	4	4	5
EPI	$(\bar{x})$	7659	7271	7019
	(s.d.)	73	59	54
	(n)	4	4	5
5HTOL	$(\bar{x})$	8329	7837	7735
	(s.d.)	39	81	76
	(n)	4	4	5
5HTP	$(\bar{x})$	7994	7818	7697
	(s.d.)	98	76	46
	(n)	4	4	5
0.005 in. Spacer				
VMA	$(\bar{x})$	5804	5998	5431
	(s.d.)	78	11	15
	(n)	2	3	3
EPI	$(\bar{x})$	6764	7283	6697
	(s.d.)	47	137	109
	(n)	2	4	4
5HTOL	$(\bar{x})$	7441	7959	7391
	(s.d.)	101	103	22
	(n)	2	4	4
5HTP	$(\bar{x})$	7433	7826	7351
	(s.d.)	58	63	36
	(n)	2	4	4
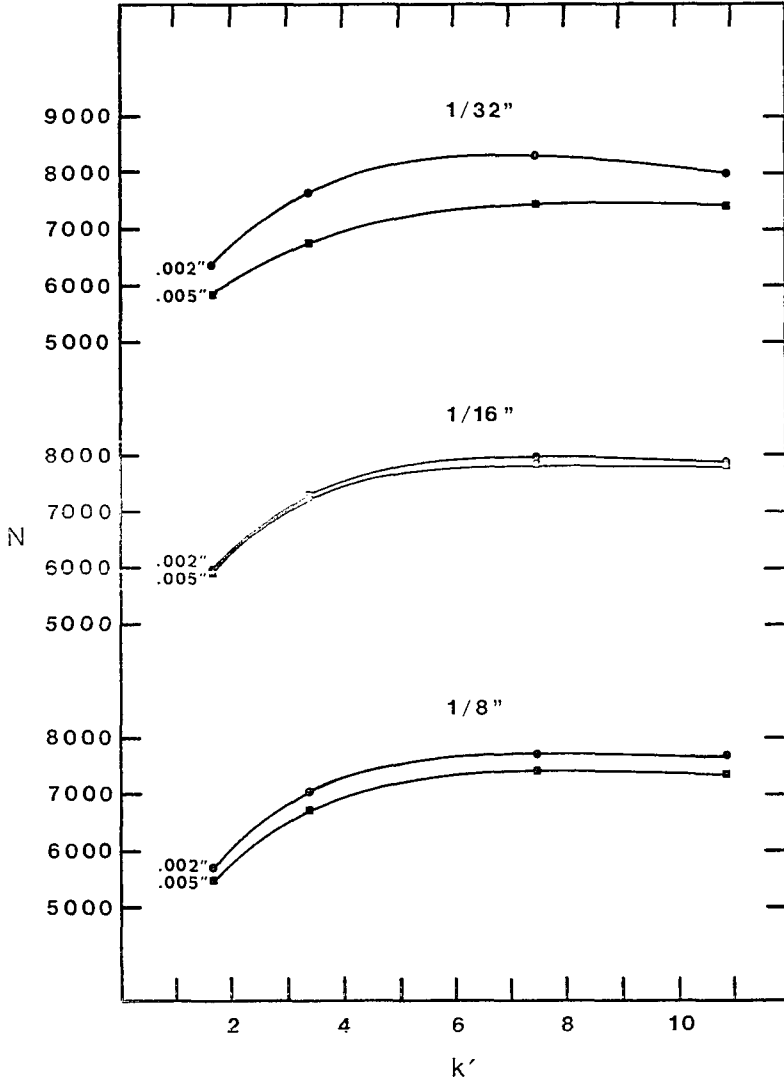
Figure 2-10.   Effect of Spacer Thickness on the Efficiency
for Various Solutes Using Three Electrode
Diameters.

electrode produces the greatest differences, while the 1/16 in. dia. produces the least. The differences between the 0.002 in. spacer and 0.005 in. spacer are significant for both the 1/32 in. dia. and 1/8 in. dia. electrodes. On the other hand, the differences for the 1/16 in. dia. electrode are not significant. Overall, these data clearly demonstrate that the effects of spacer thickness can be significant for real chromatographic peaks.

A very interesting trend can be observed from the normalized peak height and area data, as seen in Table 2-10A. The results given in this table were obtained by normalizing all the peak heights and peak areas of Table 2-9 to the corresponding heights and areas obtained with the 0.002 in. spacer and 1/8 in. dia. electrode. The values for the latter, "control" data set are presented in Table 2-10B.

Figure 2-11 shows the normalized peak heights for components with varying k' values at different electrode diameters and spacer thickness values; the results for the normalized peak areas were tabulated, but not plotted since they essentially convey the same information as the peak height data. As can be seen, the normalized peak heights for the 0.002 in. spacer are consistantly almost two times those of the 0.005 in. spacers for all electrode diameters. This is summarized for both the peak heights and peak areas in Table 2-11. This table also includes the average results of the ratios for the 0.002 in. spacer to the 0.005

TABLE 2-10A.   EFFECT OF ELECTRODE DIAMETER ON NORMALIZED
PEAK HEIGHTS AND AREAS FOR TWO DIFFERENT
SPACER THICKNESSES

Compound		Normalized* Peak Height(%) Diameter(in.)			Normalized* Peak Area(%) Diameter(in.)		
		1/32	1/16	1/8	1/32	1/16	1/8
0.002 in. Spacer							
VMA	$(\bar{x})$	16.85	36.44	100.0	15.15	36.15	100.0
	(s.d.)	0.38	0.03	0.5	0.35	0.05	1.1
	(n)	4	3	5	4	4	5
EPI	$(\bar{x})$	15.36	31.69	100.0	16.46	37.74	100.0
	(s.d.)	0.69	0.44	1.1	0.69	0.06	1.3
	(n)	4	4	5	4	3	5
5HTOL	$(\bar{x})$	15.93	37.81	100.0	14.90	38.12	100.0
	(s.d.)	0.27	0.35	1.6	0.03	0.11	1.3
	(n)	4	4	5	3	3	5
5HTP	$(\bar{x})$	15.09	35.25	100.0	14.11	34.27	100.0
	(s.d.)	0.41	0.21	2.2	0.43	0.21	2.1
	(n)	4	4	5	4	4	5
0.005 in. Spacer							
VMA	$(\bar{x})$	8.70	22.26	56.65	8.21	21.88	58.22
	(s.d.)	0.11	0.04	0.81	0.12	0.15	0.96
	(n)	2	3	4	2	3	4
EPI	$(\bar{x})$	7.22	19.14	53.00	8.38	22.16	64.46
	(s.d.)	0.02	0.17	0	0.05	0.42	0.08
	(n)	2	4	2	2	4	3
5HTOL	$(\bar{x})$	8.45	22.66	57.52	8.36	22.16	58.47
	(s.d.)	0.05	0.08	0.73	0.01	0.11	0.88
	(n)	2	4	4	2	4	4
5HTP	$(\bar{x})$	7.98	21.77	58.38	7.91	21.18	58.17
	(s.d.)	0.04	0.16	0.24	0.02	0.36	0.33
	(n)	2	4	4	2	4	4

* See Table 2-10B for control values.

TABLE 2-10B. PEAK HEIGHTS AND AREAS OBTAINED USING A 1/8
INCH DIAMETER ELECTRODE AND 0.002 INCH
SPACER THICKNESS

Compound		Peak Height (nA)	Peak Area (arbitrary units)
VMA	$(\bar{x})$	117.86	177158
	(s.d.)	0.64	2006
	(n)	5	5
EPI	$(\bar{x})$	160.58	301612
	(s.d.)	1.75	3812
	(n)	5	5
5HTOL	$(\bar{x})$	98.89	402948
	(s.d.)	1.61	5298
	(n)	5	5
5HTP	$(\bar{x})$	92.11	524665
	(s.d.)	2.04	11205
	(n)	5	5
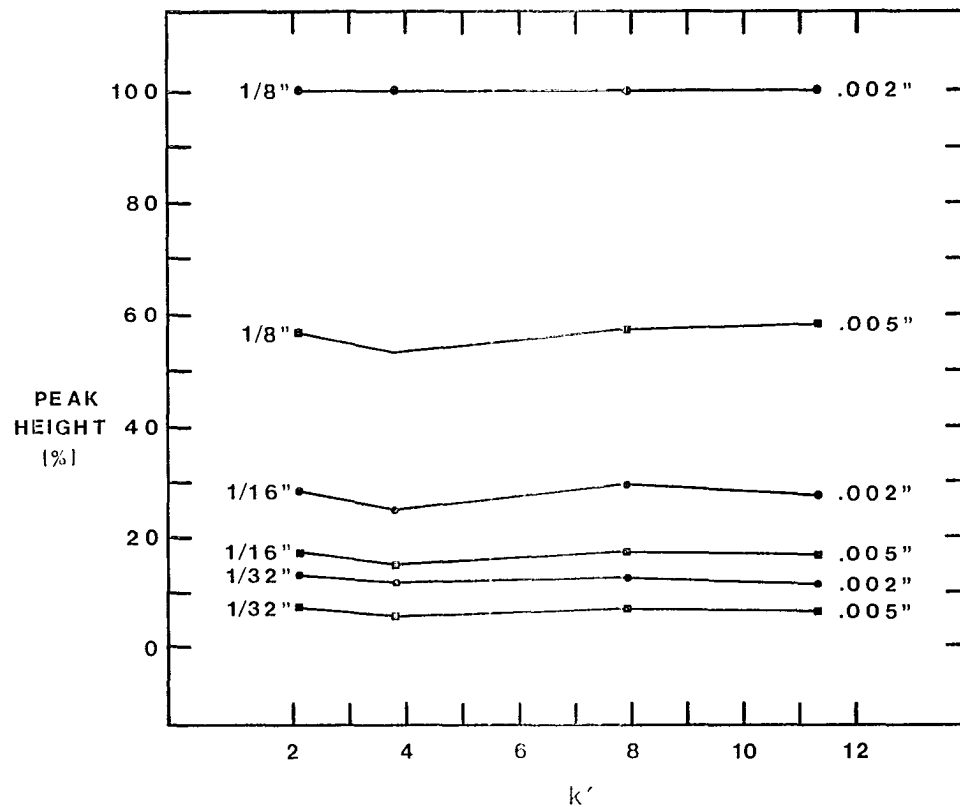
Figure 2-11   Effect of Electrode Diameter and Spacer Thickness
on the Normalized Peak Height for Various Solutes.

TABLE 2-11. AVERAGE OF NORMALIZED PEAK HEIGHTS AND PEAK AREAS FOR DIFFERENT ELECTRODE DIAMETERS AND DIFFERENT SPACER THICKNESSES

Spacer Thickness (in.)		Average* Normalized Peak Height(%) Diameter(in.)			Average* Normalized Peak Area(%) Diameter(in.)		
		1/32	1/16	1/8	1/32	1/16	1/8
0.002	$(\bar{x})$	16.01	35.30	100.0	15.16	36.57	100.0
	(s.d.)	0.62	2.62	0	0.98	1.75	0
	(n)	4	4	4	4	4	4
0.005	$(\bar{x})$	8.09	21.46	56.39	8.22	21.85	58.29
	(s.d.)	0.65	1.59	2.37	0.22	0.46	0.16
	(n)	4	4	4	4	4	4
Ratio of 0.002 in. to 0.005 in. Results		1.98	1.64	1.77	1.84	1.67	1.72
Average Ratio		1.8 ± 0.2			1.7 ± 0.1		

* Peak heights and areas obtained from 222 separate peak measurements with peaks having k′ values between 0.8 and 11.0.

in. spacer. The result shows that the peak heights produced by the 0.002 in. spacer are about 1.8 ± 0.2 times higher than the peak heights of the 0.005 in. spacer, while the peaks area produced a comparable ratio of 1.7 ± 0.1. This represents data obtained from 222 measurements with k' values ranging from 0.8 to 11 and with electrode diameters of 1/32 in., 1/16 in. and 1/8 in. Thus, these ratios should be good indicators of the effect of changing the spacer thickness from 0.005 in. to 0.002 in.

An equation which relates the limiting current for a flow channel electrode, i_L, to various operational parameters has been derived by Meyer et al.:[98]

$$i_L = 1.467 n F w C_o (Dl/h)^{2/3} (U/d)^{1/3} \qquad (2-15)$$

where n is the number of electrons in the electrochemical reaction, F is Faraday's constant, w is the width of the electrode (cm), C_o is the bulk concentration of the reactant (mole/cm^3), D is the diffusion coefficient (cm^2/s), l is the length of the electrode (cm), h is the height or thickness of the channel (cm), U is the volume flow rate (cm^3/s) and d is the width of the channel (cm). These workers established the validity of equation 2-15 using experiments with a Ag channel electrode.[98] Weber and Purdy used the linear concentration profile approximation method and derived a more general expression, which included the coulometric as well as the amperometric applications.[13] They then showed that

equation 2-15 applies for the amperometric case. Their
derived expression was confirmed by experimental data using
an LCEC cell equipped with a rectangular carbon paste elec-
trode.

By keeping all other variables constant in equation 2-
15, the limiting current is seen to be directly proportional
to the channel height (or spacer thickness) to the negative
two-thirds power:

$$i_L \propto h^{-2/3} \qquad\qquad (2-16)$$

Substituting 0.00191 in. and 0.00477 in. (from Table 2-7)
into (2-16) yields $i_L \propto 64.96$ and $i_L \propto 35.29$, respectively
for the 0.002 in. and 0.005 in. spacers. And, the ratio of
64.96 to 35.29 is 1.84, which compares very favorably with
the experimentally determined ratio of 1.7 ± 0.8 for the two
spacers.

5. Electrode diameter. The effect of varying the elec-
trode diameter on the efficiencies of compounds having vari-
ous k' values was investigated simultaneously with the ef-
fect of spacer thickness. The experimental conditions are
listed under the section entitled Spacer Thickness, and the
results are give in Tables 2-9 and 2-10. The efficiencies
and capacity factors determined for various peaks at each
electrode diameter are plotted in Figure 2-12.

In the case of the 0.002 in. spacer, Figure 2-12
clearly indicates that the efficiency increases as the dia-
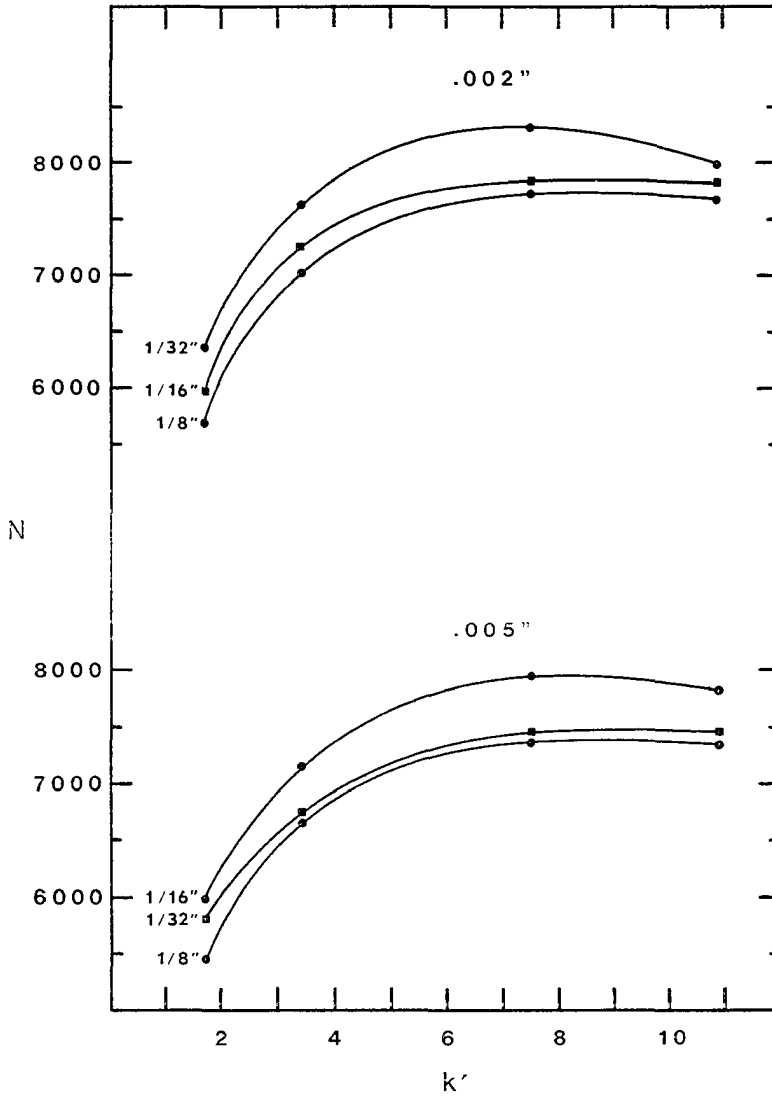
Figure 2-12.   Effect of Electrode Diameter on the Efficiency
for Various Solutes Using Two Spacer Thicknesses.

meter of the electrode decreases and the 1/32 in. dia. represents the optimum. This trend seems completely appropriate. The region of the highest linear velocity should be directly in the middle of the channel. Since calculations would indicate that laminar flow should be obtained in the channel of this electrode, the linear velocity should be expected to decrease as one moves from the center towards the edge of the channel. Band broadening by the cell implies that eluents are diffusing laterally towards the slower flow velocity regions of the channel. Since all the tested electrodes are centered in the middle of the channel, then the smallest electrode will be exposed to the relatively higher linear velocity regions of the channel. In these regions, the bands are swept across the electrode very rapidly, resulting in higher efficiencies. On the other hand, a large diameter electrode will be exposed not only to the high linear velocity regions but also to the slower regions. Any eluent that has diffused into these slower regions will be detected by the larger electrode and, thus, a larger signal will be obtained. But, since the flow in these regions is slower, the residence time is longer. Therefore, the band is broadened and efficiency is decreased.

In the case of the 0.005 in. spacer, the results are distinctly different. There is no significant difference in efficiencies obtained form the 1/32 in. and 1/8 in. dia.

electrodes.   The only exception to this statement occurs at
the smallest k' value where the efficiency is better for the
1/32 in. case.   But, the 1/16 in. dia. electrode provides
the optimum efficiency for all values of k'.   There is no
obvious explanation for this behavior.   Because of this
irregularity, however, this experiment was repeated.   The
results were very similar to those already discussed. Thus,
the original results are apparently correct. Since the three
different electrode diameters are contained in three dis-
tinct cells, this unexpected result may be due to manufac-
turing differences in the individual cells.

    The   data   of Table 2-11 can also be used to determine
the effect of varying the electrode diameter on the norma-
lized peak heights and peak areas.   The ratios for the 1/8
in. to 1/16 in., the 1/16 in. to 1/32 in., and the 1/8 in.
to 1/32 in. are determined for both 0.002 in. and 0.005 in.
spacers,   as shown in Table 2-12.   A change in electrode
diameter by a factor of two caused a change in the average
normalized peak height of a factor of 2.6 for both peak
heights and areas, while a change in diameter by a factor of
four caused a normalized peak height change of a factor of
6.6 and 6.8 for the peak heights and peak areas, respec-
tively.

    Recently, Weber et al. have reported that one equation
applies to both tubular and channel electrodes.[17] Only some
of the constants need to be changed or redefined for the two

TABLE 2-12. EFFECT OF CHANGES IN ELECTRODE DIAMETER ON
AVERAGE NORMALIZED PEAK HEIGHTS AND AREAS

2x Change in dia.	Average Ratio of Normalized Peak Heights	Average Ratio of Normalized Peak Areas
1/8 in. to 1/16 in. (0.002 in. spacer)	2.83	2.73
1/16 in. to 1/32 in. (0.002 in. spacer)	2.20	2.41
1/8 in. to 1/16 in. (0.005 in. spacer)	2.63	2.67
1/16 in. to 1/32 in. (0.005 in. spacer)	2.65	2.66
Average Result	2.6 ± .3	2.6 ± .1

4x Change in dia.		
1/8 in. to 1/32 in. (0.002 in. spacer)	6.25	6.60
1/8 in. to 1/32 in. (0.005 in. spacer)	6.97	7.09
Average Result	6.6 ± .5	6.8 ± .4

different cases.   For a flow channel electrode with a chan-
nel height (spacer thickness) of b:

$$i_L = 1.47nFC_0U(DA/bU)^{2/3} \qquad (2-17)$$

where A is the area of the electrode (cm^2).   For the tubular
electrode, one simply replaces the constant 1.47 with 1.61,
and b becomes the radius of the tube. By keeping all other
variables constant in equation 2-17, the limiting current is
seen to be directly proportional to the area of the elec-
trode raised to the two-thirds power:

$$i_L \propto A^{2/3} \qquad (2-18)$$

Substituting the experimentally employed electrode areas
into expression 2-18 yields relative values for the currents
which are used to evaluate the observed relationship between
the current and the electrode area, as shown in Table 2-13.
Theoretically, a twofold increase in electrode diameter
should cause an increase in current by a factor of 2.52,
while a fourfold increase in diameter should result in an
increase of current by a factor of 6.35.   The experimental
results of Table 2-12 (2.6 and 6.7, respectively) compare
very favorably with the theoretical results.

These results demonstrate, from both empirical and
theoretical standpoints, that the signal of the current type
of electrochemical cell increases directly with the two-
thirds power of the electrode area.   This increase is prac-

TABLE 2-13.   THEORETICALLY PREDICTED CHANGE IN CURRENT DUE
TO CHANGES IN THE ELECTRODE DIAMETER

	Electrode Diameter(in.)		
	1/32	1/16	1/8
Calculated Area(cm^2)	4.948×10^{-3}	1.979×10^{-2}	7.917×10^{-2}
Calculated i_L ($\alpha A^{2/3}$)	0.02904	0.07361	0.1844

2x Change in dia.	Predicted Ratio of Currents
1/8 in. to 1/16 in.	2.52
1/16 in. to 1/32 in.	2.52
Average	2.52 ± 0

4x Change in dia.	
1/8 in. to 1/32 in.	6.35

tically significant only if the noise of the cell does not increase proportionally. Thus, it is probably more important to consider the signal to noise ratio (SNR). It has been reported that the noise of the amperometric type of cell increases linearly with the electrode area.[11,13]

$$i_N \propto A \qquad (2-19)$$

where i_N is the current due to the noise. An expression relating the SNR for this cell to the electrode area can be obtained by dividing expression 2-18 by that of 2-19:

$$SNR \propto A^{2/3}/A = A^{-1/3} \qquad (2-20)$$

This equation indicates that the cell with the smallest possible diameter should yield the highest possible SNR.

6. Electrode material. Two types of electrode materials were investigated --- carbon paste (CP) and glassy carbon (GC). Since the actual electrode is not capable of being replaced with regard to the lower half of the cell in which it is housed, as seen in Figure 2-8, three distinct carbon paste assemblies and three distinct glassy carbon assemblies were chosen for this experiment. All electrodes were 1/8 in. dia., and all measurements were made with the same modified cell top and spacer.

Short circuited mode. The first experiment utilized a columnless system to determine the effect of the electrode material on the experimental standard deviation. The re-

sults of this experiment are presented in Table 2-14.

The experimental standard deviation for glassy carbon was 22.4 ± 0.14 µl, while the result for carbon paste was 5.32 ± 0.32 µl. A 5 µl injection was employed in both cases. These values indicate a significant difference between glassy carbon and carbon paste.

Normal mode. To investigate the effect of the observed difference on actual peaks, an experiment was conducted incorporating the 3 µm column. The results of this experiment are tabulated in Table 2-15. The effect of electrode material on efficiency is graphically displayed in Figure 2-13. This figure demonstrates the dramatic decrease in efficiency due to the use of the glassy carbon material, which is completely consistent with the results of the columnless experiment.

BAS, an LCEC manufacturer, does not recommend the use of carbon paste electrodes with mobile phases containing greater than five percent ACN concentration. They cite decreased electrode lifetime as the primary reason for this recommendation. The practical experiences of this author during the past two years have revealed that carbon paste electrodes are useful, in the current 7.5% ACN environment, for at least one month when working with injected quantities of compounds which exceed 100 ng. With injected amounts below 100 ng, however, electrode longevity is typically only one to two weeks. When carbon paste electrodes are used

TABLE 2-14. EXPERIMENTAL STANDARD DEVIATION FOR TWO
DIFFERENT ELECTRODE MATERIALS

Electrode No.		$\sigma_{t,exp}$ (min)	$\sigma_{v,exp}$ (µl)
GLASSY CARBON			
#1	($\bar{x}$)	0.011515	23.03
	(s.d.)	0.000111	0.22
	(n)	6	6
#2	($\bar{x}$)	0.010242	20.48
	(s.d.)	0.000580	1.16
	(n)	5	5
#3	($\bar{x}$)	0.011697	23.39
	(s.d.)	0.000134	0.27
	(n)	6	6
Average	($\bar{x}$)	0.011205	22.41
	(s.d.)	0.000714	1.43
	(n)	17	18
CARBON PASTE			
#1	($\bar{x}$)	0.002825	5.65
	(s.d.)	0.000102	0.20
	(n)	6	6
#2	($\bar{x}$)	0.002557	5.11
	(s.d.)	0.000005	0.04
	(n)	4	4
#3	($\bar{x}$)	0.002591	5.18
	(s.d.)	0.000140	0.28
	(n)	8	8
Average	($\bar{x}$)	0.002661	5.32
	(s.d.)	0.000159	0.32
	(n)	18	18

TABLE 2-15.   EFFECT OF ELECTRODE MATERIAL ON PEAK WIDTH
              AT HALF-HEIGHT AND EFFICIENCY

Compound*		$W_{1/2}$(min)		N	
		Glassy Carbon	Carbon Paste	Glassy Carbon	Carbon Paste
VMA	$(\bar{x})$	0.02817	0.02134	3963	6764
	(s.d.)	0.00034	0.00039	17	244
	(n)	4	4	3	4
EPI	$(\bar{x})$	0.03833	0.03175	5587	8117
	(s.d.)	0.00027	0.00032	75	163
	(n)	4	4	4	4
5HTOL	$(\bar{x})$	0.06461	0.05650	7214	9415
	(s.d.)	0.00019	0.00020	39	77
	(n)	4	4	4	4
5HTP	$(\bar{x})$	0.08933	0.08042	7338	9028
	(s.d.)	0.00047	0.00042	11	64
	(n)	4	4	3	4

 * Capacity factors for these compounds are given
   in the footnote to Table 2-6.
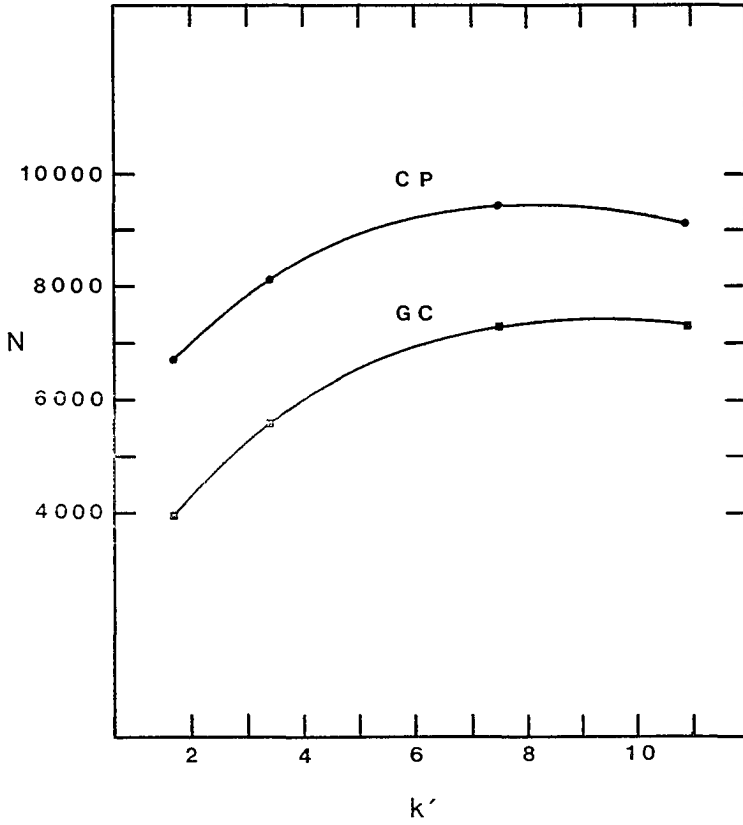
Figure 2-13.   Effects of Electrode Material on Efficiency
              for Various Capacity Factors.

with pure aqueous mobile phases, on the other hand, their lifetimes are between one and six months. Increased ACN simply leads to more rapid dissolution of the Nujol^R binder in the carbon paste electrodes, resulting in an increase in detection limits. Thus, the practical experience would appear to support the recommendation of the manufacturer for general applications. But, the results presented above show that 3 μm columns are *not* included in the general case. For systems using these columns, carbon paste is clearly the electrode material of choice in spite of the possible necessity for frequent resurfacing. The loss in efficiency obtained by switching to a glassy carbon electrode is simply too high a price to pay. Besides, even glassy carbon requires occasional resurfacing.

7. Comparison with published results. At this time, only a very limited amount of work has appeared in the literature concerning the effects of the detector cell in a 3 μm system on its overall efficiency. However, the currently obtained system standard deviation and efficiencies compare well with previously reported results. The dead volume of the current cell and the tubing combination are the lowest of all detectors. However, all the previous reports utilized a UV detector, so a direct comparison may not be appropriate.

As mentioned previously, the standard deviation associated with the injection is equal to the volume of injec-

tion divided by a constant, C. The value of C is obtained directly as the inverse of the slope of the linear regression presented in Table 2-2. Both the 1.5 ml/min and 2.0 ml/min flow rates yielded a value using this approach of 1.85. This compares very favorably to the reported C value range of 2.08 to 3.61 by Lauer and Rozing and the reported range of 1 to 2 by DiCesare et al.[90,78]

The efficiencies of individual peaks from the current report can also be compared with those reported by others. Cooke et al., for example, reported approximately 12000 theoretical plates for compounds having k' values of two to nine for the 7.5 cm, 3 μm Beckman column.[80] And, Perkin Elmer guarantees at least 12000 plates for its columns. On the other hand, the results of this work indicate between 7000 and 9000 theoretical plates (Tables 2-6, 2-9 and 2-15). But, both the work of Cooke et al. and the manufacturer's guarantee refer to an optimum mobile phase of 40% water:60% acetonitrile, while the current study employs an aqueous phase with only 7.5% acetonitrile. This difference in mobile phases is more than sufficient to account for the lower efficiencies obtained with our system.

IV. Conclusion

The dead volume associated with the 3 μm LCEC has been investigated and minimized. Pulsation was reduced to a practical limit using mechanical devices. The adequacy of the current system was demonstrated by the empirically de-

termined value of the system standard deviation, which is 2.52 µl and 3.76 µl for flow rates of 1.5 ml/min and 2.0 ml/min, respectively.

For the electrochemical detection portion of the LCEC, both the potentiostat and the detector cell have been optimized. The optimum time constant for a separation including a compound with $k' = 1$ is 0.05 s. The optimum cell is one that has a modified top, a 1/32 in. dia. carbon paste electrode, and a 0.002 in. spacer.

CHAPTER 3

OPTIMIZATION OF THE LIQUID CHROMATOGRAPHIC SEPARATION

I.   Introduction

The desire to improve has always been a prime motiva-
tor.   This desire has led to many recent advances in both
liquid chromatography and LCEC. The LCEC separation of
catecholamines, indoleamines, and related compounds is one
area that has experienced an exceptional amount of activity.
This chapter represents an attempted improvement on these
previous works. [The reader is referred to the Appendix for
a definition of the acronyms used herein for the compounds
of interest.] A brief survey of the literature associated
with biogenic amines and LCEC reveals a trend toward increa-
singly more complex and more rapid separations.

In 1976, Molnar and Horvath became one of the first
groups to demonstrate the potential usefulness of reversed-
phase liquid chromatography (RPLC) in the separation of
catecholamine related compounds.[111] Using columns filled
with 5 and 10 μm packing materials, they were able to pro-
vide an appropriate set of separations for all the inter-
mediates in the primary metabolic pathways of catechol-
amines.   The four major catecholamines were separated in

126

nine minutes on a 5 µm column.   Seven compounds associated

with the catechol-O-methyltransferase pathway were separated

in nineteen minutes.   Compounds associated with the tyrosine

hydroxylase, DOPA decarboxylase, and monoamine oxidase path-

ways were also separated.   A total of five different separa-

tion conditions were presented.   Although actual biological

samples were not investigated, this pioneering work clearly

demonstrated the applicability of this technique to the

separation of catecholamines and related compounds.

The   general utility of ion pairing agents in RPLC was

demonstrated very soon thereafter by Knox and Jurand.[100]

Ion pairing agents have nonpolar aliphatic tails with polar

head groups possessing either a positive or a negative

charge. Since these compounds are fundamentally detergents,

or soaps, the techniques incorporating them have commonly

been termed "soap chromatography". The aliphatic tails are

absorbed into the nonpolar stationary phase of the RPLC

column leaving the polar head groups projecting out into the

mobile phase.   These polar moieties greatly increase the

retention times of polar solutes such as the protonated

catecholamines.   Ion pairing agents also increase the effi-

ciency and peak symmetry of polar solutes.   Using soap

chromatography, Asmus and Freed established the separation

of eight different catecholamines and metabolites.[99]   They

also investigated the use of nitrate, sulfate, acetate and

trichloroacetate as ion pairing agents. Wagner *et al.* also

employed ion pairing RPLC in 1979 to separate eight cate-
cholamines and related compounds,[101] while Riley et al.
reported the resolution of tryptophan and three of its
metabolites in four minutes using the same basic ap-
proach.[102]

In 1981, Joseph et al. established an ion pairing RPLC
determination of DA, NE, and five related metabolites for
tissue samples, requiring thirty minutes and an ethyl ace-
tate extraction sample pretreatment.[103] Kempf and Mandel
separated NE, DA, 5HT and four metabolites in twenty minutes
employing two different columns and two different mobile
phases.[104] Using a 5 µm ion paired RPLC column, Kilts et
al. separated DA, 5HT and four metabolites in twelve mi-
nutes.[105]

In 1982, Ishikawa et al. used two different mobile
phases with a single column to separate fourteen com-
pounds.[106] One mobile phase separated nine compounds in
eighteen minutes, while the other required an additional
eighteen minutes to separate the remaining five. Wagner
et al., following up their previous work, were able to
quantitate fourteen compounds in sixty minutes using an
isocratic system.[107]

In 1983, with a multiple electrode LCEC, Mayer and
Shoup were able to determine seven catecholamines, indole-
amines, and related metabolites in fifteen minutes.[60] In a
rather novel approach, Nakagawa et al. used a crown ether

(18-crown-6) with RPLC to separate six catecholamines in eight minutes.[110]

Finally, this year Lasley *et al.* separated thirteen metabolites of TYR and TP in thirty minutes using an isocratic 5 μm RPLC system.[108] Applying this separation, they measured neurotransmitter turnover rates in various discrete regions of the rat brain.

Considering these previously employed systems, we will, in this chapter, attempt to optimize the separation of catecholamines, indoleamines, and related metabolites on the new 3 μm columns. This optimization will focus on selection of the proper amounts and kinds of mobile phase components.

II. Experimental

A. Instrumentation

The LCEC setup used for these studies has been previously described in Chapter 2. However, one modification has been incorporated to provide minimal operator time during data acquisition. The Rheodyne loop injector has been replaced with an automated sample injector, namely the WISP model 710B from Waters Associates, Inc. of Milford, MA. The connecting tube supplied with the WISP to go from the injector to the column was replaced with a 1/16 in. o.d., 0.006 in. i.d., 6 cm long, polished piece of stainless steel tubing. This modification was necessary to reduce the dead volume of the system to an acceptable level for 3 μm col-

umns. The column, as a result, had to be mounted directly in front of the injector portion of the WISP so that it protruded through the access door. The Plexiglas[R] window on the door of the WISP also had to be removed to accomodate the 3 μm column. However, no adverse effects on the operation of the WISP have been observed as a result of this relatively minor modification in the past two years.

A Beckman Ultrasphere[R], 3 μm, ODS, 4.6 mm x 7.5 cm column (part no. 244247) was used exclusively in the detailed investigation of the effect of mobile phase composition on the capacity factor for individual compounds. An acceptable separation for the desired compounds on both the Perkin Elmer HS-3, 4.6 mm x 10 cm (part no. 258-1501) and the newer 4.6 mm x 8.5 cm column was also produced using the final conditions obtained for the Beckman unit as a guideline.

The modified electrochemical detector with a low dead volume described in Chapter 2 is the same detector that was used for the studies reported in this chapter. The time constant was set at 0.05 s. The carbon paste cell had a 1/8 in. dia. working electrode and a 0.002 in. spacer with the modified top.

B. Reagents and Preparations

1. __Mobile phase.__ The sources and purities of the chemicals used to prepare the mobile phase were given in Chapter 2. A complete description of the procedure for

preparation of the mobile phase has also been previously outlined in Chapter 2. A reasonably comprehensive set of mobile phases, each containing different amounts of individual components, were prepared and evaluated. The exact composition of each mobile phase is given below in the Procedures section.

2. <u>Standards</u>. Twenty-four catecholamines, indoleamines, metabolites and related compounds were investigated. The source for each compound is given in Chapter 2, while the acronyms for each appear in the Appendix. Stock solutions having concentrations of ca. 1.00 m$\underline{M}$ for each solute to be tested were initially prepared in a solution containing 1.0 m$\underline{M}$ HCl. These stock standards were stored at 4°C and used within two months of preparation. Working solutions were prepared on the day of the experiment by diluting the stock standard solutions 1:1000 with the 1.0 m$\underline{M}$ HCl. The working concentrations for each compound were, thus, approximately 1x10^{-6} $\underline{M}$.

C. Procedure

The primary purpose of this investigation was to obtain a separation for the majority of the desired compounds requiring the shortest possible amount of time. This was accomplished in two steps. The first step involved establishing the effects of various mobile phase components on the capacity factor for each of the twenty-four compounds.

This data was then compiled and used to identify the optimal mobile phase composition(s).

Due to the complete lack of reports on appropriate 3 μm separations, an optimized mobile phase for a 5 μm column was used as a starting point for the current investigation.[75] The buffer for this system consisted of 0.10 $\underline{M}$ citric acid, 0.09 m$\underline{M}$ SOS, and 7.5% methanol (volume/volume basis). The final solution was titrated to a pH of 4.8 with solid NaOH. However, manufacturers now recommend the use of acetonitrile instead of methanol. The acetonitrile/water combination offers a lower viscosity than comparable methanol/water mixtures, thus allowing the entire system to be operated at a lower pressure for a given flow rate. Another advantage of acetonitrile is that it is less toxic than methanol. As a result, the organic modifier of the starting mobile phase was changed from 7.5% methanol to 7.5% acetonitrile. Additionally, 0.05 m$\underline{M}$ EDTA was added to complex any stray metal ions, and, thus, hopefully provide a lower detector noise level.

1. Effect of mobile phase composition on capacity factor.

pH experiments. Due to the innate characteristics of the silica based packing material, the useful pH range of the column is limited to two and seven. Beyond these limits, the packing material will slowly dissolve in the mobile phase. The pH values initially selected for investi-

gation were 2.00, 2.50, 3.50, 4.00, 4.50 and 5.00. The region between pH 5 and 7 was not investigated because the amino acid solutes exist as zwitterions in this pH region and, thus, are only slightly retained by the column. The concentrations of the other components during the study for pH effects were fixed at 0.10 M citric acid, 0.09 mM SOS, 0.05 mM EDTA, and 7.5% ACN. The various mobile phases to be tested were titrated to the desired value of pH with solid NaOH.

SOS experiments. The most commonly reported ion pairing agent concentrations are in the sub-millimolar to millimolar range. Thus, the concentrations of SOS investigated were 0.00 mM, 0.03 mM, 0.09 mM, 0.30 mM and 1.00 mM. The five resultant mobile phases contained one of the above concentrations of SOS along with 0.10 M citric acid, 7.5% ACN, and 0.05 mM EDTA. They were each titrated to a pH of 4.8 with solid NaOH.

ACN experiments. The acetonitrile percentages investigated were 2.5, 5.0, 7.5, and 10.0%. The remaining mobile phase components were 0.10 M citric acid, 0.09 mM SOS, and 0.05 mM EDTA. The mobile phases were titrated to a final pH of 4.8 with solid NaOH.

2. Separation optimization. The previously described mobile phases were tested with each compound to construct plots of the capacity factor versus each of pH, the concentration of SOS, and the concentration of ACN. The collection

of plots was then used to identify regions of apparently optimal separation. The mobile phases predicted to yield the most desirable separations are selected, prepared, and evaluated. The following criteria were used to identify appropriate mobile phase compositions.

Among the twenty-four compounds, the separation and adequate resolution of some of the compounds was deemed to be more important than that of the others. For this purpose, the compounds were divided into three categories. The compounds of the greatest interest were labelled Priority 1. Possible internal standards were labelled Priority 2. The compounds of least importance were labelled Priority 3. The resultant list of compounds is given in Table 3-1. A useful mobile phase would, hopefully, resolve all the compounds listed under Priority 1 and at least one of the compounds listed under Priority 2. The mobile phase that accomplished or came closest to accomplishing this task and, additionally, resolved the most compounds from Priority 3 would then be selected as the optimum.

D. Calculations

1. Capacity factor, k'. See Chapter 2, Section E.1.

2. Efficiency, N. See Chapter 2, Section E.2.

3. Resolution, R. Resolution is a measure of the degree of separation between two adjacent peaks. An R value less than 1.00 indicates fairly severe overlapping. A value of R greater than 2.00 indicates baseline resolution between

TABLE 3-1.   COMPOUND PRIORITY ASSIGNMENTS

Priority 1	Priority 2	Priority 3
DA	DHBA	DOPEG
DOPA	EPIN	MEL
DOPAC	N-MET	MET
EPI		MHPG
HVA		N-Ac-5HT
NE		TP
NM		TYR
3MT		VMA
5HIAA		5MT
5HT		
5HTOL		
5HTP		

the peaks. By definition,

$$R = 2[(t_{r,2} - t_{r,1})/(W_2 + W_1)] \qquad (3-1)$$

where t_r is the peak retention time and W is the peak width measured at the baseline, as shown in Figure 3-1.

III. Results and Discussion

A. **Effect** **of** **mobile** **phase** **composition** **on** **capacity** **factor**. The results of these experiments are presented in Tables 3-2, through 3-4 as well as Figures 3-2 through 3-4. Each reported value represents the average of at least four separate determinations.

1. **pH effect**. The results of the initial pH experiments are given in Table 3-2. The data clearly show that the effect of pH on the capacity factor is highly dependent on the nature of the compound examined. The twenty-four compounds can be conveniently divided, for this reason, into four categories based on the functional groups they possess. The four groups are neutrals, amino acids, acids, and amines. This categorization is presented in Table 3-5.

A capacity factor *versus* pH plot has been constructed for each of the four categories, as seen in Figure 3-2. MEL and 5MT have been omitted from the plots because of their extremely large capacity factors. A quick look at Table 3-2, however, reveals that the behavior of MEL and 5MT, respectively, corresponds in general to that of the neutrals
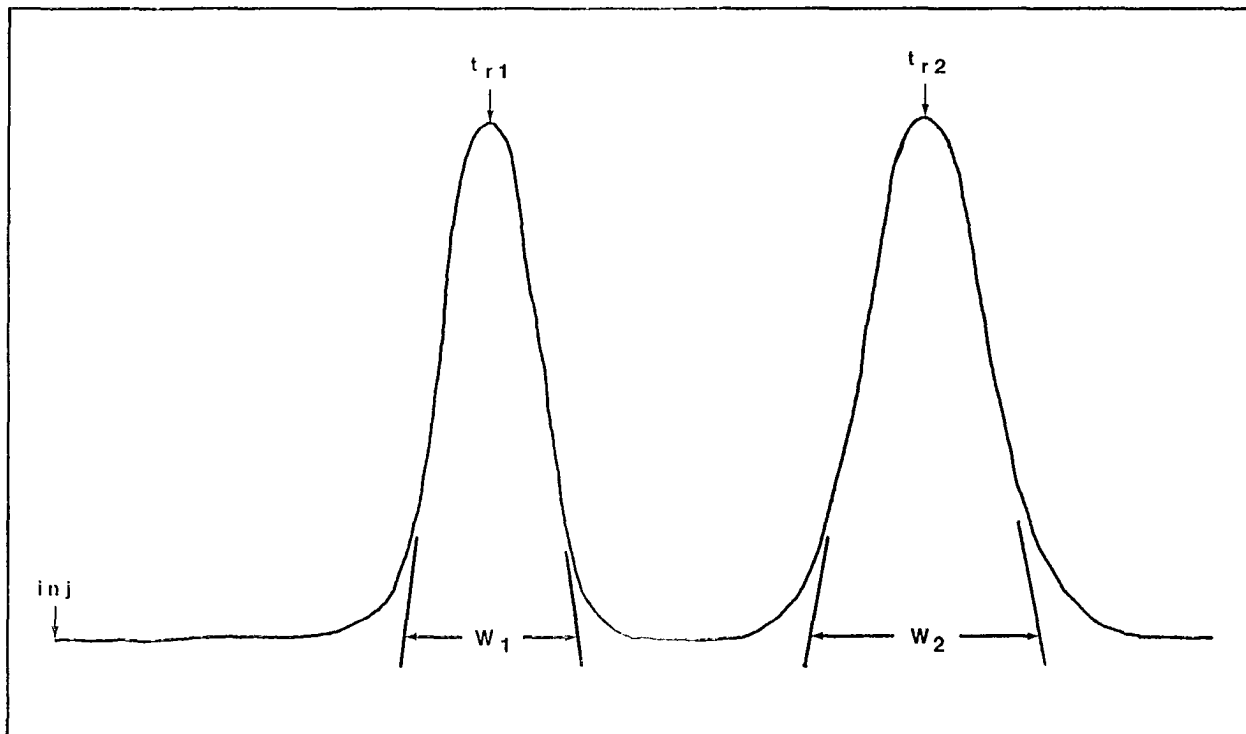
Figure 3-1.   Determination of Resolution Between Adjacent Peaks.

TABLE 3-2.   EFFECT OF pH ON CAPACITY FACTOR

| | Capacity Factor, k' | | | | | | |
| | pH | | | | | | |
Compound	2.00	2.50	3.00	3.50	4.00	4.50	5.00
DA	3.42	2.00	1.60	1.24	1.18	0.98	0.82
DHBA	2.32	1.25	1.02	0.79	0.70	0.57	0.47
DOPA	2.62	0.90	0.40	0.21	0.08	0.03	0.02
DOPAC	3.07	2.67	2.78	2.47	2.22	1.43	0.64
DOPEG	0.42	0.26	0.29	0.25	0.28	0.28	0.29
EPI	1.93	1.02	0.80	0.62	0.54	0.44	0.36
EPIN	4.23	2.59	2.03	1.54	1.50	1.28	1.08
HVA	8.96	8.22	8.02	7.26	6.42	4.24	2.01
MEL	55.20	52.58	49.89	45.22	48.45	48.85	48.58
MET	3.99	2.44	1.90	1.42	1.41	1.19	1.01
MHPG	1.01	0.84	0.86	0.79	0.98	0.87	0.86
NE	1.52	0.73	0.57	0.43	0.36	0.27	0.24
NM	2.37	1.66	1.30	1.00	0.92	0.76	0.65
N-Ac-5HT	7.13	6.35	6.45	5.96	6.55	6.46	6.08
N-MET	12.27	7.69	6.21	4.92	4.81	4.20	3.57
TP	41.71	18.94	9.26	4.28	2.98	2.40	2.14
TYR	4.44	1.64	0.77	0.33	0.24	0.14	0.12
VMA	1.08	0.84	0.76	0.45	0.26	0.04	0.00
3MT	8.58	5.56	4.35	3.33	3.25	2.81	2.36
5HIAA	5.97	5.27	5.52	5.03	4.91	3.61	1.97
5HT	10.03	6.10	5.09	4.16	3.91	3.39	2.88
5HTOL	4.50	4.01	4.21	3.94	4.42	4.37	4.22
5HTP	8.49	3.46	1.83	0.94	0.71	0.60	0.54
5MT	80.26	53.55	40.31	31.01	30.52	27.53	22.79
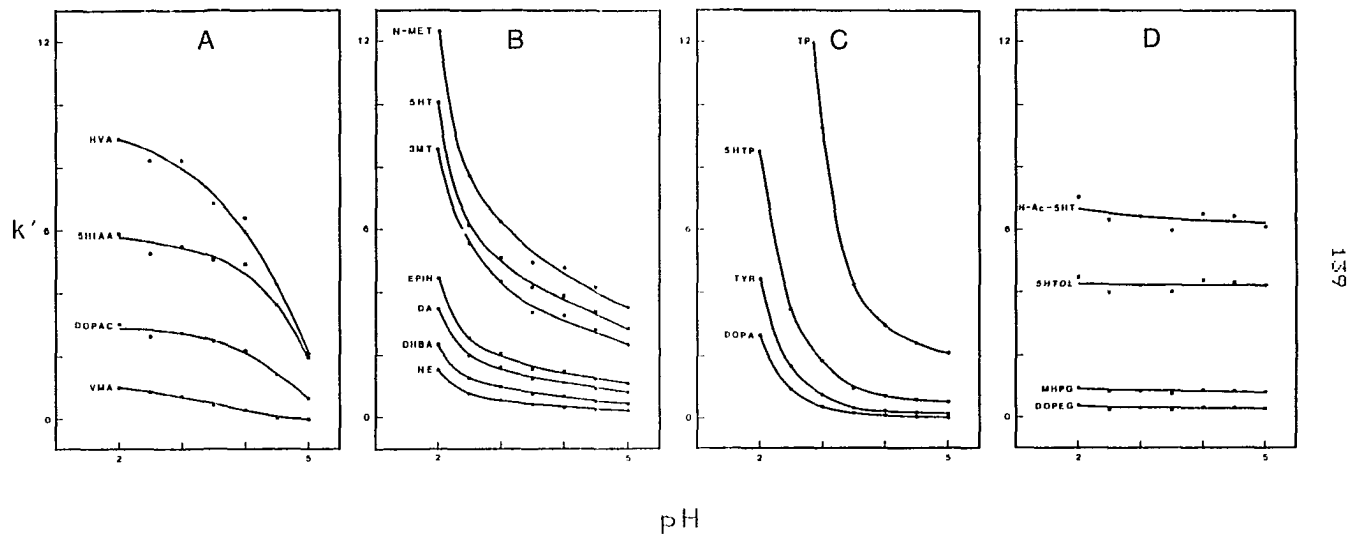
Figure 3-2. Effect of pH on the Capacity Factor for Acids (A),
Amines (B), Amino Acids (C), and Neutrals(D).

TABLE 3-5.   CLASSIFICATION OF COMPOUNDS

Acids	Amines	Amino Acids	Neutrals
DOPAC	DA	DOPA	DOPEG
HVA	DHBA	TP	MEL
VMA	EPI	TYR	MHPG
5HIAA	EPIN	5HTP	N-Ac-5HT
	MET		5HTOL
	NE		
	NM		
	N-MET		
	3MT		
	5HT		
	5MT		

and the amines. All the amines included in Table 3-5 are also, notably, not included in the amine plot of Figure 3-2. The proximity of the individual curves for many of the amines would simply obscure the observation of their general behavior. The purpose of the plots is simply to demonstrate the general effects of pH on the capacity factors of the four different types of compounds. Thus, representative compounds are completely adequate to establish the relevant trends.

The plot for the acids reveals an inverse relationship between the capacity factor and the pH of the mobile phase. This result reflects exactly the behavior expected. At pH values higher than its pK_a, an acid is deprotonated and, thus, negatively charged. The charged form of the acid has much less affinity for the stationary phase than the proto-nated, neutral molecule. Thus, the charged species will have a shorter retention time and a smaller capacity factor. At pH values near the pK_a, the capacity factor of the acids should increase rapidly as a function of decreasing pH. Finally, at pH values considerably below the pK_a, the capa-city factor should be relatively large and, again, pH inde-pendent. The k' *vs.* pH plot should resemble, in this way, a classical potentiometric titration curve. The VMA curve in Figure 3-2 matches this description fairly well. Two pH independent regions for VMA are clearly visible, but only a gradual, rather than the predicted sharp, change occurs in

the capacity factor near the "endpoint". The sharpness of the endpoint in this case may be masked by the small overall change in the capacity factor. If the curves for the other three acids were extended to higher pH values, the final pH independent region would also be expected to become visible in their plots.

Four other research groups have investigated, for RPLC, the effect of pH on the capacity factor of the acid metabolites of biogenic amines.[75,99,105,109] At least one of the four acids listed in Table 3-5 was examined in each of these reports. The published results are very similar to the data shown in Figure 3-2. This is in spite of the fact that the previous work was all completed with 5 and 10 μm columns. The behavior observed by Molnar and Horvath is almost identical to the results of the current work.[109]

The plot for the amines in Figure 3-2 shows an inverse dependence of the capacity factor on pH. Instead of the levelling effect at low pH observed with the acids, the amines exhibit a more rapidly increasing capacity factor as the pH is lowered. At pH values above three, the capacity factors for the amines appear to to be relatively stable. Six reports[75,99,101,105,109,110] on the RPLC effects of pH on the capacity factor for amines have appeared in the literature. For the pH range used in the current investigation, the clear consensus of these reports is that the capacity factor is *independent* of pH. From pH 5 to pH 7, on

the other hand, the capacity factor of the amines reportedly increases quite dramatically. The work of Nakagawa *et al.* also reports a similar increase with pH except that, in this case, it began at a pH of 4 instead of 5.[110] No substantial increase was observed in capacity factors as the pH was lowered from 3 to 2 in any of the papers. Fundamentally, one would expect the pH curves for the amines to resemble potentiometric titration curves of weak bases. Indeed, the results of the published reports are completely consistant with this expectation. The amines are all positively charged molecules in the pH range of 2 to 5 and no substantial change in k' is reported for this region. In the pH range of 5 to 7, the protonated amines are beginning to experience deprotonation to the neutral molecules, with the pK_a values for deprotonation being approximately 8 to 10. The neutral molecules have an increased affinity for the stationary phase, and, thus, the capacity factor increases as the pH is raised.

The results of the current work show a set of relatively constant capacity factors for the amines at slightly acidic (pH 4-5) conditions. These values then increase dramatically as the pH decreases, as was seen in Figure 3-2. Since the amines do not undergo any protonation or deprotonation reactions in this pH range, other components of the mobile phase must be affecting the capacity factors. There are three major components of the mobile phase that

may experience acid/base alterations in the pH range of 2 to 5. They are citric acid, EDTA and SOS. Citric acid has an initial acid dissociation constant given by $pK_{a,1}$ = 3.13. Thus, it is predominantly in the fully protonated, neutral form below pH 3 and predominantly in a negatively charged form above pH 3. The neutral form of citric acid would be expected to be more attracted to the stationary phase than the charged form. If hydrogen bonding occurs between the amines and the neutral citric acid, then this might partially explain why the capacity factors of the amines increase as the pH decreases. If this is the actual mechanism, however, one would expect that the sharpest increase in capacity factors should be observed around a pH equal to the $pK_{a,1}$ of citric acid. But, this does not exactly correspond with the actual curves, which, instead, exhibit the sharpest change nearer a pH value of 2. EDTA also experiences a change in its degree of protonation in this pH range. It has $pK_{a,1}$ and $pK_{a,2}$ values of 1.68 and 2.00, respectively. Although these values seemingly correspond quite well with the rises observed in the amine curves, the concentration of the EDTA (0.05 m$\underline{M}$) would be expected to be too low to exert a substantial effect on the capacity factors of the amines. One previous paper also used this same concentration of EDTA in the mobile phase without experiencing any dependency for the amine capacity factors on pH.[101] Thus, it would appear unlikely that EDTA is the cause of the

pH dependence of the amines. Finally, the only other compo-
nent that might change its form in this pH range is SOS. At
low pH values, SOS may begin to assume an uncharged, neutral
form. The amount of SOS adsorbed onto the stationary phase
is, of course, dependent on its affinity for the mobile and
stationary phases. And, the uncharged form would be expect-
ed to have a higher affinity for the stationary phase. But,
how this or the resultant, modified stationary phase would
interact with the protonated amines is difficult to predict.

A more interesting possibility is obtained by comparing
the current results to those obtained by Bulawa.[75] His
mobile phase roughly matched the current one with two excep-
tions: (1) methanol was used instead of acetonitrile, and
(2) no EDTA was used. His work was also completed on a 5 μm
reversed-phase column instead of a 3 μm one. He notably did
not observe the increase in amine k′ values as the pH de-
clined. Since all the other mentioned reports also did not
use acetonitrile, and since one of those reports would
apparently rule out the possible involvement of EDTA,[101] we
are left with the finger of suspicion pointing to acetonit-
rile. Our current feeling is that this effect is probably
due to both acetonitrile and another, presently unidentified
component of the mobile phase. But, the actual mechanism
remains fundamentally unknown.

The overall effect of pH on the amino acids is very
similar to that of the amines, as shown in Figure 3-2.

Closer inspection of the amino acid curves, however, reveals a much greater dependence on pH than that observed for the amines. The very sharp capacity factor increase observed as the pH is lowered from 3.5 to 2 is at least partially due to protonation of the neutral zwitterion to form a positively charged species. This species is then readily attracted to the absorbed, negatively charged SOS molecules on the stationary phase. Values of pK_a for the reverse process (deprotonation) are on the order of 2 to 3. But, a portion of the increase in k' is probably also due to the unexplained process mentioned above for the amines.

Several papers using 5 and 10 μm packing materials have reported on the pH dependence of capacity factors for the amino acids.[75,99,101] The results of the current report agree very well with the previous work. Basically, the reported data indicate the pH dependency of amino acids to be greater in magnitude than that observed for the amines.

The neutral plot of Figure 3-2 shows that the capacity factors of the neutral compounds are relatively independent of pH. The majority of the functional groups for the neutral compounds are hydroxy and methoxy groups. These groups are basically pH insensitive in the range examined. Thus, the plot for the neutral compounds appears to be quite reasonable. This result agrees with the report of Bulawa.[75]

2. SOS effect. The results of Table 3-3 exhibit two basic trends. In fact, the twenty-four compounds only need

TABLE 3-3. EFFECT OF SOS CONCENTRATION ON CAPACITY FACTOR

	Capacity Factor, k′				
	SOS(m$\underline{M}$)				
Compound	0.00	0.03	0.09	0.30	1.00
DA	0.55	1.67	3.35	6.82	15.02
DHBA	0.33	1.06	2.14	4.36	9.61
DOPA	0.44	1.04	1.86	3.57	7.79
DOPAC	3.37	3.36	3.52	3.19	3.14
DOPEG	0.42	0.42	0.44	0.34	0.40
EPI	0.27	0.92	1.86	3.59	7.57
EPIN	0.73	2.17	4.33	8.62	18.95
HVA	10.67	10.62	10.91	9.96	9.32
MEL	64.03	63.86	67.76	62.57	60.99
MET	0.72	2.11	4.23	8.19	17.49
MHPG	1.18	1.16	1.20	1.04	1.06
NE	0.19	0.66	1.33	2.66	5.62
NM	0.47	1.42	2.88	5.62	12.03
N-Ac-5HT	7.97	7.98	8.32	7.79	7.81
N-MET	2.30	6.27	12.46	25.55	55.29
TP	7.04	17.11	31.38	73.12	159.35
TYR	0.77	1.81	3.18	6.23	13.48
VMA	1.21	1.16	1.22	1.05	1.03
3MT	1.66	4.69	9.22	18.63	40.73
5HIAA	6.43	6.46	6.76	6.25	6.06
5HT	1.81	4.96	9.83	20.50	44.76
5HTOL	4.94	4.97	5.19	4.81	4.77
5HTP	1.60	3.65	6.43	12.58	26.82
5MT	14.33	39.90	88.80	173.39	393.84

to be subdivided into two categories to explain the effect of SOS. The first group, which shows a dependence on SOS consists of the amines and the amino acids of Table 3-5. The second group, which is independent of SOS, is composed of the acids and the neutral compounds.

The capacity factors of both the amines and the amino acids show a marked and relatively direct dependence on SOS, as seen in Figure 3-3. The trend denoted by this plot is that which is generally anticipated. At a given pH, increasing the concentration of SOS in the mobile phase leads to an increase in the total amount of SOS absorbed in the stationary phase. The resultant increase in negative charge associated with the stationary phase leads to an increased attraction for the positively charged amines and partially positively charged amino acids. Thus, these species will be retained longer and experience an increase in their capacity factors.

A literature search revealed that only one paper has reported the effect of SOS on the capacity factor for these compounds.[75] The next most relevant report used heptane-sulfonate as the ion pairing agent instead of sodium octyl sulfate.[105] Since these two detergents are very similar in structure, their effects on capacity factors should be quite similar. Indeed, the effect of both detergents on the capacity factors of amines and amino acids was very comparable to that observed in the current study.
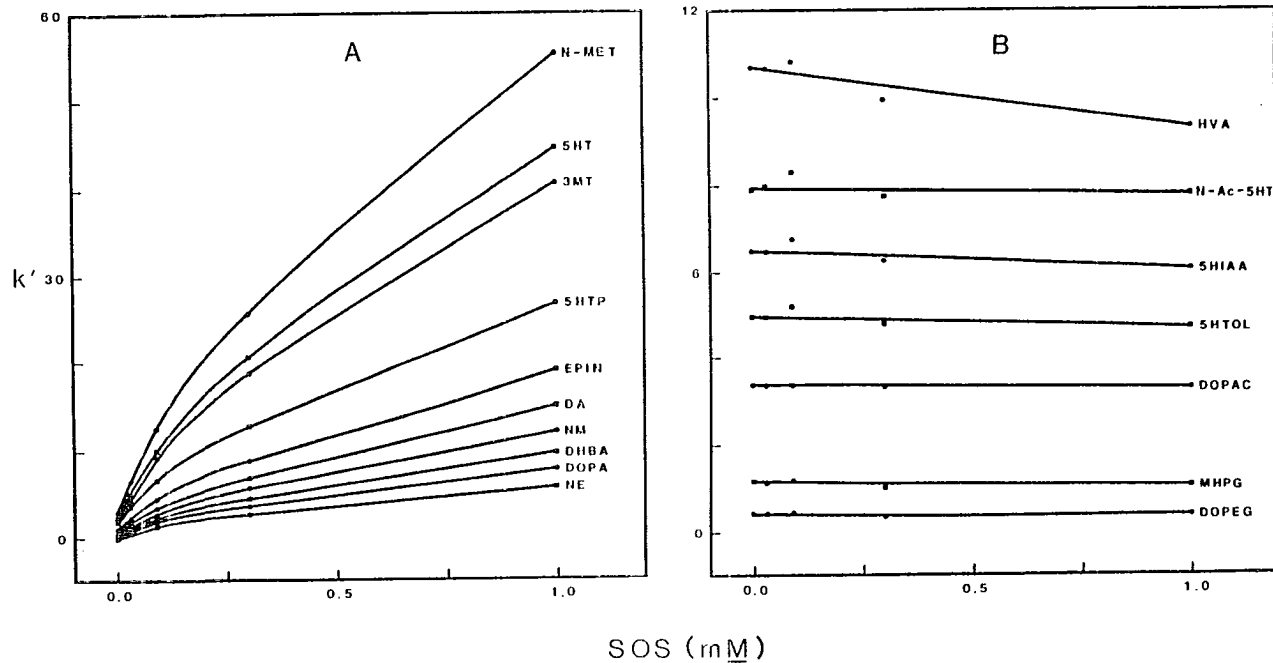
Figure 3-3.   Effect of SOS on the Capacity Factors for
(A) Amines and Amino Acids and (B) Acids
and Neutrals.

The capacity factors of the acids and the neutrals appear to be relatively independent of the concentration of SOS. However, a closer look at the data for the acids reveals a very slight inverse dependence of k' on SOS. This trend is also quite reasonable. Since both the SOS modified stationary phase and the acids are negatively charged at pH 4.80, they will repel one another. Increasing the amount of SOS in the stationary phase will, thus, simply decrease the attraction of the deprotonated acids to that phase and, likewise, decrease their capacity factors. On the other hand, the neutral compounds would be predicted to have no interaction whatsoever with the SOS molecules. Thus, their capacity factors should be, and are, independent of SOS concentration.

Asmus and Freed, investigating the use of trichloroacetate and nitrate as ion pairing agents, found that these agents act very similar to conventional ion pairing agents.[99] Since both of these anions are negatively charged, increasing their concentration should, by the same arguments as given above, slightly decrease the capacity factors of the acid compounds. Indeed, this is the result that was reported. The current results are also supported by other relevant investigations reported in the literature.[75,105]

3. __ACN effect.__ Although the capacity factor effects of ACN appear to be very similar for the four basic types of compounds of Table 3-5, they were divided into four separate

plots to avoid congestion, as seen in Figure 3-4. Overall, the capacity factors are inversely proportional to the concentration of ACN, *i.e.*, as the ACN increases, the capacity factors decrease. This is very reasonable. As the ACN and, thus, the nonpolar character of the mobile phase is increased, the affinity of the organic solutes for the mobile phase relative to the stationary phase will be increased. This has the effect of decreasing the retention times and, thus, the capacity factors.

Only one published paper has reported on the effect of ACN concentration on the capacity factors of these compounds.[60] The results of that report are completely consistent with the current investigation. Several reports, on the other hand, have appeared using methanol, instead of ACN, as the organic modifier in the mobile phase.[60,75,105] The general trends observed in these reports are also consistent with the current results on ACN.

One particularly interesting phenomenon in the ACN plot is the crossover of the 3MT, 5HT and N-MET curves. Normally, when the performance of a column being used for brain neurochemical determinations begins to deteriorate, one of the first observable problems involves the resolution between 3MT and 5HT. The separation between these two peaks decreases until they are almost completely overlapping. Figure 3-4 reveals that the separation of these compounds might be advantageously recovered by merely changing the ACN
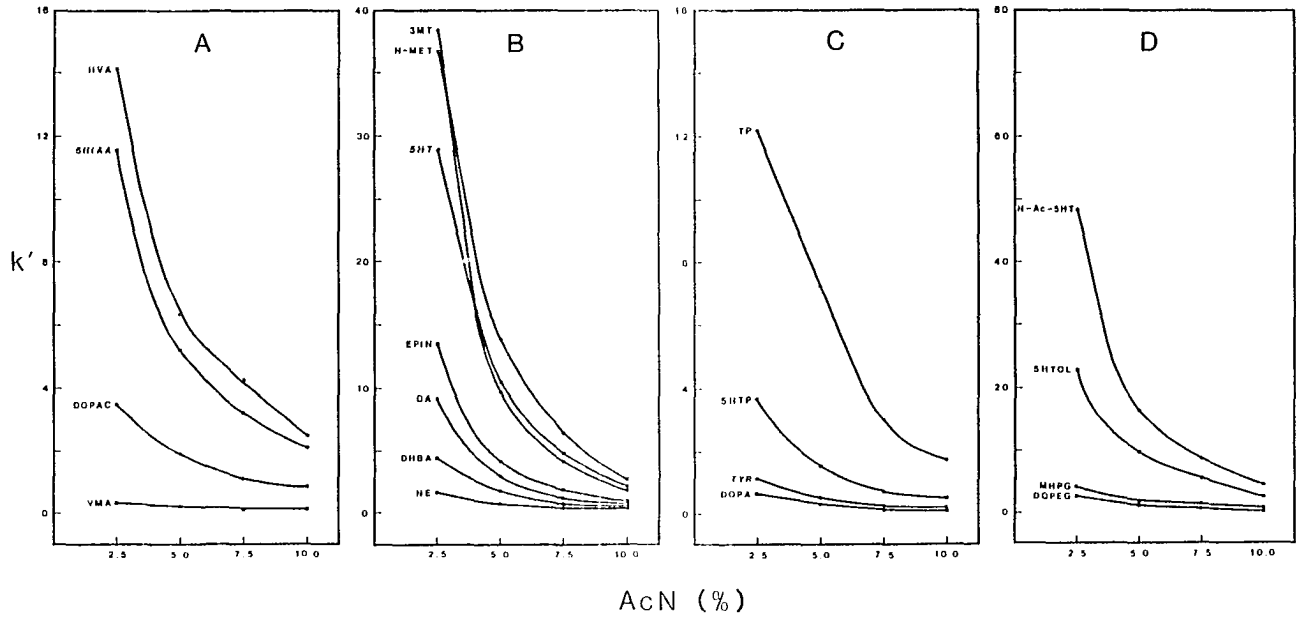
Figure 3-4. Effect of Acetonitrile on the Capacity Factor
for Acids (A), Amines (B), Amino Acids (C),
and Neutrals (D).

TABLE 3-4.   EFFECT OF ACN CONCENTRATION ON CAPACITY FACTOR

| | Capacity Factor, k' | | | |
| | ACN(%) | | | |
Compound	2.50	5.00	7.50	10.00
DA	9.03	2.93	1.23	0.73
DHBA	4.40	1.61	0.70	0.49
DOPA	0.68	0.32	0.04	0.14
DOPAC	3.46	1.89	1.13	0.86
DOPEG	1.18	0.70	0.34	0.42
EPI	3.39	1.30	0.56	0.45
EPIN	13.49	4.03	1.81	0.96
HVA	14.12	6.32	4.25	2.44
MEL	N.D.*	N.D.*	N.D.*	35.11
MET	12.32	3.71	1.75	0.91
MHPG	4.07	1.97	1.13	0.86
NE	1.55	0.78	0.32	0.33
NM	5.60	2.13	0.97	0.65
N-Ac-5HT	48.22	16.46	8.80	4.70
N-MET	36.66	13.93	6.42	2.61
TP	12.17	5.27	3.01	1.72
TYR	1.16	0.57	0.22	0.21
VMA	0.29	0.20	0.01	0.13
3MT	38.38	9.65	4.01	1.81
5HIAA	11.58	5.20	3.21	2.12
5HT	28.83	10.42	4.75	2.16
5HTOL	22.64	9.53	5.64	3.34
5HTP	3.65	1.49	0.70	0.50
SMT	N.D.*	N.D.*	N.D.*	16.58

* Values not determined.

concentration to either less than four percent or greater than six percent. This approach could extend the useful lifetime of the column by perhaps a few months.

   B.   Optimization of the mobile phase.   From the previous discussions concerning mobile phase components, it should be clear that pH exhibits the greatest selectivity with regard to its effect on the capacity factors of the individual compounds.   All four different classes of compounds exhibit distinctly different pH dependencies.   On the other hand, SOS separates the compounds into only two major groups, and the effect of ACN is almost identical for all of the twenty-four compounds.

   Since pH appears to have the greatest selectivity, it can be initially used to produce a crude separation.   Next, SOS can be used to refine the separation until all desired compounds are adequately resolved.   Finally, the ACN content will be increased to obtain the least amount of time required for each sample.

   The experimental results of Table 3-2 were plotted for the Priority 1 compounds of Table 3-1 to obtain a single capacity factor *versus* pH plot.   The result is depicted in Figure 3-5.   This plot can be used to locate the most promising pH regions for the separation of the desired compounds. As can be seen, the region above pH 3.5 is practically useless due to the congestion of the amines.   The best regions are to be found where the curves are all well separ-
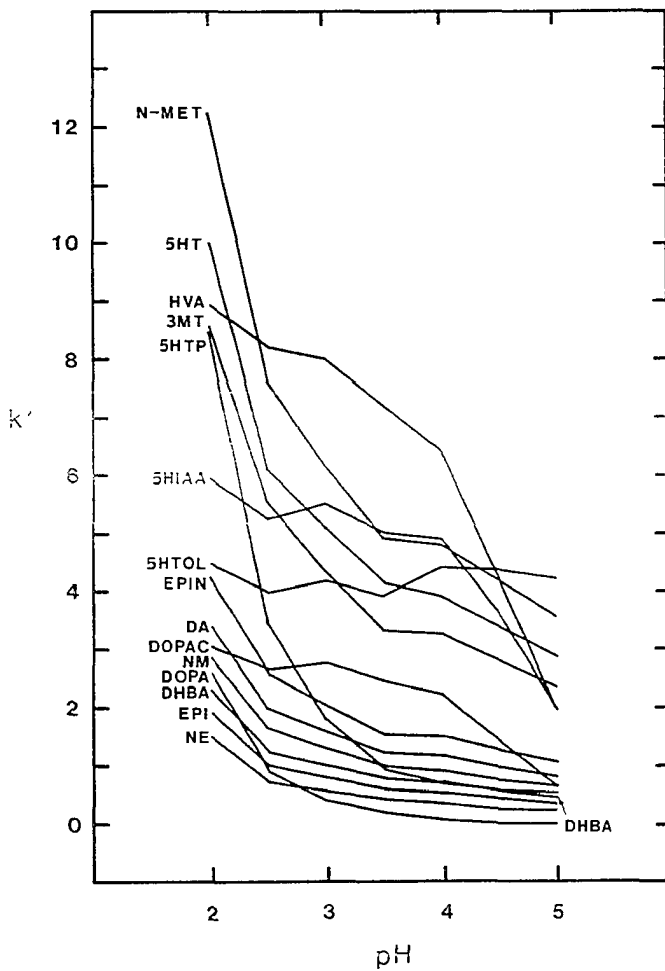
Figure 3-5.   Effect of pH on the Capacity Factor for
              Priority 1 and Priority 2 Compounds.

ated or, at least, where the minimum number of adjacent curves are overlapping. Two such regions are present in Figure 3-5. They are at pH values of 2.3 and 2.7. With this piece of information, a decision was made to more carefully evaluate the pH region between 2.25 and 2.75. The results of six different mobile phases, each 0.1 pH unit apart, revealed the optimum pH to be 2.50. The mobile phase at this pH value produced a chromatogram with only two pairs of overlapping peaks. The first overlapping pair was 5HIAA and 3MT, while the second pair was HVA and N-MET.

In order to obtain an overall view of the effect of SOS on the capacity factor of the desired compounds, the Priority 1 and 2 compounds of Table 3-3 were then compiled into a single graph, as shown in Figure 3-6. This plot indicates two approaches to resolve the overlapping pairs. One approach involves decreasing the SOS concentration from its then current value of 0.09 m$\underline{M}$ so that 3MT elutes before 5HIAA and N-MET elutes prior to HVA. But, this would clearly produce a very congested chromatogram. Thus, the only logical alternative is to increase the SOS concentration. Scanning across the curves of Figure 3-6, four possible SOS concentrations are revealed. These are at 0.15, 0.3, 0.6 and 0.9 m$\underline{M}$ SOS. Since one of the objectives of this optimization is to minimize the time required for the separation, the lowest necessary SOS concentration would appear most desirable due to its associated shorter retention times.
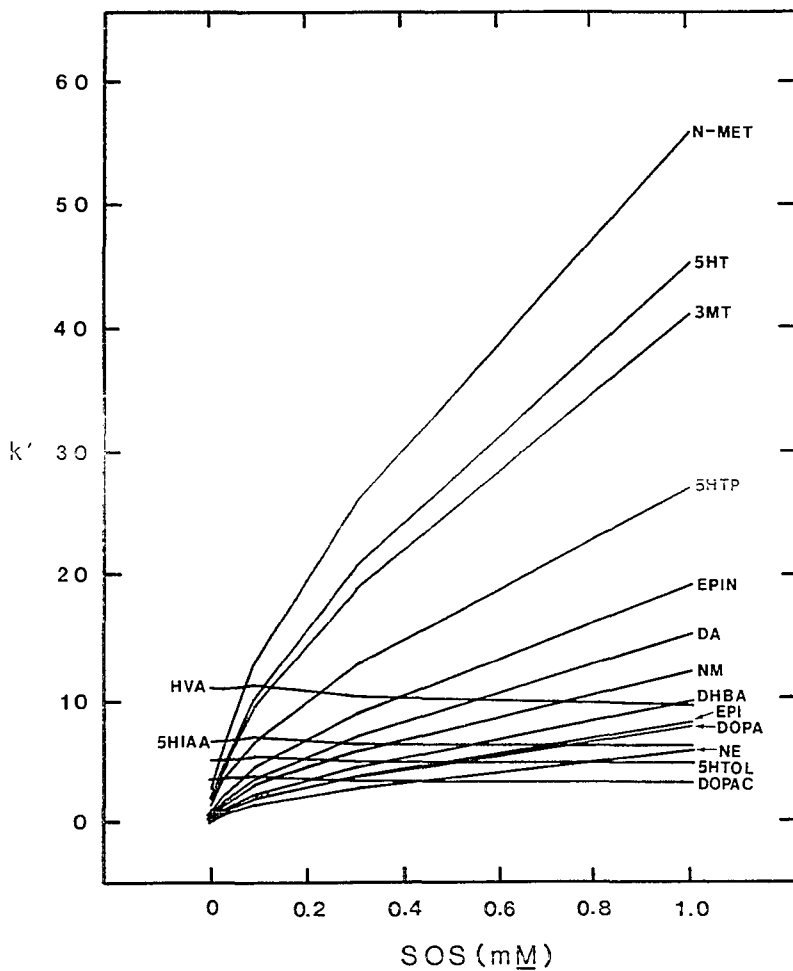
Figure 3-6. Effect of SOS on the Capacity Factor for
Priority 1 and Priority 2 Compounds.

Thus, SOS concentrations in the range of 0.1 to 0.2 m$\underline{M}$ were more closely evaluated. The results of this investigation showed an optimum SOS concentration of 0.175 m$\underline{M}$.

At this point, the optimization process has resulted in the separation of fifteen compounds including all the compounds from Table 3-1 listed as Priority 1 and Priority 2. The separation requires about 6.5 minutes. In an attempt to further decrease the required analysis time, the effects of ACN, as shown in Figure 3-7, were compiled. This plot shows that the retention times of the individual compounds can all be reduced by increasing the ACN concentration above the then current value of 7.5%. But, our experience from the use of 10% ACN, mentioned in Chapter 2, had already indicated a very short carbon paste electrode lifetime and a high background noise associated with higher ACN values. Thus, we decided to leave the ACN value at 7.5%.

An alternative route to shortening the time of analysis simply involves increasing the flow rate. By increasing the flow rate from 1.5 ml/min to 2.2 ml/min, the total time required was reduced from 6.5 minutes to less than 4.5 minutes. Greater increases in flow rate, however, produce losses in efficiency and instrumental pressure problems. The resultant chromatogram revealed several regions in which there were no compounds. Investigation of the capacity factors of the Priority 3 compounds showed that several could be added to the separation without affecting either
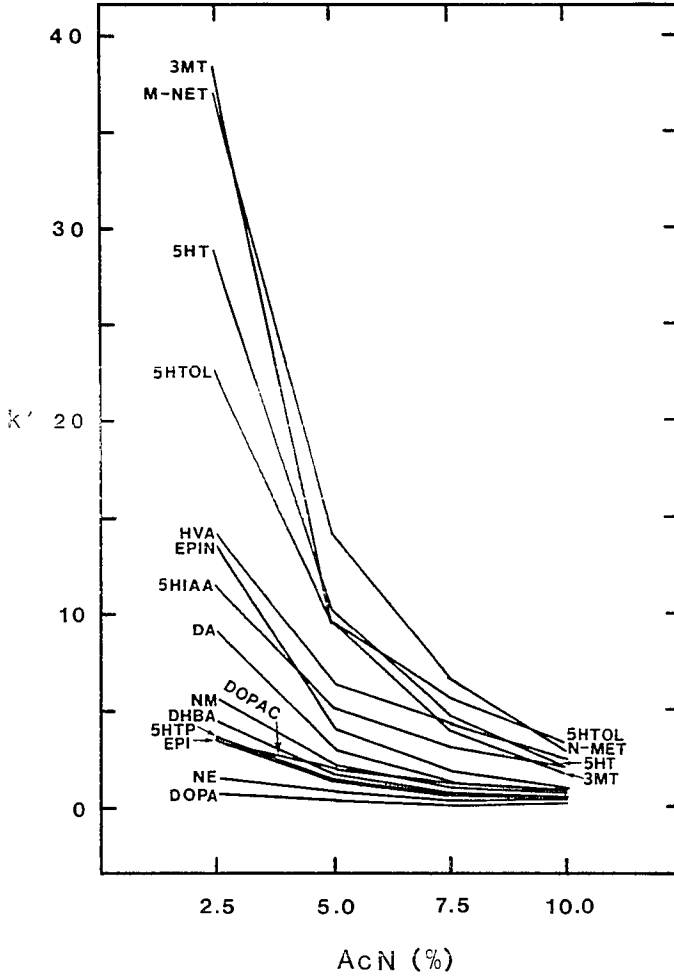
Figure 3-7. Effect of Acetonitrile on the Capacity Factor
for Priority 1 and Priority 2 Compounds.

the achieved efficiency or the total analysis time. Thus, DOPEG, VMA and N-Ac-5HT were added. TP, 5MT and MEL were also observed to elute after the last solute, N-MET. They are completely resolved from one another and could, thus, be added to the current separation. But, inclusion of these compounds would drastically increase the required time for analysis.

The final optimized mobile phase for the Beckman column includes 0.175 m$\underline{M}$ SOS, 7.5% ACN, 0.1 $\underline{M}$ citric acid, and 0.05 m$\underline{M}$ EDTA; it has a pH of 2.50. The optimum flow rate is 2.2 ml/min. This system can currently resolve eighteen compounds in less than four and a half minutes, as seen in Figure 3-8. The resolution values achieved are at least 1.5 for all adjacent peak pairs.

Perkin Elmer column. A good starting point for the optimization of the mobile phase for the reversed-phase 3 μm Perkin Elmer 10 cm column would certainly appear to be the previously optimized mobile phase for the Beckman reversed-phase 3 μm column. Initial experiments employing this approach, however, resulted in extreme tailing of the amine peaks. In some cases, efficiences of less than a thousand theoretical plates were observed. Communications with the distributor (BAS), fortunately, shed some light on the situation. The tailing was thought to be due to unreacted silyl functional groups on the stationary phase. In any case, the suggested addition of diethylamine to the mobile
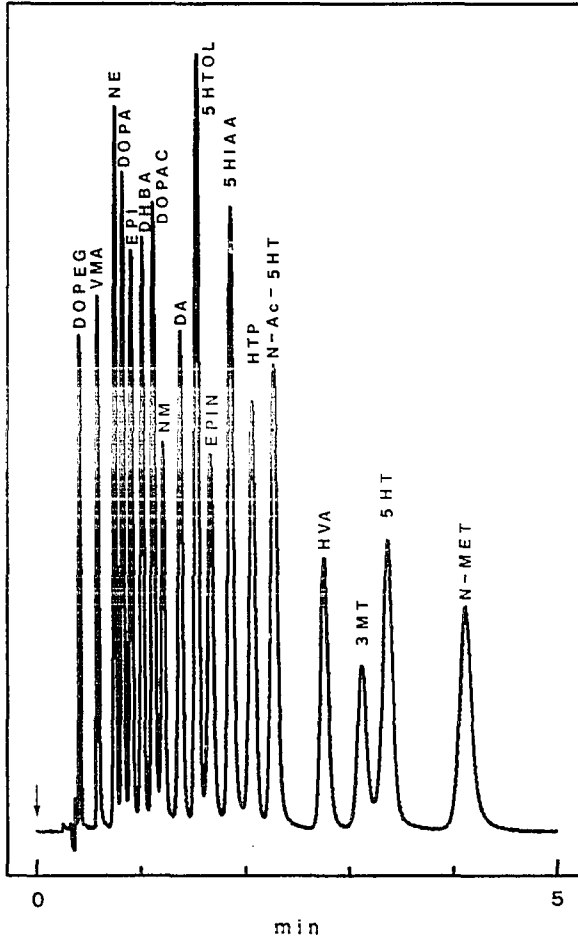
Figure 3-8. Separation of Eighteen Biogenic Amine Related
Compounds on the Beckman Column.

phase remedied the problem. All subsequent mobile phases for Perkin Elmer columns incorporated 0.06% (vol/vol) of DEA.

The Perkin Elmer column was optimized in roughly the same manner as the Beckman column. The optimum pH determined was 2.45, which is just slightly lower than the value previously obtained for the Beckman column. The results of the SDS optimization indicated the best value to be 0.255 m$\underline{M}$. Finally, the flow rate was increased to 1.85 ml/min without any adverse effect on the separation.

Under these optimal conditions, the Perkin Elmer column can also resolve the same 18 compounds as mentioned above for the Beckman unit, but the separation requires approximately seven minutes. This longer time is primarily due to the length of the Perkin Elmer column, which is 10 cm instead of the 7.5 cm of the Beckman column. This 25% increase in length significantly increases the back pressure of the column, which, correspondingly, limits the maximum flow rate that can be employed. The combination of the flow rate limitation, the 25% increase in the void volume, and the roughly 25% increase in efficiency all contribute to the observed increase in the total required separation time. A sample chromatogram showing the separation of the eighteen compounds by the Perkin Elmer 10 cm column is presented in Figure 3-9.

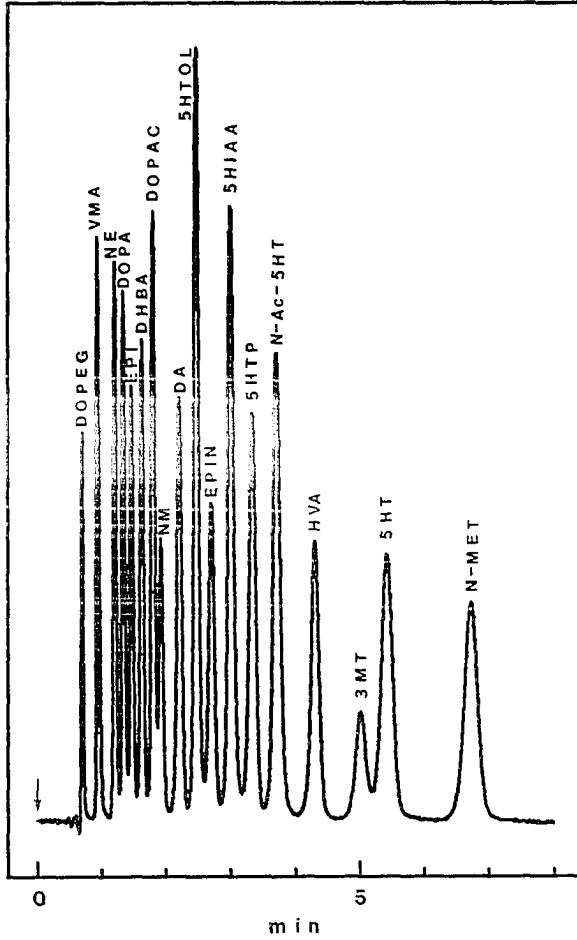Due to the higher efficiency of the Perkin Elmer col-

Figure 3-9. Separation of Eighteen Biogenic Amine Related
Compounds on the 10 cm Perkin Elmer Column.

umn, our laboratory adopted this column for routine determi-
nations of catecholamines, indoleamines, related compounds,
and related enzyme activities for both rat and mouse
brains.[112,113] The additional efficiency afforded by the
column is particularly helpful in resolving the early elu-
ting catecholamines such as NE, DOPA and EPI from the sol-
vent front, as shown in Figure 3-10.

Very recently, Perkin Elmer has replaced the 10 cm
columns with columns having a length of only 8.3 cm. They
claim that the new 8.3 cm columns are equivalent to the
previous 10 cm columns in efficiency due to improved column
packing techniques. Optimizing the new 8.3 cm column re-
quired just a slight pH modification of the previously
established mobile phase for the 10 cm column. The new
optimum pH is 2.55 instead of 2.45. Due to the shorter
length of the column, the flow rate could be increased
slightly from 1.85 ml/min to 2.0 ml/min. But, a chromato-
gram showing the separation of the same eighteen compounds
mentioned above by the 8.3 cm column (Figure 3-11) still
revealed a time requirement of approximately seven minutes.

A quick perusal of Figures 3-8, 3-9 and 3-11 readily
demonstrates the superiority of the latest column and mobile
phase combinations to the user who has done similar or
related separations with the 5 or 10 μm columns.

To partially quantitate the performance of the latest
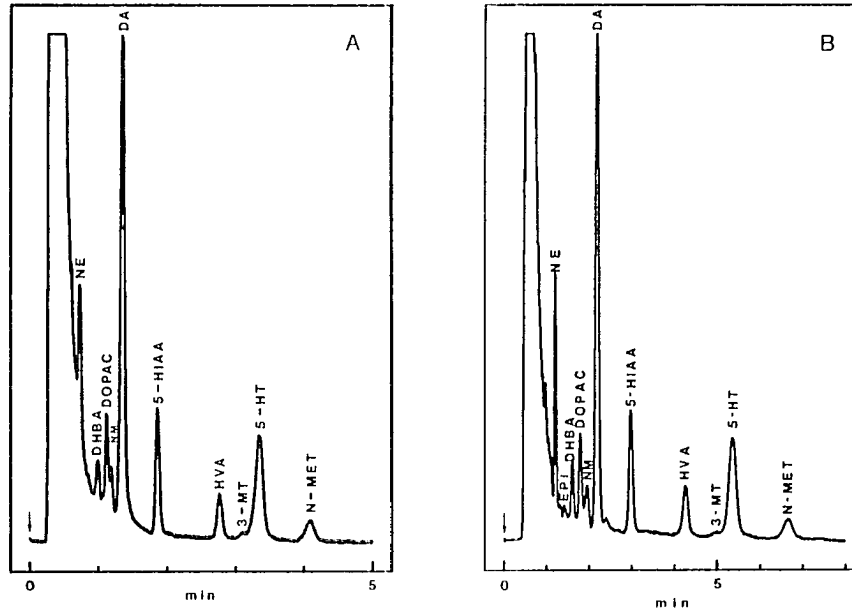column, the efficiency and resolution of adjoining peaks

Figure 3-10.   Whole Mouse Brain Determinations Using Beckman
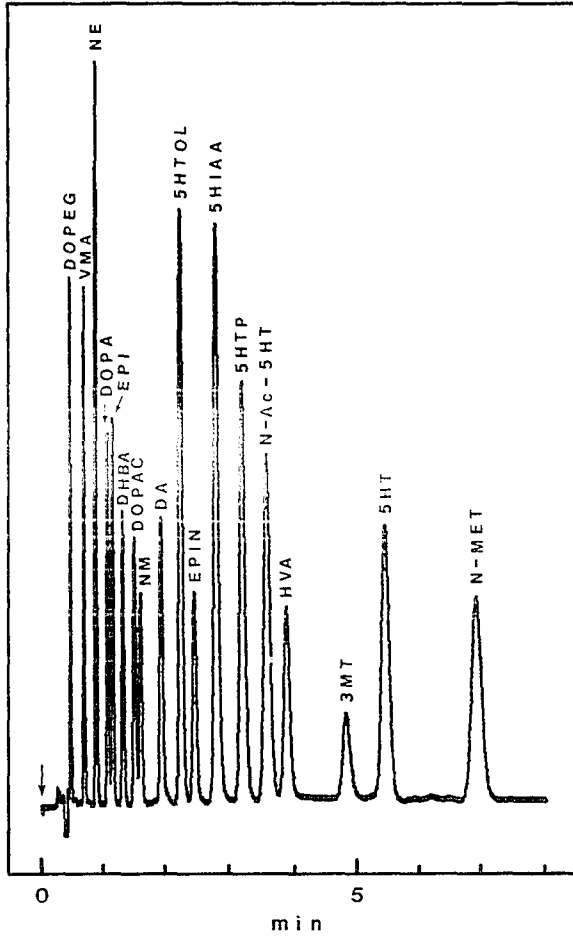(A) and 10 cm Perkin Elmer (B) Columns.

Figure 3-11.   Separation of Eighteen Biogenic Amine Related
                Compounds on the 8.3 cm Perkin Elmer Column.

were measured for all 18 resolved compounds. The efficiency was measured by both the second moment (equation 2-2) and the width of the peak at half-height (equation 2-5). The results of these calculations are tabulated in Table 3-6. Determinations of the efficiency by the second moment method are known to be extremely sensitive to baseline assignments. With eighteen compounds in one chromatogram, consistent baseline designation is difficult at best. Thus, variability in the determination of efficiency is inevitable. On the other hand, measurement of efficiency by the width at half-height is totally insensitive to peak shapes. The use of this method with tailing peaks can easily result in overes-timations of the efficiency by more than one hundred per-cent. The efficiency determined by the width at half-height is expected, from practical experience, to be approximately one-quarter to one-third higher than that determined by the second moment method. The results of Table 3-6 generally agree with these predictions. Determinations of the effi-ciency for early eluting peaks are especially difficult. The calculated efficiency for the very first peak, DOPEG, by both methods is clearly unacceptable. Although there are notable discrepencies between the two methods, the apparent, overall efficiency for these compounds is seen to be ap-proximately six to eight thousand theoretical plates. Per-kin Elmer guarantees such columns to contain at least twelve thousand theoretical plates. Considering the nature of

TABLE 3-6.   EFFICIENCY AND RESOLUTION DETERMINED BY SECOND
             MOMENT AND BY WIDTH AT HALF-HEIGHT FOR THE 8.3
             CM PERKIN ELMER COLUMN

Compound	$N(\sigma)$	$N(W_{1/2})$	R
DOPEG	497	13870	
			$\}---\rightarrow$ 8.44
VMA	1601	5481	
			$\}---\rightarrow$ 4.85
NE	3871	6753	
			$\}---\rightarrow$ 3.73
DOPA	7230	6388	
			$\}---\rightarrow$ 1.48
EPI	6960	7072	
			$\}---\rightarrow$ 2.91
DHBA	5076	7348	
			$\}---\rightarrow$ 2.83
DOPAC	11066	7539	
			$\}---\rightarrow$ 1.35
NM	7866	7748	
			$\}---\rightarrow$ 4.09
DA	3675	7892	
			$\}---\rightarrow$ 3.35
5HTOL	6798	7875	
			$\}---\rightarrow$ 2.01
EPIN	5698	8017	
			$\}---\rightarrow$ 2.95
5HIAA	5158	7576	
			$\}---\rightarrow$ 2.97
5HTP	5616	7520	
			$\}---\rightarrow$ 2.33
N-Ac-5HT	5790	6881	
			$\}---\rightarrow$ 1.83
HVA	6991	8500	
			$\}---\rightarrow$ 4.92
3MT	4542	7802	
			$\}---\rightarrow$ 2.78
5HT	7415	9438	
			$\}---\rightarrow$ 5.84
N-MET	6348	9677	

these compounds and the use of a non-optimal (according to
the manufacturer) mobile phase, the results of Table 3-6 are
very respectable.

The resolutions of Table 3-6 clearly show that most of
the originally desired twenty-four compounds have been ade-
quately separated, with the possible exception of three
pairs of peaks. The poorest pair of the currently resolved
compounds is DOPAC and NM. In spite of a resolution of only
1.35, however, Figure 3-11 shows that the two compounds are
approximately 80% resolved. Quantitation of these com-
pounds, thus, should not be a major problem using commonly
available integration or peak height approaches.

IV. Conclusion

Separation of eighteen compounds with resolutions grea-
ter than 1.0 has been demonstrated on all three of the
tested three micron columns. The total time required for
separation is less than five minutes for the Beckman column
and approximately seven minutes for both of the Perkin Elmer
columns. The higher efficiency Perkin Elmer columns would
appear to provide a better separation for the early eluting
compounds commonly found in actual tissue samples. The
final, optimum mobile phase composition for each of the
three columns is presented in Table 3-7.

TABLE 3-7. OPTIMAL MOBILE PHASE CHARACTERISTICS

	Column		
Component	Beckman	Perkin Elmer (10cm)	Perkin Elmer (8.3cm)
Citric Acid ($\underline{M}$)	0.100	0.100	0.100
Na$_2$EDTA (m$\underline{M}$)	0.050	0.050	0.050
SOS (m$\underline{M}$)	0.175	0.255	0.255
DEA (% vol/vol)	O	0.060	0.060
ACN (% vol/vol)	7.5	7.5	7.5
pH	2.50	2.45	2.55
Flow Rate(ml/min)	2.20	1.95	2.00

REFERENCES

1. Hadden N., Baumann, F., MacDonald, F., Munk, M., Stevenson, R., Gere, D., Zamaroni, F., Majors, R. "Basic Liquid Chromatography"; Varian Aerograph: Walnut Creek, CA., 1971, Chapter 1.

2. Kemula, W. *Rocz. Chem.* 1952, *26*, 281.

3. Kissinger, P. T.; Refshauge, C.; Dreiling, R.; Adams, R. N. *Anal. Letters* 1973, *6*, 465-477.

4. Shoup, R. E., Ed. "Recent Reports on Liquid Chromatography/Electrochemistry"; Bioanalytical Systems: West Lafayette, IN., 1982, Chapter 2.

5. Karger, B. L., Snyder, L. R., Horvath, C. "An Introduction to Separation Science"; John Wiley & Sons: New York, 1973.

6. Snyder, L. R., Kirkland, J. J. "Introduction to Modern Liquid Chromatography", 2nd ed.; John Wiley & Sons: New York, 1979.

7. Blank, C. L. *J. Chromatogr.* 1976, *117*, 35-46.

8. Bard, A. J., Faulkner, L. R. "Electrochemical Methods"; John Wiley & Sons: New York, 1980, Chapter 13.

9. Paul, D. W.; Ridgeway, T. H.; Heineman, W. R. *Anal. Chim. Acta* 1983, *146*, 125-134.

10. Shoup, R. E.; Kissinger, P. T. *Chem. Instru.* 1976, 7, 171-177.

11. Lankelma, J.; Poppe, H. *J. Chromatogr.* 1976, *125*, 375-388.

12. Swartzfager, D. G. *Anal. Chem.* 1976, *48*, 2189-2192.

13. Weber, S. G.; Purdy, W. C. *Anal. Chim. Acta* 1978, *100*, 531-544.

14. Hirata, Y.; Lin, P. T.; Novotny, M.; Wightman, R. M.
     J. Chromatogr. 1980, *181*, 287-294.

15. Pinkerton, T. C.; Hajizadeh, K.; Deutsch, E.;
     Heineman, W. R. *Anal. Chem.* 1980, *52*, 1542-1544.

16. Beauchamp, R.; Boing, P.; Fombon, J. J.; Facussel, J.;
     Breant, M.; Georges, J.; Porthault, M.; Vittori, O. *J.
     Chromatogr.* 1981, *204*, 123-130.

17. Elbicki, J. M.; Morgan, D. M.; Weber, S. G. *Anal.
     Chem.* 1984, *56*, 978-985.

18. Lund, W.; Hannisdal, M.; Greibrokk, T. *J. Chromatogr.*
     1979, *173*, 249-261.

19. Stulik, K.; Pacakova, V. *J. Chromatogr.* 1981, *208*,
     269-278.

20. Stulik, K.; Pacakova, V.; Starkova, B. *J. Chromatogr.*
     1981, *213*, 41-46.

21. Patthy, M.; Gyenge, R.; Salat, J. *J. Chromatogr.* 1982,
     241, 131-139.

22. Gunasingham, H.; Fleet, B. *Anal. Chem.* 1983, *55*, 1409-
     1414.

23. Fleet, B.; Little, J. *J. Chromatogr. Sci.* 1974, *12*,
     747-752.

24. Stais, K.; Krejei, M. *J. Chromatogr.* 1982, *235*, 21-29.

25. Buchta, R. C.; Papa, L. J. *J. Chromtogr. Sci.* 1976,
     14, 213-219.

26. Armentrout, D. N.; McLean, J. D.; Long, M. W. *Anal.
     Chem.* 1979, *51*, 1039-1045.

27. Stulik, K.; Pacakova, V. *J. Chromatogr.* 1980, *192*,
     135-141.

28. Rubinson, R. A.; Gilbert, T. W.; Mark, J. H. *Anal.
     Chem.* 1980, *52*, 1549-1551.

29. Lown, J. A.; Koile, R.; Johnson, D. C. *Anal. Chim.
     Acta* 1980, *116*, 33-39.

30. Takata, Y.; Muto, G. *Anal. Chem.* 1973, *45*, 1864-1868.

31. Johnson, D. C.; Larochelle, J. *Talanta* 1973, *20*, 959-
     971.

32. Takata, Y.; Fujita, K. *J. Chromatogr.* **1975**, *108*, 255-263.

33. Eggli, R.; Asper, R. *Anal. Chim. Acta* **1978**, *101*, 253-259.

34. Schieffer, G. W. *Anal. Chem.* **1980**, *52*, 1994-1998.

35. ESA Model 5100A Coulochem Electrochemical Detector, ESA, Bedford, MA. 01730, (Sales literature).

36. Wasa, T.; Musha, S. *Bull. Chem. Soc. Japan* **1975**, *48*, 2176-2181.

37. Hanekamp, H. B.; Vogt, W. H.; Bos, P.; Frei, R. W. *Anal. Lett.* **1979**, *12*, 175-189.

38. PAR Model 310 Polarographic Detector, Princeton Applied Research, Princeton, NJ. (Sales literature).

39. Model TL-9A, Bioanalytical Systems, West Lafayette, IN. 47906 (Sales literature).

40. Anderson, J. L.; Chesney, D. J. *Anal. Chem.* **1980**, *52*, 2156-2161.

41. Fenn, R. J.; Siggia, S.; Curran, D. J. *Anal. Chem.* **1978**, *50*, 1067-1073.

42. Tjaden, U. R.; Lankelma, J.; Poppe, H.; Muusge, R. G. *J. Chromatogr.* **1976**, *125*, 275-286.

43. Taylor, L. R.; Johnson, D. C. *Anal. Chem.* **1974**, *46*, 262-266.

44. Larochelle, J. H.; Johnson, D. C. *Anal. Chem.* **1978**, *50*, 240-243.

45. Stulik, K.; Pacakova, V. *J. Electroanal. Chem.* **1981**, *129*, 1-24.

46. Wightman, R. M.; Paik, E. C.; Borman, S.; Dayton, M. A. *Anal. Chem.* **1978**, *50*, 1410-1414.

47. Caudill, W. L.; Howell, J. O.; Wightman, R. M. *Anal. Chem.* **1982**, *54*, 2532-2535.

48. Caudill, W. L.; Ewing, A. G.; Jones, S.; Wightman, R. M. *Anal. Chem.* **1983**, *55*, 1877-1881.

49. Curran, D. J.; Fougas, T. P. *Anal. Chem.* **1984**, *56*, 672-678.

50. Schieffer, G. W. *Anal. Chem.* 1981, *53*, 126-127.

51. Kissinger, P. T. *Anal. Chem.* 1977, *49*, 447A-456A.

52. Dieker, J. W.; Van Der Linder, W. E.; Poppe, H. *Talanta* 1979, *26*, 511-518.

53. Samuelsson, R.; Osteryoung, J. O.; Osteryoung, J. *Anal. Chem.* 1980, *52*, 2215-2216.

54. Samuelsson, R.; Osteryoung, J. *Anal. Chim. Acta* 1981, *123*, 97-105.

55. Stastug, M.; Volf, R.; Benadikova, H.; Vit, I. *J. Chromatogr. Sci.* 1983, *21*, 18-24.

56. Roston, D. A.; Shoup, R. E.; Kissinger, P. T. *Anal. Chem.* 1982, *54*, 1417A-1434A.

57. Schieffer, G. W. *Anal. Chem.* 1980, *52*, 1994-1998.

58. Allison, L. A.; Shoup, R. E. *Anal. Chem.* 1983, *55*, 8-12.

59. Elchisak, M. A. *J. Chromatogr.* 1983, *264*, 119-127.

60. Meyer, G. S.; Shoup, R. E. *J. Chromatogr.* 1983, *255*, 533-544.

61. Ikenoyn, S.; Hiroshima, M.; Ohmae, M.; Kawabe, K. *Chem. Pharm. Bull.* 1980, *28*, 2941-2947.

62. Shimada, K.; Tamaka, M.; Nambara, T. *Anal. Lett.* 1980, *3*, 1129-1136.

63. Caudill, W. L.; Houck, G. P.; Wightman, R. M. *J. Chromatogr.* 1982, *227*, 331-339.

64. Johnson, D. C. "1984 Abstracts", 1984 Pittsburgh Conference on Analytical Chemistry and Applied Spectroscopy, Atlantic City, N.J., March 1984, Abstract 139.

65. Matsuda, H. *J. Electroanal. Chem.* 1967, *15*, 109-127.

66. Matsuda, H. *J. Electroanal. Chem.* 1968, *16*, 153-164.

67. Yamada, J.; Matsuda, H. *J. Electroanal. Chem.* 1973, *44*, 189-198.

68. Blank, C. L.; Pike, R. *Life Sci.* 1976, *18*, 859-866.

69. Sasa, S.; Blank, C. L. *Anal. Chem.* 1977, *49*, 354-359.

70. Robinson, C. P.; Blank, C. L.; Haines, H.; Francis, J. *Comp. Biochem. Physiol.* 1978, *61C*, 215-221.

71. Sasa, S.; Blank, C. L.; Wenke, D. C.; Sczupak, C. A. *Anal. Chim. Acta* 1978, *100*, 531-544.

72. Sasa, S.; Blank, C. L. *Anal. Chim. Acta* 1979, *104*, 29-45.

73. Wong, P. Ph.D. Dissertation, The University of Oklahoma, 1980.

74. Blank, C. L., Wong, P., Bulawa, M., Lin, P. "Function and Regulation of Monoamine Enzymes", Usidin, E., Weiner, N., Youdim, M. B. H., Eds.; MacMillan: London, 1981; pp.759-770.

75. Bulawa, M. C. Ph.D. Dissertion, The University of Oklahoma, 1981.

76. Cooke, N. H. C.; Olsen, K. *J. Chromatogr. Sci.* 1980, *18*, 512-524.

77. DiCesare, J. L.; Dong, M. W.; Ettre, L. S. *Chromatographia* 1981, *14*, 257-268.

78. DiCesare, J. L.; Dong, M. W.; Atwood, J. G. *J. Chromatogr.* 1981, *217*, 369-386.

79. Dong, M. W.; DiCesare, J. L. *J. Chromatogr. Sci.* 1982, *20*, 49-54.

80. Cooke, N. H. C.; Archer, B. G.; Olsen, K.; Berick, A. *Anal. Chem.* 1982, *54*, 2277-2283.

81. Scott, R. P.; Kucera, J. *J. Chromatogr.* 1978, *169*, 51-72.

82. Tsuda, T.; Novotny, M. *Anal. Chem.* 1978, *50*, 271-275.

83. Knox, J. H.; Gilbert, M. T. *J. Chromatogr.* 1979, *186*, 405-418.

84. Guiochon, G. *J. Chromatogr.* 1979, *185*, 3-26.

85. Lochmuller, C. H.; Sumner, M. *J. Chromatogr. Sci.* 1980, *18*, 154-165.

86. Reese, C. E.; Scott, R. P. W. *J. Chromatogr. Sci.* 1980, *18*, 479-486.

87. Knox, J. H. *J. Chromatogr. Sci.* 1980, *18*, 453-461.

88. Scott, R. P. W.; Simpson, C. F. *J. Chromatogr. Sci.* 1982, *20*, 62-66.

89. Kirkland, J. J.; Yau, W. W.; Stoklosa, H.; J. Dilks, C. H. *J. Chromatogr. Sci.* 1977, *15*, 303-316.

90. Lauer, H. H.; Rozing, G. P. *Chromatographia* 1981, *14*, 641-647.

91. Scott, R. P. W.; Katz, E. *J. Chromatogr.* 1982, *253*, 159-178.

92. Cooke, N. H. C.; Olsen, K. *J. Chromatogr. Sci.* 1980, *18*, 512-524.

93. Unger, K. K.; Messer, W. J.; Krebs, K. F. *J. Chromatogr. 1978, 149* 1-12.

94. Grushka, E.; Myers, M. N.; Schettler, P. D.; Giddings, J. C. *Anal. Chem.* 1969, *41*, 889-892.

95. Sternberg, J. C. "Advances in Chromatography", vol. 2; Giddings, J. C., Killer, R. A., Eds.; Marcel Dekker, New York: 1966, Chapter 6.

96. Wonnacott, T. H., Wonnacott, R. J. "Regression: A Second Course in Statistics"; John Wiley & Sons: New York, 1981, Chapters 3-4.

97. Nikelly, J. G.; Ventura, D. A. *Anal. Chem.* 1979, *51*, 1586-1588.

98. Meyer, R. E.; Banta, M. C.; Lantz, P. M.; Posey, F. A. *J. Electroanal. Chem.* 1971, *30*, 345-358.

99. Asmus, P. A.; Freed, C. R. *J. Chromatogr.* 1979, *169*, 303-311.

100. Knox, J. H.; Jurand, J. *J. Chromatogr.* 1975, *110*, 103-115.

101. Wagner, J.; Palfreyman, M.; Zraika, M. *J. Chromatogr.* 1979, *164*, 41-54.

102. Riley, C. M.; Tomlinson, E.; Jefferies, T. M.; Redfern, P. H. *J. Chromatogr.* 1979, *162*, 153-161.

103. Joseph, M. H.; Kadam, B. V.; Risby, D. *J. Chromatogr.* 1981, *226*, 361-368.

104. Kemph, E.; Mandel, P. *Anal. Biochem.* 1981, *112*, 223-

231.

105. Kilts, C.; Breese, G. R.; Mailman, R. B. *J. Chromatogr.* **1981**, *225*, 347-357.

106. Ishikawa, K.; McGaugh, J. L. *J. Chromatogr.* **1982**, *229*, 35-46.

107. Wagner, J.; Vitali, P.; Palfreyman, M. G.; Zraika, M.; Huot, S. *J. Neurochem.* **1982**, *38*, 1241-1254.

108. Lasley, S. M.; Michaelson, I. A.; Greenland, R. D.; McGinnis, P. M. *J. Chromatogr.* **1984**, *305*, 27-42.

109. Molnar, I.; Horvath, C. *Clin. Chem.* **1976**, *22*, 1497-1502.

110. Nakagawa, T.; Shibukawa, A.; Uno, T. *J. Chromatogr.* **1983**, *254*, 27-34.

111. Molnar, I.; Horvath, C. *J. Chromatogr.* **1978**, *145*, 371-381.

112. Lin, P. Y. T.; Blank, C. L. *Current Separations* **1983**, *5*, 3-6.

113. Lin, P. Y. T.; Bulawa, M. C.; Wong, P.; Lin, L.; Scott, J.; Blank, C. L. *J. Liq. Chromatogr.* **1984**, *7*, 509-538.

APPENDIX

CATECHOLAMINES AND INDOLEAMINES--METABOLIC

PATHWAYS AND NOMENCLATURE

Catecholamines and indoleamines are important neuro-
chemicals in the brain and other regions of the body. They
serve as messengers between neighboring and remote nerve
cells as well as hormonal agents, in which case they are
normally carried to the site of action *via* the circulatory
system. Due to their role as transmitters of information in
the nervous system, they are commonly referred to as neuro-
transmitters. Four very important such neurotransmitters
are dopamine (DA), norepinephrine (NE), epinephrine (EPI),
and serotonin (5-hydroxytryptamine or 5HT). In normal con-
centrations, these compounds appear to have a variety of
effects on psychological, behavioral, and physiological
functions. An improper amount or utilization of these com-
pounds by the body has been implicated in a number of dis-
orders, including the well-documented loss of striatal dopa-
mine in Parkinson's Disease. Due to their known and poten-
tial importance in these and other areas, these transmitters
and their metabolites have experienced a great deal of
investigation in the past few decades. The major biosynthe-
tic and catabolic pathways have become well established.

178

Some of the most commonly studied neurotransmitters, along with related precursors and metabolites are given in Tables A-1 and A-2. Included in the tables are compounds which are frequently employed as standards in the determinations of these compounds. The acronyms employed in this dissertation have also been incorporated into the table as an easy point of reference for the reader.

The three primary catecholamine neurotransmitters (DA, NE, and EPI) share a common biosynthetic pathway. This pathway, shown in Figure A-1, begins with the readily available amino acid, L-tyrosine (TYR). Obtained from dietary sources or from the precursor L-phenylalanine *via* a hepatic metabolic pathway, TYR is converted initially to 3,4-dihydroxyphenylalanine (L-DOPA) by the enzyme tyrosine hydroxylase (TH). This transformation represents the rate limiting step in the biosynthesis of the catecholamines. The enzymatic conversion *in vivo* requires molecular oxygen (O_2) and tetrahydrobiopterin (BH_4) as cofactors. DOPA is decarboxylated to form dopamine (DA) with the enzyme DOPA decarboxylase (DDC) using pyridoxal-5´-phosphate as a cofactor. DA, in turn, is converted, in cells which contain dopamine-β-hydroxylase (DβH), to norepinephrine (NE). DβH requires molecular oxygen, ascorbic acid, and Cu^{2+} as cofactors. NE may then be transformed into epinephrine (EPI), also commonly known as adrenaline, in those cells which contain phenethanolamine-N-methyltransferase (PNMT). This final biosyn-

TABLE A-1. CATECHOLAMINE RELATED COMPOUNDS

Acronym	Compound [Salt form]*	Formula Weight	
		Salt	Free Base
DA	dopamine (3-hydroxytyramine) [hydrochloride]	189.64	153.18
DHBA	3,4-dihydroxybenzylamine [hydrobromide]	220.07	139.15
DOPA	L-3,4-dihydroxyphenylalanine	197.19	
DOPAC	3,4-dihydroxyphenylacetic acid	168.15	
DOPEG	3,4-dihydroxyphenylglycol	170.16	
EPI	epinephrine (adrenaline) [bitartrate]	333.30	183.21
EPIN	deoxyepinephrine (N-methyl-dopamine) [hydrochloride]	203.70	167.24
HVA	homovanillic acid	182.18	
MET	metanephrine [hydrochloride]	233.70	197.24
MHBA	4-hydroxy-3-methoxybenzyl-amine [hydrochloride]	189.64	153.15
MHPG	4-hydroxy-3-methoxyphenyl-glycol [piperazine]	454.52	184.19
3MT	4-hydroxy-3-methoxypheneth-ylamine [hydrochloride]	203.67	167.21
4MT	3-hydroxy-4-methoxypheneth-ylamine [hydrochloride]	203.67	167.21
NE	L-norepinephrine (noradrena-line) [hydrochloride]	205.64	169.18
NM	normetanephrine [hydro-chloride]	219.67	183.21
TYR	L-tyrosine	181.19	
VMA	vanillylmandelic acid (4-hy-droxy-3-methoxymandelic)	198.17	

TABLE A-2.　INDOLEAMINE RELATED COMPOUNDS

Acronym	Compound [Salt form]*	Formula Weight	
		Salt	Free Base
N-Ac-5HT	N-acetylserotonin (N-acetyl-5-hydroxytryptamine	218.26	
5HIAA	5-hydroxyindole-3-acetic acid	191.19	
5HT	5-hydroxytryptamine(seroton-in)[creatine sulfate+H_2O]	387.40 (+)405.43	176.22
5HTOL	5-hydroxytryptophol	177.21	
5HTP	5-hydroxy-L-tryptophan	220.23	
MEL	melatonin	232.28	
N-MET	N_o-methyl-5-hydroxytrypta-mine [oxalate]	280.29	190.25
5MT	5-methoxytryptamine [hydrochloride]	226.71	190.25
TP	L-tryptophan	204.23	
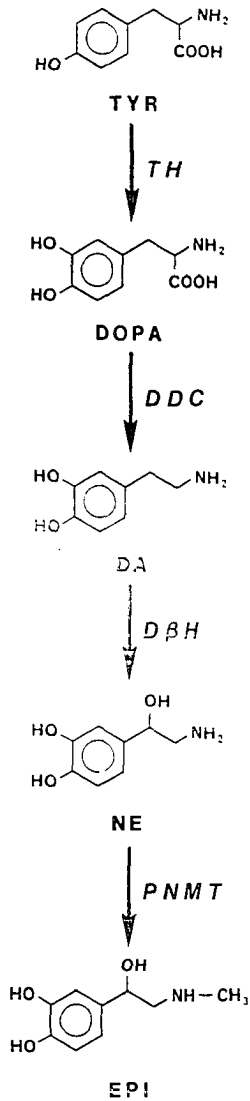
Figure A-1. Biosynthetic Pathway of Dopamine (DA), Norepinephrine (NE), and Epinephrine (EPI).

thetic enzyme employs S-adenosylmethionine (SAM) as the cofactor.

Catabolism of the catecholamines primarily involves two enzymes: monoamine oxidase (MAO) and catechol-O-methyl-transferase (COMT). Examples of the chemical transformations produced by these enzymes are given in Figure A-2. MAO is relatively nonspecific and will use virtually any primary or secondary monoamine as a substrate, converting it to a short-lived aldehyde intermediate. The aldehyde is then converted either to an acid, by the action of aldehyde dehydrogenase (AD), or to an alcohol, by the action of aldehyde reductase (AR). The presence of a methyl group on the carbon atom adjacent to the amine, *i.e.*, the α-carbon, on the ethylamine side chain notably leads to a great reduction or complete elimination of the reactivity of the amine toward MAO. COMT is also a nonspecific enzyme. It methylates one of the two hydroxy groups of virtually any catechol-containing compound. Some limited degree of selectivity is usually demonstrated for one of the particular hydroxy groups over the other. In the case of the catecholamines, the 3-position is preferred over the 4-position, where the numbering is with respect to the alkyl side chain. SAM and Mg^{2+} are used as cofactors for COMT. Using these catabolic pathways, the major metabolite obtained from DA in the *mammalian brain* is HVA, while the *major metabolites* of NE and EPI are, respectively, MHPG and VMA.
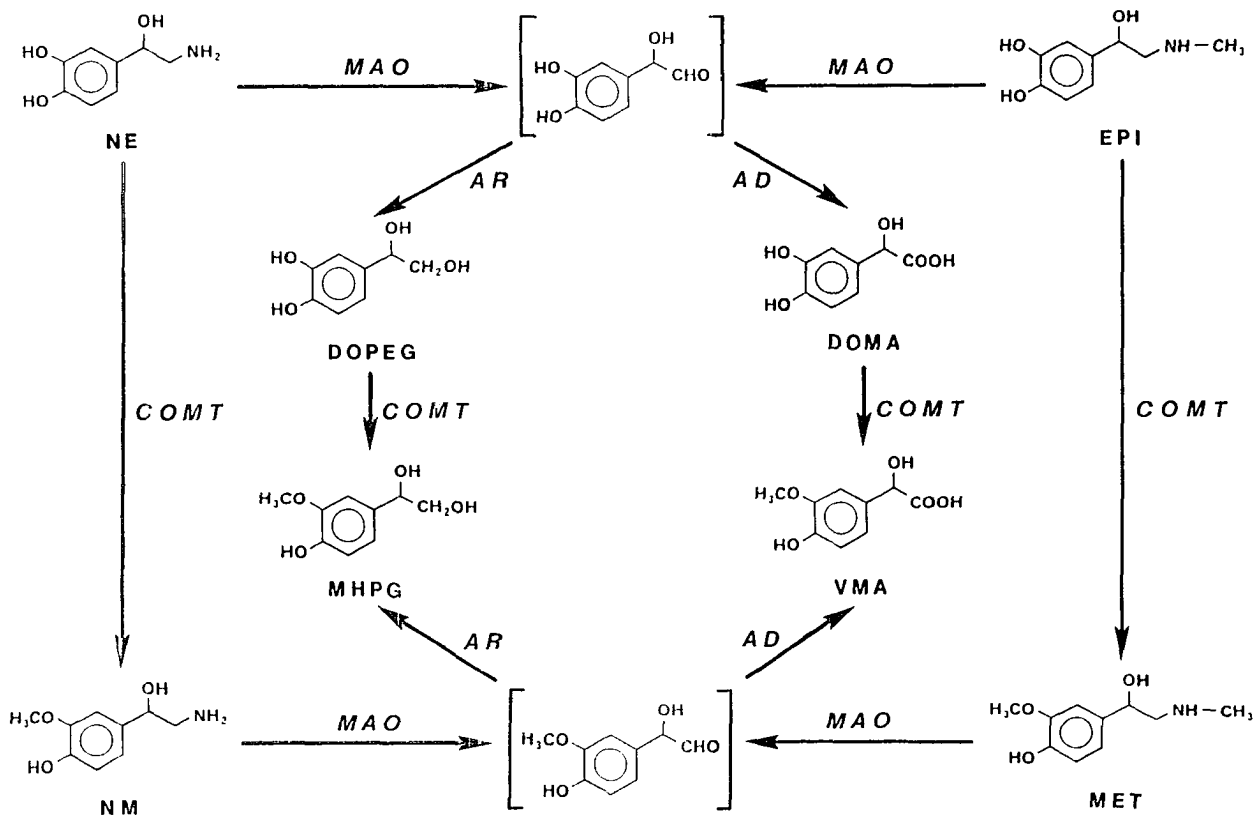
Figure A-2. Catabolic Pathways of Norepinephrine (NE) and Epinephrine (EPI).

The biosynthesis of serotonin, or 5-hydroxytryptamine
(5HT), begins with L-tryptophan (TP). In a manner analagous
to the catecholamine pathway, the first step involves the
hydroxylation of TP by the enzyme tryptophan hydroxylase
(TPH), leading to formation of 5-hydroxytryptophan (5HTP).
Oxygen and tetrahydrobiopterin are, again, essential cofac-
tors in this process. Like TH in the catecholamine biosyn-
thetic pathway, TPH represents the rate limiting step in the
formation of the transmitter serotonin. 5-Hydroxytryptophan
decarboxylase converts 5HTP into 5HT, as shown in Figure A-
3.

Catabolism of 5HT primarily involves MAO. Coupled with
AD and AR, respectively, this leads to the formation of 5-
hydroxyindole-3-acetic acid (5HIAA) and 5-hydroxytryptophol
(5HTOL). These pathways are presented in Figure A-4.

In the pineal gland, the enzyme N-acetyltransferase (N-
AcT) becomes important in the metabolism of 5HT. N-AcT
converts 5HT into N-acetylserotonin (N-Ac-5HT), as shown in
Figure A-5. This compound may then be converted into mela-
tonin (MEL) by hydroxyindole-0-methyltransferase (HIOMT).
Melatonin has been frequently implicated in a variety of
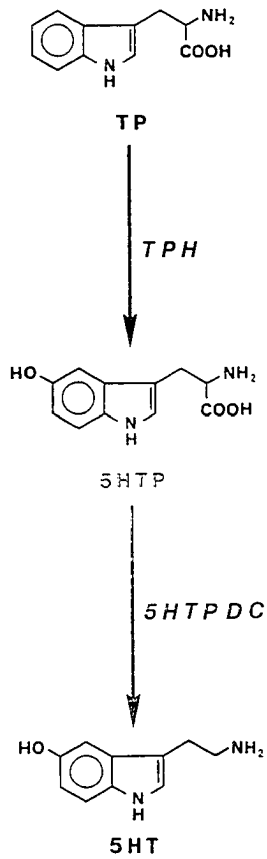diurnal behavioral and physiological effects.

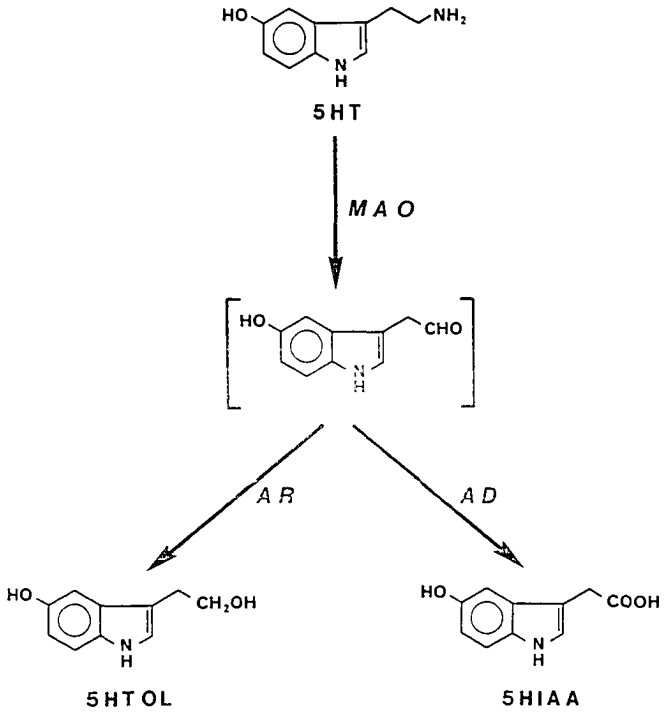Figure A-3.   Biosynthetic Pathway of Serotonin (5HT).
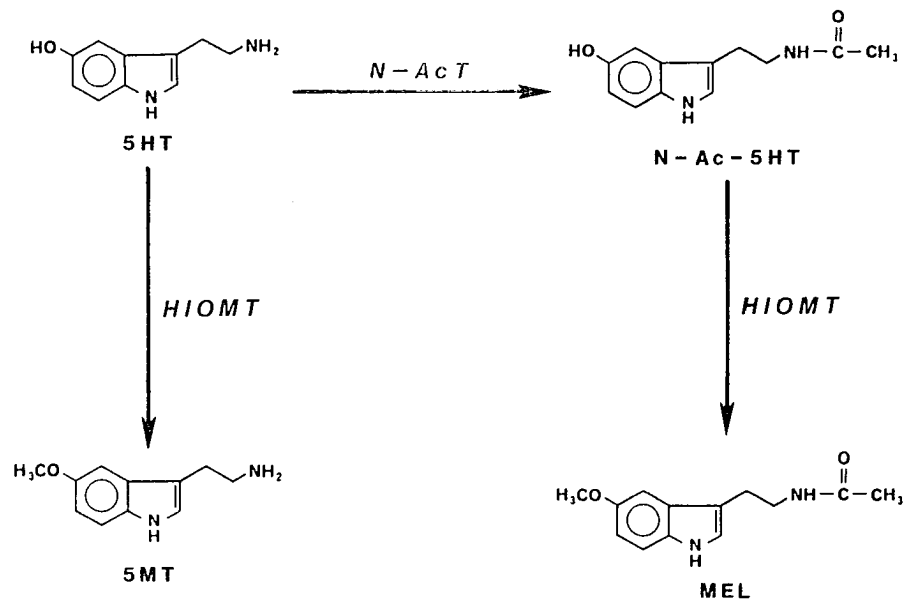
Figure A-4. Catabolic Pathways of Serotonin (5HT).

Figure A-5. Biosynthetic Pathway of Melatonin (MEL).